UNIVERSITAT ROVIRA I VIRGILI
IMPROVEMENT OF MONTE CARLO ALGORITHMS AND INTERMOLECULAR POTENCIALS FOR THE MODELLING OF ALKANOLS, ESTHERS, TRIOPHENES AND AROMATICS
Javier Pérez Pellitero
ISBN: 978-84-691-0377-7/DL: T.2195-2007

UNIVERSITAT ROVIRA I VIRGILI

IMPROVEMENT OF MONTE CARLO ALGORITHMS AND INTERMOLECULAR POTENTIALS FOR THE MODELLING OF ALKANOLS, ETHERS, THIOPHENES AND AROMATICS

A dissertation submitted to the
Department of Chemical Engineering
Universitat Rovira i Virgili
for the degree of
Philosophiæ Doctor (Ph. D)

presented by

JAVIER PÉREZ PELLITERO

UNIVERSITAT ROVIRA I VIRGILI
IMPROVEMENT OF MONTE CARLO ALGORITHMS AND INTERMOLECULAR POTENCIALS FOR THE MODELLING OF ALKANOLS, ESTHERS, TRIOPHENES AND AROMATICS
Javier Pérez Pellitero
ISBN: 978-84-691-0377-7/DL: T.2195-2007

El sota signant Dr. **ALLAN D. MACKIE**

FA CONSTAR:

Que el present treball que porta per títol:

IMPROVEMENT OF MONTE CARLO ALGORITHMS AND INTERMOLECULAR POTENTIALS FOR THE MODELLING OF ALKANOLS, ETHERS, THIOPHENES AND AROMATICS

i que presenta el sr **JAVIER PÉREZ PELLITERO** per optar al grau de Doctor per la Universitat Rovira i Virgili, ha estat realitzat sota la seva direcció i que tots els resultats presentats i la seva anàlisi són fruit de la investigació realitzada per l'esmentat doctorand.

I perque se'n prengui coneixement i tingui els efectes corresponents, signa aquest certificat

Allan D. Mackie
Professor Titular
Departament d'Enginyeria Química
Universitat Rovira i Virgili

Tarragona 09 de juliol de 2007

UNIVERSITAT ROVIRA I VIRGILI
IMPROVEMENT OF MONTE CARLO ALGORITHMS AND INTERMOLECULAR POTENCIALS FOR THE MODELLING OF ALKANOLS, ESTHERS, TRIOPHENES AND AROMATICS
Javier Pérez Pellitero
ISBN: 978-84-691-0377-7/DL: T.2195-2007

En primer lugar quisiera expresar mi agradecimiento a los Dres. Allan Mackie y Philippe Ungerer por haber dirigido este trabajo, sin cuya acertada dirección no hubiera sido posible. También mi agradecimiento para el Dr. Josep Bonet por su inestimable colaboración e ilustrativas discusiones durante estos años. No menos reconocido el agradecimiento a la Dra. Flor Siperstein que también me ha guiado durante gran parte de este trabajo.

Quiero agradecer también la cálida acogida dispensada por el Dr. Carlos Nieto durante mi estancia en París así como a todos los compañeros del Institut Français du Pétrole, en particular Véronique Lachet, quien ha colaborado en la dirección de este trabajo en su última etapa.

Desde luego estos 4 años no hubieran sido lo mismo sin la presencia de los inquilinos del laboratorio 221, los que ya estaban a mi llegada: Henry y Saravana, Alessandro que lo hizo casi al mismo tiempo y los últimos en hacerlo Asfaw, Ashenafi y Belay. Gracias a todos por su inestimable compañia, y en especial, mi agradecimiento para Teresa, siempre capaz de hacerte la vida un 10% más fácil. Tambien a todos los compañeros de fatigas: Ronnie, Rafa, Noe, Gavaldá, y muchos otros.

Como no, mi más sentido agradecimiento a mis padres por haberme permitido llegar hasta aquí con su apoyo y soporte. Eso sí tiene mérito... También a mis hermanos y otros familiares por estar ahí cuando hay que estar.

A Anni por haberme dado su apoyo durante todo este tiempo y también mi agradecimiento a todos los amigos que compartieron buenos ratos durante este tiempo haciendo este trabajo mucho más liviano y llevadero: Toni, Anna, Cristines, Olga, Lluis, Carles, Moi, Alberto, Patri, Miguel y muchisimos más que no caben ...

Finalmente, mi agradecimiento a la Universitat Rovira i Virgili, Institut Français du Pétrole, Generalitat de Catalunya y Ministerio de Educación y Ciencia por haber hecho posible con su financiación la realización de esta tesis.

UNIVERSITAT ROVIRA I VIRGILI
IMPROVEMENT OF MONTE CARLO ALGORITHMS AND INTERMOLECULAR POTENCIALS FOR THE MODELLING OF ALKANOLS, ESTHERS, TRIOPHENES AND AROMATICS
Javier Pérez Pellitero
ISBN: 978-84-691-0377-7/DL: T.2195-2007

Resumen

Durante la última década y paralelamente al incremento de la velocidad de computación, las técnicas de simulación molecular se han erigido como una importante herramienta para la predicción de propiedades físicas de sistemas de interés industrial. Estas propiedades resultan esenciales en las industrias química y petroquímica a la hora de diseñar, optimizar, simular o controlar procesos. El actual coste moderado de computadoras potentes hace que la simulación molecular se convierta en una excelente opción para proporcionar predicciones de dichas propiedades. En particular, la capacidad predictiva de estas técnicas resulta muy importante cuando en los sistemas de interés toman parte compuestos tóxicos o condiciones extremas de temperatura o presión debido a la dificultad que entraña la experimentación a dichas condiciones.

La simulación molecular proporciona una alternativa a los modelos termofísicos utilizados habitualmente en la industria como es el caso de las ecua-

UNIVERSITAT ROVIRA I VIRGILI
IMPROVEMENT OF MONTE CARLO ALGORITHMS AND INTERMOLECULAR POTENCIALS FOR THE MODELLING OF ALKANOLS, ESTHERS, TRIOPHENES AND AROMATICS
Javier Pérez Pellitero
ISBN: 978-84-691-0377-7/DL: T.2195-2007

ciones de estado, modelos de coeficientes de actividad o teorías de estados correspondientes, que resultan inadecuados al intentar reproducir propiedades complejas de fluidos como es el caso de las de fluidos que presentan enlaces de hidrógeno, polímeros, etc. En particular, los métodos de Monte Carlo (MC) constituyen, junto a la dinámica molecular, una de las técnicas de simulación molecular más adecuadas para el cálculo de propiedades termofísicas. Aunque, por contra del caso de la dinámica molecular, los métodos de Monte Carlo no proporcionan información acerca del proceso molecular o las trayectorias moleculares, éstos se centran en el estudio de propiedades de equilibrio y constituyen una herramienta, en general, más eficiente para el cálculo del equilibrio de fases o la consideración de sistemas que presenten elevados tiempos de relajación debido a su bajos coeficientes de difusión y altas viscosidades.

Los objetivos de esta tesis se centran en el desarrollo y la mejora tanto de algoritmos de simulación como de potenciales intermoleculares, factor considerado clave para el desarrollo de las técnicas de simulación de Monte Carlo. En particular, en cuanto a los algoritmos de simulación, la localización de puntos críticos de una manera precisa ha constituido un problema para los métodos habitualmente utilizados en el cálculo de equlibrio de fases, como es el método del colectivo de GIBBS. La aparición de fuertes fluctuaciones de densidad en la región crítica hace imposible obtener datos de simulación en dicha región, debido al hecho de que las simulaciones son llevadas a cabo en una caja de simulación de longitud finita que es superada por la longitud de correlación. Con el fin de proporcionar una ruta adecuada para la local-

UNIVERSITAT ROVIRA I VIRGILI
IMPROVEMENT OF MONTE CARLO ALGORITHMS AND INTERMOLECULAR POTENCIALS FOR THE MODELLING OF ALKANOLS, ESTHERS, TRIOPHENES AND AROMATICS
Javier Pérez Pellitero
ISBN: 978-84-691-0377-7/DL: T.2195-2007

ización de puntos críticos tanto de componentes puros como mezclas binarias, la primera parte de esta tesis está dedicada al desarrollo y aplicación de métodos adecuados que permitan superar las dificultades encontradas en el caso de los métodos convencionales. Con este fin se combinan estudios de escalado del tamaño de sitema con técnicas de "Histogram Reweighting" (HR). La aplicación de estos métodos se ha mostrado recientemente como mucho mejor fundamentada y precisa para el cálculo de puntos críticos de sistemas sencillos como es el caso del fluido de Lennard-Jones (LJ). En esta tesis, estas técnicas han sido combinadas con el objetivo de extender su aplicación a mezclas reales de interés industrial. Previamente a su aplicación a dichas mezclas reales, el fluido de Lennard-Jones, capaz de reproducir el comportamiento de fluidos sencillos como es el caso de argón o metano, ha sido tomado como referencia en un paso preliminar.

A partir de simulaciones realizadas en el colectivo gran canónico y recombinadas mediante la mencionada técnica de "Histogram Reweighting" se han obtenido los diagramas de fases tanto de fluidos puros como de mezclas binarias. A su vez se han localizado con una gran precisión los puntos críticos de dichos sistemas mediante las técnicas de escalado del tamaño de sistema. Con el fin de extender la aplicación de dichas técnicas a sistemas multicomponente, se han introducido modificaciones a los métodos de HR evitando la construcción de histogramas y el consecuente uso de recursos de memoria. Además, se ha introducido una metodología alternativa, conocida como el cálculo del cumulante de cuarto orden o parametro de Binder, con el fin de hacer más directa la localización del punto crítico. En particular, se pro-

UNIVERSITAT ROVIRA I VIRGILI
IMPROVEMENT OF MONTE CARLO ALGORITHMS AND INTERMOLECULAR POTENCIALS FOR THE MODELLING OF ALKANOLS, ESTHERS, TRIOPHENES AND AROMATICS
Javier Pérez Pellitero
ISBN: 978-84-691-0377-7/DL: T.2195-2007

ponen dos posibilidades, en primer lugar la intersección del parámetro de Binder para dos tamaños de sistema diferentes, o la intersección del parámetro de Binder con el valor conocido de la correspondiente clase de universalidad combinado con estudios de escalado.

Por otro lado, y en un segundo frente, la segunda parte de esta tesis está dedicada al desarrollo de potenciales intermoleculares capaces de describir las energías inter e intramoleculares de las moléculas involucradas en las simulaciones. En la última década se han desarrolldo diferentes modelos de potenciales para una gran variedad de compuestos. Uno de los más comunmente utilizados para representar hidrocarburos y otras moléculas flexibles es el de átomos unidos, donde cada grupo químico es representado por un potencial del tipo de Lennard-Jones. El uso de este tipo de potencial resulta en una significativa disminución del tiempo de cálculo cuando se compara con modelos que consideran la presencia explícita de la totalidad de los átomos. En particular, el trabajo realizado en esta tesis se centra en el desarrollo de potenciales de átomos unidos anisotrópicos (AUA), que se caracterizan por la inclusión de un desplazamiento de los centros de Lennard-Jones en dirección a los hidrógenos de cada grupo, de manera que esta distancia se convierte en un tercer parámetro ajustable junto a los dos del potencial de Lennard-Jones.

En la segunda parte de esta tesis se han desarrollado potenciales del tipo AUA-4 para diferentes familias de compuesto que resultan de interés industrial como son los tiofenos, alcanoles y éteres. En el caso de los tiofenos este interés es debido a las cada vez más exigentes restricciones medioambientales que obligan a eliminar los compuestos con presencia de azufre. De aquí la

UNIVERSITAT ROVIRA I VIRGILI
IMPROVEMENT OF MONTE CARLO ALGORITHMS AND INTERMOLECULAR POTENCIALS FOR THE MODELLING OF ALKANOLS, ESTHERS, TRIOPHENES AND AROMATICS
Javier Pérez Pellitero
ISBN: 978-84-691-0377-7/DL: T.2195-2007

creciente de necesidad de propiedades termodinámicas para esta familia de compuestos para la cual solo existe una cantidad de datos termodinámicos experimentales limitada. Con el fin de hacer posible la obtención de dichos datos a través de la simulación molecular hemos extendido el potencial intermolecular AUA-4 a esta familia de compuestos. En segundo lugar, el uso de los compuestos oxigenados en el campo de los biocombustibles ha despertado un importante interés en la industria petroquímica por estos compuestos. En particular, los alcoholes más utilizados en la elaboración de los biocombustibles son el metanol y el etanol. Como en el caso de los tiofenos, hemos extendido el potencial AUA-4 a esta familia de compuestos mediante la parametrización del grupo hidroxil y la inclusión de un grupo de cargas electrostáticas optimizadas de manera que reproduzcan de la mejor manera posible el potencial electrostático creado por una molecula de referencia en el vacío. Finalmente, y de manera análoga al caso de los alcanoles, el último capítulo de esta tesis la atención se centra en el desarrollo de un potencial AUA-4 capaz de reproducir cuantitativamente las propiedades de coexistencia de la familia de los éteres, compuestos que son ampliamente utilizados como solventes.

UNIVERSITAT ROVIRA I VIRGILI
IMPROVEMENT OF MONTE CARLO ALGORITHMS AND INTERMOLECULAR POTENCIALS FOR THE MODELLING OF ALKANOLS, ESTHERS, TRIOPHENES AND AROMATICS
Javier Pérez Pellitero
ISBN: 978-84-691-0377-7/DL: T.2195-2007

Contents

UNIVERSITAT ROVIRA I VIRGILI
IMPROVEMENT OF MONTE CARLO ALGORITHMS AND INTERMOLECULAR POTENCIALS FOR THE MODELLING OF ALKANOLS, ESTHERS, TRIOPHENES AND AROMATICS
Javier Pérez Pellitero
ISBN: 978-84-691-0377-7/DL: T.2195-2007

UNIVERSITAT ROVIRA I VIRGILI
IMPROVEMENT OF MONTE CARLO ALGORITHMS AND INTERMOLECULAR POTENCIALS FOR THE MODELLING OF ALKANOLS, ESTHERS, TRIOPHENES AND AROMATICS
Javier Pérez Pellitero
ISBN: 978-84-691-0377-7/DL: T.2195-2007

UNIVERSITAT ROVIRA I VIRGILI
IMPROVEMENT OF MONTE CARLO ALGORITHMS AND INTERMOLECULAR POTENCIALS FOR THE MODELLING OF ALKANOLS, ESTHERS, TRIOPHENES AND AROMATICS
Javier Pérez Pellitero
ISBN: 978-84-691-0377-7/DL: T.2195-2007

UNIVERSITAT ROVIRA I VIRGILI
IMPROVEMENT OF MONTE CARLO ALGORITHMS AND INTERMOLECULAR POTENCIALS FOR THE MODELLING OF ALKANOLS, ESTHERS, TRIOPHENES AND AROMATICS
Javier Pérez Pellitero
ISBN: 978-84-691-0377-7/DL: T.2195-2007

List of Figures

UNIVERSITAT ROVIRA I VIRGILI
IMPROVEMENT OF MONTE CARLO ALGORITHMS AND INTERMOLECULAR POTENCIALS FOR THE MODELLING OF ALKANOLS, ESTHERS, TRIOPHENES AND AROMATICS
Javier Pérez Pellitero
ISBN: 978-84-691-0377-7/DL: T.2195-2007

UNIVERSITAT ROVIRA I VIRGILI
IMPROVEMENT OF MONTE CARLO ALGORITHMS AND INTERMOLECULAR POTENCIALS FOR THE MODELLING OF ALKANOLS, ESTHERS, TRIOPHENES AND AROMATICS
Javier Pérez Pellitero
ISBN: 978-84-691-0377-7/DL: T.2195-2007

UNIVERSITAT ROVIRA I VIRGILI
IMPROVEMENT OF MONTE CARLO ALGORITHMS AND INTERMOLECULAR POTENCIALS FOR THE MODELLING OF ALKANOLS, ESTHERS, TRIOPHENES AND AROMATICS
Javier Pérez Pellitero
ISBN: 978-84-691-0377-7/DL: T.2195-2007

UNIVERSITAT ROVIRA I VIRGILI
IMPROVEMENT OF MONTE CARLO ALGORITHMS AND INTERMOLECULAR POTENCIALS FOR THE MODELLING OF ALKANOLS, ESTHERS, TRIOPHENES AND AROMATICS
Javier Pérez Pellitero
ISBN: 978-84-691-0377-7/DL: T.2195-2007

List of Tables

UNIVERSITAT ROVIRA I VIRGILI
IMPROVEMENT OF MONTE CARLO ALGORITHMS AND INTERMOLECULAR POTENCIALS FOR THE MODELLING OF ALKANOLS, ESTHERS, TRIOPHENES AND AROMATICS
Javier Pérez Pellitero
ISBN: 978-84-691-0377-7/DL: T.2195-2007

UNIVERSITAT ROVIRA I VIRGILI
IMPROVEMENT OF MONTE CARLO ALGORITHMS AND INTERMOLECULAR POTENCIALS FOR THE MODELLING OF ALKANOLS, ESTHERS, TRIOPHENES AND AROMATICS
Javier Pérez Pellitero
ISBN: 978-84-691-0377-7/DL: T.2195-2007

Introduction

Parallel with the increase of computer speed, in the last decade, molecular simulation techniques have emerged as important tools to predict physical properties of systems of industrial interest. These properties are essential in the chemical and petrochemical industries in order to perform process design, optimization, simulation and process control. The actual moderate cost of powerful computers converts molecular simulation into an excellent tool to provide predictions of such properties. In particular, the predictive capability of molecular simulation techniques becomes very important when dealing with extreme conditions of temperature and pressure as well as when toxic compounds are involved in the systems to be studied due to the fact that experimentation at such extreme conditions is difficult and expensive.

Consequently, alternative processes must be considered in order to obtain the required properties. Chemical and petrochemical industries have made intensive use of thermophysical models including equations of state [1] [2] [3], activity coefficients models [4] and corresponding state theories [5]. These predictions present the advantage of providing good approximations with minimal computational needs. However, these models are often inadequate when only a limited amount of information is available to determine the necesary parameters, or when trying to reproduce complex fluid properties such as that of molecules which exhibit hydrogen bonding, polymers, etc. In addition, there is no way for dynamical properties to be estimated in a consistent manner.

UNIVERSITAT ROVIRA I VIRGILI
IMPROVEMENT OF MONTE CARLO ALGORITHMS AND INTERMOLECULAR POTENCIALS FOR THE MODELLING OF ALKANOLS, ESTHERS, TRIOPHENES AND AROMATICS
Javier Pérez Pellitero
ISBN: 978-84-691-0377-7/DL: T.2195-2007

Molecular simulation provides an alternative way to provide equilibrium and dynamic properties. The term "molecular simulation" refers to computational methods in which the molecular structure is explicitly taken into account and presents the advantage of providing a unified theoretical framework based on statistical mechanics to model fluid properties for industrial applications. In principle, it is possible to model every kind of molecule at any temperature or pressure in any mixture. Depending on the type of problem to be addressed, molecular structure can be specified either at very high resolution with every single electron, or at coarser levels where the smallest particles represent atoms or parts of the molecules. In this way molecular simulation is clearly intimately related with the field of nanotechnology.

In order to calculate thermodynamic properties, one of the main objectives of this work, only molecular structures at the coarser level are considered, that is atoms or groups of atoms. To address the calculation of thermophysical properties, two molecular simulation techniques can be emphasized: molecular dynamics (MD), in which the equations of motion are solved to obtain equilibrium as well as transport properties [6], and Monte Carlo (MC) simulation which focuses on the equilibrium properties through the use of statistical methods. Although, unlike molecular dynamics, Monte Carlo techniques do not provide the user with information about the molecular process or trajectories of the molecules in the system they are generally more efficient for the calculation of phase equilibria or dealing with systems exhibiting high relaxation times, i.e those having low diffusion coefficients and high viscosities.

Despite the fact that since the appearance of the first computers, the growth of computer speed has been maintained, the applicability of both molecular dynamics and Monte Carlo simulation is constrained by the maximum number of particles in the system. Consequently, exploiting the full advantages of these techniques requires the development and improvement of simulation algorithms, which constitutes a key mission in the development of Monte Carlo techniques. In particular, the location of critical points is one of the cases where, despite their simplicity, conventional Monte Carlo techniques like the Gibbs Ensemble method [7], have difficulties to accurately locate the critical point. This is due to the strong density fluctuations characterizing the critical region [8][9]. The divergent correlation length for the energy and density makes it impossible to obtain directly simulation data in this region, due to the fact that the simulations are performed in a finite system where the correlation length is cut by the size of the simulation box.

UNIVERSITAT ROVIRA I VIRGILI
IMPROVEMENT OF MONTE CARLO ALGORITHMS AND INTERMOLECULAR POTENCIALS FOR THE MODELLING OF ALKANOLS, ESTHERS, TRIOPHENES AND AROMATICS
Javier Pérez Pellitero
ISBN: 978-84-691-0377-7/DL: T.2195-2007

Although the study of the critical points of mixtures is of great practical relevance, little work has been done until now. Monte Carlo(MC) simulation has been shown to be an effective tool to study the equilibrium properties of fluids[10][11] and algorithms such as the Gibbs ensemble Monte Carlo (GEMC)[7][12], have simplified the determination of phase coexistence properties. A simple procedure to determine the critical locus consists on applying scaling laws[13] to the data obtained with the GEMC algorithm. However this methodology usually results in an overestimation of the critical temperature because of the appearance of the large density fluctuations mentioned before. Although direct simulations are not possible in the vicinity of the critical point, molecular simulation adequately represents the near-critical scaling behavior providing a highly effective route to the thermodynamic limit from simulations of finite size. In this way, finite size scaling studies [14](FSS) combined with histogram reweighting (HR) techniques [15][16] have been recently shown as much more precise and well founded methodologies for the calculation of the critical point of simple fluids and binary mixtures such as the Lennard-Jones (LJ) fluid. The LJ fluid is considered as a reference model to test and analyze new methodologies and furthermore its use allows to simulate accurately atomistic fluids, and have been the subject of a number of theoretical and simulation studies. For instance, Wilding and Bruce[17] used FSS to estimate the critical constants of the LJ fluid. Also other works have been done later [18][19] but only Potoff and Panagiotopoulos [20] have extended the analysis to simple binary mixtures.

In this thesis, the HR and FSS techniques are combined with the main goal of extending the application of these methodologies to the calculation of the vapor-liquid equilibrium and critical point of real mixtures. Before applying the methodologies to the real mixtures of industrial interest, the Lennard-Jones fluid has been taken as a reference model and as a preliminary step. In this case, the predictions are affected only by the omnipresent statistical errors, but not by the accuracy of the model chosen to reproduce the behavior of the real molecules or the interatomic potential [21] used to calculate the configurational energy of the system.

The simulations have been performed in the grand canonical ensemble (GCMC)using the GIBBS code [22]. Liquid-vapor coexistences curves have been obtained from HR techniques for pure fluids and binary mixtures, while critical parameters were obtained from FSS in order to close the phase envelope of the phase diagrams. In order to extend the calculations to multicomponent systems modifications to the conventional HR techniques have been introduced in order to avoid the construction of histograms and the consequent need for large memory resources. In addition an alternative methodol-

UNIVERSITAT ROVIRA I VIRGILI
IMPROVEMENT OF MONTE CARLO ALGORITHMS AND INTERMOLECULAR POTENCIALS FOR THE MODELLING OF ALKANOLS, ESTHERS, TRIOPHENES AND AROMATICS
Javier Pérez Pellitero
ISBN: 978-84-691-0377-7/DL: T.2195-2007

ogy known as the fourth order cumulant calculation [23], also known as the Binder parameter, has been implemented to make the location of the critical point more straightforward. In particular, we propose the use of the fourth order cumulant calculation considering two different possibilities: either the intersection of the Binder parameter for two different system sizes or the intersection of the Binder parameter with the known value for the system universality class combined with a FSS study.

The development of transferable potential models able to describe the inter and intra-molecular energies of the molecules involved in the simulations constitutes an important field in the improvement of Monte Carlo techniques. In the last decade, potential models, also referred to as force fields, have been developed for a wide range of compounds[24, 10, 25]. One of the most common approaches for modeling hydrocarbons and other flexible molecules is the use of the united-atoms model, where each chemical group is represented by one Lennard-Jones center. This scheme results in a significant reduction of the computational time as compared to all-atoms models since the number of pair interactions goes as the square of the number of sites. Improvements on the standard united-atoms model, where typically a 6-12 Lennard-Jones center of force is placed on top of the most significant atom, have been proposed. For instance, Errington *et al.* have used a Buckingham exp-6 potential [26], where 3 parameters are involved in each center of force and the repulsive part of the LJ interaction is replaced by an exponential term. Chen *et al.* have introduced additional sites on the centers of the C-H bonds[27]. Also, Ungerer *et al.* [28] have obtained the AUA 4 model by reparameterizing the initial Anisotropic United Atom (AUA) model proposed by Toxvaerd[29] [30]. The AUA model consists of a displacement of the Lennard-Jones centers of force towards the hydrogen atoms, converting the distance of displacement into a third adjustable parameter.

In this thesis we have developed AUA 4 intermolecular potentials for three different families of compounds. The family of ethers is of great importance due to their applications as solvents. The other two families, thiophenes and alkanols, play an important roles in the oil and gas industry. Thiophene due to current and future environmental restrictions and alkanols due ever higher importance and presence of biofuels in this industry.

In the case of thiophenes, due to the increasing requirements for sulfur removal from fuel, there has been a constant growth of interest in these compounds in the petroleum industry. The reason for lowering sulfur level include the environmental effects of acid rain so produced when sulfur com-

UNIVERSITAT ROVIRA I VIRGILI
IMPROVEMENT OF MONTE CARLO ALGORITHMS AND INTERMOLECULAR POTENCIALS FOR THE MODELLING OF ALKANOLS, ESTHERS, TRIOPHENES AND AROMATICS
Javier Pérez Pellitero
ISBN: 978-84-691-0377-7/DL: T.2195-2007

pounds are emitted to the atmosphere, oxidized to sulfur oxides, and later scavenged by atmospheric precipitation as sulfuric acid. Sulfur containing molecules must either be removed or converted into hydrocarbons and H_2S in order to accomplish the strict limits in sulfur emissions imposed by the environmental laws. Since the family of thiophenes is much more resistant than thiols or sulfides to known conversion processes, adsorption is currently being considered as an alternative. In particular, the most difficult compounds to remove from liquid fuels are typically dibenzothiophene(DBT) and its derivatives [31]. Hence, there is a strong need for thermodynamic data for this compound for which only limited vapor-equilibrium data can be found in the literature. To supply this data, we obtain in Chapter 3 an optimized intermolecular potential for the sulfur group of the thiophene family aimed at giving a quantitative description of both liquid and coexistence properties, based on an extension of the AUA 4 intermolecular potentials already given in previous works[32, 28].

The increasing popularity of the use of oxygenated compounds in the field of biocombustibles has given rise to a strong interest in the family of alkanols in the petroleum industry. In particular, the simplest and most commonly used alcohols in the elaboration of biodiesels are methanol and ethanol. In Chapter 4, we obtain an optimized intermolecular potential for the hydroxyl group of the alcohols family aimed at giving a quantitative description of both liquid and coexistence properties, based on an extension of the AUA 4 intermolecular potentials already given in previous works[32, 28]. Several models have been proposed to investigate the behavior of alkanols [33][34][35] mainly at ambient temperature and density. Vapor-liquid coexistence curves from methanol to hexanol have been obtained in [36], by combining the charges of the OPLS (optimized potential for liquid simulation) force field with the hydroxyl group Lennard-Jones (LJ) parameters derived by Van Leeuwen in [37] and the alkyl groups of the Siepmann-Karaborni-Smit(SKS) [38] force field. The OPLS force field was found to not to be transferable to high temperatures and longer chains. Despite the model of Van Leeuwen behaves much better, it requires the methyl groups of the different alcohols to be specifically readapted. More recently, in 2001 Chen *et al* [39] have extended the TraPPE [25](Transferable Potentials for Phase Equilibria) force field to several primary, secondary and tertiary alcohols. In this work, we obtain an optimized intermolecular potential and electrostatic set of charges for the hydroxyl group of the alcohols family aimed at giving a quantitative description of the coexistence properties, based on an extension of the AUA 4 intermolecular potentials. Our aim is to keep using the same set of LJ parameters for the alkyl chain as the previously optimized for alkanes, without the need of defining additional "pseudo-atoms".

UNIVERSITAT ROVIRA I VIRGILI
IMPROVEMENT OF MONTE CARLO ALGORITHMS AND INTERMOLECULAR POTENCIALS FOR THE MODELLING OF ALKANOLS, ESTHERS, TRIOPHENES AND AROMATICS
Javier Pérez Pellitero
ISBN: 978-84-691-0377-7/DL: T.2195-2007

Finally in Chapter 5, we devote our attention to the extension of the AUA 4 intermolecular potentials to the family of ethers, which are widely used as solvents. As in the case of alkanols, a set of electrostatic charges is proposed to reproduce the electrostatic potential of such compounds prior to the optimization of the oxygen group Lennard-Jones parameters.

UNIVERSITAT ROVIRA I VIRGILI
IMPROVEMENT OF MONTE CARLO ALGORITHMS AND INTERMOLECULAR POTENCIALS FOR THE MODELLING OF ALKANOLS, ESTHERS, TRIOPHENES AND AROMATICS
Javier Pérez Pellitero
ISBN: 978-84-691-0377-7/DL: T.2195-2007

Chapter 1

FUNDAMENTALS

UNIVERSITAT ROVIRA I VIRGILI
IMPROVEMENT OF MONTE CARLO ALGORITHMS AND INTERMOLECULAR POTENCIALS FOR THE MODELLING OF ALKANOLS, ESTHERS, TRIOPHENES AND AROMATICS
Javier Pérez Pellitero
ISBN: 978-84-691-0377-7/DL: T.2195-2007

1.1 Statistical Mechanics

Statistical mechanics is primarily concerned with the calculation of properties of condensed matter sytems. It constitutes the application of statistics, which includes mathematical tools for dealing with large populations, to the field of mechanics, which is concerned with the motion of particles or objects when subjected to a force. It provides a framework for relating the microscopic properties of individual atoms and molecules to the macroscopic or bulk properties of materials that can be observed in everyday life, therefore explaining thermodynamics as a natural result of statistics and mechanics (classical and quantum) at the microscopic level. Instead of looking for exact solutions, we deal with the probabilities of the system being in one state or another, hence the name statistical mechanics. The fundamental postulate in statistical mechanics (also known as the equal a priori probability postulate) holds the following:

Given an isolated system in equilibrium, it is found with equal probability in each of its accessible microstates.

This postulate is a fundamental assumption in statistical mechanics. It states that a system in equilibrium does not have any preference for any of its available microstates. Given Ω microstates at a particular energy, the probability of finding the system in a particular microstate is

$$p = 1/\Omega \tag{1.1}$$

This postulate is necessary because it allows one to conclude that for a system at equilibrium, the thermodynamic state (macrostate) which could result from the largest number of microstates is also the most probable macrostate of the system.

1.2 Statistical Thermodynamics

Statistical thermodynamics is based on the fundamental assumption that all possible configurations of a given system, which satisfy the given boundary

UNIVERSITAT ROVIRA I VIRGILI
IMPROVEMENT OF MONTE CARLO ALGORITHMS AND INTERMOLECULAR POTENCIALS FOR THE MODELLING OF ALKANOLS, ESTHERS, TRIOPHENES AND AROMATICS
Javier Pérez Pellitero
ISBN: 978-84-691-0377-7/DL: T.2195-2007

conditions such as energy, volume and number of particles, are equally likely to occur. The overall system will therefore be in the statistically most probable configuration. Statistical thermodynamics is the study of the microscopic behavior of thermodynamic systems using probability theory. Statistical thermodynamics, generally, provides a molecular level interpretation of thermodynamic quantities such as work, heat, free energy, and entropy. The goal of statistical thermodynamics is to understand and to interpret the measurable macroscopic properties of materials in terms of the properties of their constituent particles and the interactions between them.

This is done by connecting thermodynamic functions to quantum-mechanic equations. As an example, from a classical thermodynamics point of view we might ask what is it about a thermodynamic system of gas molecules, such as methane CH_4, that determines the free energy characteristic of that compound? Classical thermodynamics does not provide the answer. If, for example, we were given spectroscopic data, of this body of gas molecules, such as bond length, bond angle, bond rotation, and flexibility of the bonds in CH_4 we should see that the free energy could not be other than it is. To prove this true, we need to bridge the gap between the microscopic realm of atoms and molecules and the macroscopic realm of classical thermodynamics. From physics, statistical mechanics provides such a bridge by teaching us how to conceive of a thermodynamic system as an assembly of units. More specifically, it demonstrates how the thermodynamic parameters of a system, such as temperature and pressure, are interpretable in terms of the parameters descriptive of such constituent atoms and molecules.

1.3 Statistical Ensembles

1.3.1 Canonical Ensemble

In the canonical ensemble, also known as the NVT ensemble, the number of particles, volume and temperature are fixed for all systems belonging to the same ensemble. Temperature is fixed by bringing the different systems in contact with a large heat bath. The quantity

$$Q(N,V,T) \equiv \frac{1}{N!h^{3N}} \int d\overrightarrow{r}\, d\overrightarrow{p}\, e^{-E(\overrightarrow{r},\overrightarrow{p})/k_BT} \tag{1.2}$$

UNIVERSITAT ROVIRA I VIRGILI
IMPROVEMENT OF MONTE CARLO ALGORITHMS AND INTERMOLECULAR POTENCIALS FOR THE MODELLING OF ALKANOLS, ESTHERS, TRIOPHENES AND AROMATICS
Javier Pérez Pellitero
ISBN: 978-84-691-0377-7/DL: T.2195-2007

is called the canonical partition function. Taking into account that the total energy of the system can be also expressed as a sum of the kinetic and potential contributions, it can be also written as the product of the kinetic (ideal gas) and potential(excess) parts:

$$Q(N,V,T) = Q^{id}_{NVT} Q^{ex}_{NVT} \tag{1.3}$$

where for an atomic system:

$$Q^{id}_{NVT} = \frac{V^N}{N!\Lambda^{3N}} \tag{1.4}$$

being Λ the thermal de Broglie wavelength:

$$\Lambda^2 = \frac{h^2}{2\pi mkT} \tag{1.5}$$

For the excess part, we can write:

$$Q^{ex}_{NVT} = \frac{1}{V^N} \int d\overrightarrow{r}\, e^{-U(\overrightarrow{r})/k_B T} \tag{1.6}$$

First of all, the partition function is a normalizing factor in the calculation of averages over the canonical ensemble. For example, the internal energy may be written as

$$U \equiv \langle E \rangle = \frac{1}{Q(N,V,T)} \frac{1}{N!h^{3N}} \int d\overrightarrow{r}\, d\overrightarrow{p}\, E e^{-E(\overrightarrow{r},\overrightarrow{p})/k_B T} \tag{1.7}$$

But the great practical importance of the partition function stems from its close relation to Helmholtz free energy $A(N,V,T)$, which itself is a central object of thermodynamics. The relation between the two is

$$Q(N,V,T) = e^{-\beta A(N,V,T)} \tag{1.8}$$

UNIVERSITAT ROVIRA I VIRGILI
IMPROVEMENT OF MONTE CARLO ALGORITHMS AND INTERMOLECULAR POTENCIALS FOR THE MODELLING OF ALKANOLS, ESTHERS, TRIOPHENES AND AROMATICS
Javier Pérez Pellitero
ISBN: 978-84-691-0377-7/DL: T.2195-2007

where $\beta \equiv 1/kT$. We can prove this from the identity $dlnx/dx = 1/x$ and the chain rule for differentiation, we then see that Eqn. 1.7 implies

$$U \equiv \langle E \rangle = - \left(\frac{\partial}{\partial \frac{1}{kT}} ln \frac{1}{N! h^{3N}} \int d\overrightarrow{r}\, d\overrightarrow{p}\, e^{-E(\overrightarrow{r},\overrightarrow{p})/k_B T} \right)_{V,N} \tag{1.9}$$

The argument of the logarithm in Eqn. 1.9 is the partition function defined in Eqn. 1.2. Equation 1.9 is then

$$U = -k \left[\frac{\partial ln Q(N,V,T)}{\partial (1/T)} \right]_{V,N} \tag{1.10}$$

The last expression can be compared with the Gibbs-HelmHoltz equation of thermodynamics:

$$U = \left[\frac{\partial (A/T)}{\partial (1/T)} \right]_{V,N} \tag{1.11}$$

where A is the HelmHoltz free energy. This lead us to the next expression relating the free energy A and the partition function $Q(N,V,T)$

$$A = -kT ln Q(N,V,T) + T\phi(V,N) \tag{1.12}$$

where $\phi(V,N)$ is an unknown function of those variables that are fixed in the differentiations in Eqns. 1.9 and 1.11. In [40] it is shown that ϕ is independent of the volume and it is associated with an arbitrary choice for the zero of entropy. Following the universally accepted convention of taking that arbitrary function of N to be zero we obtain:

$$A = -kT ln Q(N,V,T) \tag{1.13}$$

All other thermodynamic quantities may now be obtained from $A(N,V,T)$.

UNIVERSITAT ROVIRA I VIRGILI
IMPROVEMENT OF MONTE CARLO ALGORITHMS AND INTERMOLECULAR POTENCIALS FOR THE MODELLING OF ALKANOLS, ESTHERS, TRIOPHENES AND AROMATICS
Javier Pérez Pellitero
ISBN: 978-84-691-0377-7/DL: T.2195-2007

For instance, the pressure is given by

$$P = -\left(\frac{\partial A}{\partial V}\right)_T \tag{1.14}$$

Similarly, entropy and Gibbs' free energy are calculated from

$$S = -\left(\frac{\partial A}{\partial T}\right)_V \quad \text{and} \quad G = A + PV \tag{1.15}$$

1.3.2 Grand Canonical Ensemble

In the grand canonical ensemble, once again a small system is put in contact wit a large one. However, this time we do not only permit the exchange of energy but also the crossing over of particles from one subsystem to the other.

As before, we can write down the probability density in the phase space of the smaller system; it depends now both on the number of particles N and on $\{\vec{r}_i, \vec{p}_i; i = 1, \dots N\}$, as follows:

$$p(\vec{r}, \vec{p}; N) \propto e^{\mu N/kT} e^{-E(\vec{r},\vec{p})/kT} \tag{1.16}$$

Summing this density over all possible values of N and integrating - at each N - over all $\{\vec{r}_i, \vec{p}_i; i = 1, \dots N\}$ we obtain the grand partition function

$$\Xi(\mu, V, T) \equiv \sum_{N=0}^{\infty} e^{N\mu/kT} Q(N, V, T) \tag{1.17}$$

The appropriate thermodynamic function in this case is PV:

$$PV = kTln\Xi(\mu, V, T) \tag{1.18}$$

1.3.3 Isothermal-Isobaric (NPT) Ensemble

In the isothermal-isobaric ensemble the probability density is proportional to

UNIVERSITAT ROVIRA I VIRGILI
IMPROVEMENT OF MONTE CARLO ALGORITHMS AND INTERMOLECULAR POTENCIALS FOR THE MODELLING OF ALKANOLS, ESTHERS, TRIOPHENES AND AROMATICS
Javier Pérez Pellitero
ISBN: 978-84-691-0377-7/DL: T.2195-2007

$$p(\vec{r},\vec{p};N) \propto e^{-(E(\vec{r},\vec{p})+PV)/kT} \tag{1.19}$$

The quantity appearing in the exponent, when averaged, gives the thermodynamic enthalpy $H = \langle E(\vec{r},\vec{p})\rangle + P\langle V\rangle$. In this case the appropriate partition function is:

$$Q(N,P,T) = \sum_{\Gamma}\sum_{V} e^{-(E(\vec{r},\vec{p})+PV)/kT} = \sum_{V} e^{-PV/kT} Q_{N,V,T} \tag{1.20}$$

where the volume has now joined the list of microscopic quantities comprising the state point Γ. That is why the partition function includes the summation over all possible volumes:

This summation can also be written as an integral, choosing some basic unit V_0 to make $Q(N,P,T)$ dimensionless. Finally, in quasi-classical form we can write for an atomic system:

$$Q(N,P,T) = \frac{1}{N!}\frac{1}{h^{3N}}\frac{1}{V_0}\int dV \int drdp e^{-(E(\vec{r},\vec{p})+PV)/kT} \tag{1.21}$$

The Gibbs free energy G is in this case the corresponding thermodynamic function:

1.3.4 Gibbs Ensemble

In molecular simulation, first-order phase transitions are often located by computing the thermodynamic properties of the individual phases, then finding the point where the temperature, pressure and chemical potentials of both phases are equal. This way of proceeding has the limitation that the two coexisting phases have a relatively large fraction of particles residing in or near the interface which divides both phases. The fraction of particles in the interface depends on the system size which forces the use of large systems if accurate equilibrium properties are required. Unfortunately, for such large systems, long equilibration times are needed, not only because the systems contain many particles, but also because equilibration times in two-phase systems tend to be longer than those in homogeneous systems. That is why in the mid-1980s Panagiotopoulos [7] devised a new computational method, usually

UNIVERSITAT ROVIRA I VIRGILI
IMPROVEMENT OF MONTE CARLO ALGORITHMS AND INTERMOLECULAR POTENCIALS FOR THE MODELLING OF ALKANOLS, ESTHERS, TRIOPHENES AND AROMATICS
Javier Pérez Pellitero
ISBN: 978-84-691-0377-7/DL: T.2195-2007

referred to as the *Gibbs ensemble method* which resulted in a very significant reduction of the computational time and became at present the most used technique to study vapor-liquid and liquid-liquid equilibria.

The success of the Gibbs ensemble method relies on the possibility of exchanging particles between the two coexisting phases which are simulated in different boxes. Particularly, the main disadvantage of this method appears, as in the case of the Grand Canonical ensemble, when the efficiency of these insertions decreases, being not very efficient at low temperatures or for very dense liquid phases.

The necessary condition for the coexistence of two or more phases $I, II, \ldots$ is the equality of pressures $P_I = P_{II} = \ldots = P$, temperatures $T_I = T_{II} = \ldots = T$ and chemical potentials of all species $\mu_I^\alpha = \mu_{II}^\alpha = \ldots = \mu^\alpha$. Although one could think that the best ensemble to simulate phase equilibria would be at constant chemical potential, pressure and temperature, this ensemble does not exist because only intensive parameters are fixed. This means that the extensive parameters are unbounded. As we have seen in previous sections, this variable is the total number of particles N in the case of the isothermal-isobaric ensemble or the volume V in the grand canonical ensemble. The reason why the Gibbs ensemble is able to simulate phase equilibria, is that despite the differences between chemical potentials in the different phases $\Delta\mu = 0$, the absolute values are not determined.

The Gibbs ensemble method can be derived following the same approach developed in the previous sections. We focus on the version of the Gibbs ensemble where the total number of particles and total volumes are fixed; that is, the total system is at N, V, T conditions. The description of the alternative N, P, T version can be found in [41]

For a system of N particles distributed over two volumes V_1 and $V_2 = V - V_1$, we can write the expression for the partition function where the particles interact with each other in volume 1 but behave like an ideal gas in volume 2:

$$Q(N, V_1, V_2, T) = \sum_{n_1=0}^{N} \int ds_2^{N-n_1} \int ds_1^{n_1} exp[-\beta U(s_1^{n_1})] \tag{1.22}$$

Now we consider the case that the particles in both volumes are subject to the same intermolecular interactions and that the volumes V_1 and V_2 can

UNIVERSITAT ROVIRA I VIRGILI
IMPROVEMENT OF MONTE CARLO ALGORITHMS AND INTERMOLECULAR POTENCIALS FOR THE MODELLING OF ALKANOLS, ESTHERS, TRIOPHENES AND AROMATICS
Javier Pérez Pellitero
ISBN: 978-84-691-0377-7/DL: T.2195-2007

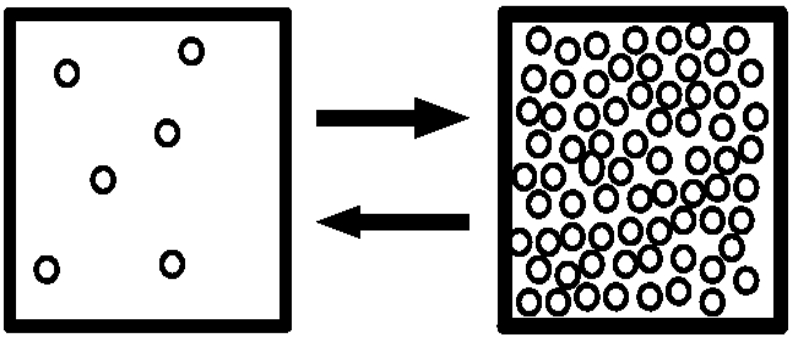

Figure 1.1: Scheme of the Gibbs ensemble method in which two systems can exchange both volume and particles in such a way that the total volume V and the total number of particles N are conserved

change subject to the restriction that the sum of the volumes $V = V_1 + V_2$ remains constant, where the two volumes correspond to those of the simulation boxes which are schematically shown in figure 1.1. In this case, we have to integrate over the volume V_1 which gives the next expression for the partition function [42] [43]:

$$Q_{GIBBS}(N,V,T) \equiv \sum_{n_1=0}^{N} \frac{1}{V\Lambda^{3N} n_1!(N-n_1)!} \int_0^V dV_1 V_1^{n_1}(V-V_1)^{N-n_1} \times \times \int ds_1^{n_1} exp[-\beta U(s_1^{n_1})] \int ds_2^{N-n_1} exp[-\beta U(s_2^{N-n_1})] \tag{1.23}$$

According to these expressions it follows that the probability of finding a configuration with n_1 particles in box 1 with a volume V_1 and positions $s_1^{n_1}$ and $s_2^{N-n_1}$ is given by:

$$p(n_1, V_1, s_1^{n_1}, s_2^{N-n_1}) \propto \frac{V_1^{N_1(V-V_1)^{N-n_1}}}{n_1!(N-n_1)!} exp\left(-\beta[U(s_1^{n_1}) + U(s_2^{N-n_1})]\right) \tag{1.24}$$

UNIVERSITAT ROVIRA I VIRGILI
IMPROVEMENT OF MONTE CARLO ALGORITHMS AND INTERMOLECULAR POTENCIALS FOR THE MODELLING OF ALKANOLS, ESTHERS, TRIOPHENES AND AROMATICS
Javier Pérez Pellitero
ISBN: 978-84-691-0377-7/DL: T.2195-2007

1.4 Monte Carlo methods

Monte Carlo methods are a widely used class of computational algorithms for simulating the behavior of various physical and mathematical systems, and for other computations. They are distinguished from other simulation methods (such as molecular dynamics) by being stochastic, that is nondeterministic by using random or pseudo-random numbers as opposed to deterministic algorithms.

Monte Carlo simulation methods are especially useful in studying systems with a large number of coupled degrees of freedom, such as liquids, disordered materials, strongly coupled solids, and cellular structures. More broadly, Monte Carlo methods are useful for modeling phenomena with significant uncertainty in inputs, such as the calculation of risk in business. A classic use is for the evaluation of definite integrals, particularly multidimensional integrals with complicated boundary conditions.

1.4.1 Monte Carlo integration

In mathematics, Monte Carlo (MC) integration is numerical quadrature using pseudo-random numbers. That is, Monte Carlo integration methods are algorithms for the approximate evaluation of definite integrals, usually multidimensional ones. The usual algorithms evaluate the integrand at a regular grid. Monte Carlo methods, however, randomly choose the points at which the integrand is evaluated.

The traditional Monte Carlo algorithm distributes the evaluation points uniformly over the integration region.

The algorithm computes an estimate of a multidimensional definite integral of the form,

$$I = \int_{x_l}^{x_u} \int_{y_l}^{y_u} f(x, y, \ldots)\, dx\, dy \ldots = \int_V f(x, y, \ldots)\, dx\, dy \ldots \tag{1.25}$$

over the hypercube with volume V defined by $.(x, y, ...)|x_l \leq x \leq x_u, y_l \leq y \leq y_u, ...$ The basic Monte Carlo algorithm samples points uniformly from

UNIVERSITAT ROVIRA I VIRGILI
IMPROVEMENT OF MONTE CARLO ALGORITHMS AND INTERMOLECULAR POTENCIALS FOR THE MODELLING OF ALKANOLS, ESTHERS, TRIOPHENES AND AROMATICS
Javier Pérez Pellitero
ISBN: 978-84-691-0377-7/DL: T.2195-2007

the integration region to estimate the integral and its error. Suppose that the sample has size N and denote the points in the sample by $x_1, ..., x_N$. Then the estimate for the integral is given by

$$E(f;N) = V \cdot \langle f \rangle = V \frac{1}{i_{max}} \sum_{i=1}^{i_{max}} f(x_i), \tag{1.26}$$

where $\langle f \rangle$ denotes the sample mean of the integrand.

The variance in this result can be estimated using

$$\sigma^2(E;N) = \frac{V}{N} \sum_{i=1}^{N} (f(x_i) - \langle f \rangle)^2. \tag{1.27}$$

The configurational integral of the canonical ensemble $Z(N,V,T) = \int drexp(-\beta E(r))$ can be estimated using

$$Z(N,V,T) \approx \frac{V^N}{i_{max}} \sum_{i=1}^{i_{max}} exp(-\beta E(i)) \tag{1.28}$$

In our case, for thermodynamic type functions, the use of conventional sample mean integration would result in having a large number of the trials that give a very small contribution to the average. An accurate estimation of $Z(N,V,T)$ for a dense liquid using a uniform sample mean method is beyond the capabilities of current computers as well as for the foreseeable future. However the problem can be solved using a sample mean integration where the random coordinates are chosen from a non-uniform distribution. In this way, techniques such as importance sampling are used to improve the results of the basic Monte Carlo algorithm

1.4.2 Importance sampling

Importance sampling techniques choose random configurations from a distribution $\rho(x)$ which allows the function evaluation to be concentrated in the region of space that makes a significant contribution to the integral. If we

UNIVERSITAT ROVIRA I VIRGILI
IMPROVEMENT OF MONTE CARLO ALGORITHMS AND INTERMOLECULAR POTENCIALS FOR THE MODELLING OF ALKANOLS, ESTHERS, TRIOPHENES AND AROMATICS
Javier Pérez Pellitero
ISBN: 978-84-691-0377-7/DL: T.2195-2007

consider the canonical ensemble, the desired integral is:

$$\langle A\rangle_{NVT} = \int drdp\rho_{NVT}(\vec{r},\vec{p})A(\vec{r},\vec{p}) \tag{1.29}$$

being the integrand $f = \rho_{NVT}A$. We can estimate the integral by choosing configurations at random from a chosen distribution ρ using:

$$\langle A\rangle_{NVT} = \left\langle \frac{A\rho_{NVT}}{\rho} \right\rangle_{trials} \tag{1.30}$$

For most fuctions $A(dr, dp)$, the integrand is significant only where the distribution of the ensemble ρ_{NVT} is significant. Then choosing $\rho = \rho_{NVT}$ gives a good estimate of the integral. In this case we can write:

$$\langle A\rangle_{NVT} = \langle A\rangle_{trials} \tag{1.31}$$

The difficulty lies now in how to generate a sequence of configurations so that by the end of the simulation each state has been generated with the appropriate probability. To do that, we use a Markov chain constructed in a way that its limiting distribution is ρ_{NVT}. A Markov chain is a generated sequence of trials satisfying the condition that the outcome of each trial depends only on the outcome of the previous trial. In natural systems, the physical variables take values according to the thermodynamic conditions of the system and the imposed constraints. There are different forms to generate these sequences of configurations, the most well known and popular is the Metropolis method, which is described in the next section:

1.4.3 The Metropolis method

The basic principle of the Metropolis method is to find the transition probability $\pi(o \to n)$ of taking the system from an old state o into any new state n. Supposing that the probability of finding the system in a state o is $\rho(o)$ and $\rho(n)$ for the state n, at the equilibrium the condition of detailed balance must be satisfied:

UNIVERSITAT ROVIRA I VIRGILI
IMPROVEMENT OF MONTE CARLO ALGORITHMS AND INTERMOLECULAR POTENCIALS FOR THE MODELLING OF ALKANOLS, ESTHERS, TRIOPHENES AND AROMATICS
Javier Pérez Pellitero
ISBN: 978-84-691-0377-7/DL: T.2195-2007

$$\rho(o)\pi(o \to n) = \rho(n)\pi(n \to o) \tag{1.32}$$

Metropolis *et al* suggested the first scheme to generate a suitable trajectory in the canonical ensemble. This solution is often known as the asymmetrical solution. This solution considers two cases for two different states o and n.

$$\pi_{on} = \alpha_{on} \qquad \rho_n \geq \rho_o \qquad o \neq n \tag{1.33}$$

$$\pi_{on} = \alpha_{on}\frac{\rho_n}{\rho_o} \qquad \rho_n < \rho_o \qquad o \neq n \tag{1.34}$$

where α_{on} is also known as the underlying matrix of the Markov chain

If the system remains in the same state:

$$\pi_{oo} = 1 - \sum_{n \neq o} \pi_{on} \tag{1.35}$$

The procedure to apply the Metropolis method is described next:

- In order to change the configuration of the system, a random movement is generated. For instance, a given atom i is chosen randomly and displaced from its position r_i^o to a new position r_i^n chosen with equal probability inside a given volume $\mathcal{V}$
- The appropriate element of the transition matrix depends on the relative probabilities of the initial and final states o and n. According to eqns 1.33 and 1.34, we consider two cases depending on the difference in configurational energy $\Delta U = U_n - U_o$:
  - If $\Delta U \leq 0$ then the probability of the new state n is greater than the probability of the old state o. Eqn 1.33 applies and the new configuration is accepted
  - If $\Delta U > 0$ then the probability of the new state n is lower than the probability of the old state o. Eqn 1.34 applies and the new configuration is accepted with a probability ρ_n/ρ_o by comparing this value with a number generated at random ξ in the interval (0,1). If

UNIVERSITAT ROVIRA I VIRGILI
IMPROVEMENT OF MONTE CARLO ALGORITHMS AND INTERMOLECULAR POTENCIALS FOR THE MODELLING OF ALKANOLS, ESTHERS, TRIOPHENES AND AROMATICS
Javier Pérez Pellitero
ISBN: 978-84-691-0377-7/DL: T.2195-2007

the new configuration is rejected the atom remains in the old position and the old configuration is recounted as a new state in the sequence of generated configurations.

A new configuration is generated while the average values of the different physical variables are calculated according to:

$$\langle A \rangle = \frac{1}{\mathcal{N}} \sum_{i=1}^{N} A(\Gamma_i) \tag{1.36}$$

where $\mathcal{N}$ is the total number of configurations generated during the simulation and $A(\Gamma_i)$ the value of the physical property A at the configuration i.

The Metropolis method ensures that the different configurations are generated according to the appropriate probabilities of these configurations. The algorithm makes use of a specific acceptance probabilty for each of the different ensembles as will be explained in the next section:

1.5 Simulations in the different ensembles

1.5.1 Simulations in the Canonical Ensemble

As described in section 1.3.1 in the canonical ensemble, the total volume V, number of particles N and temperature T are fixed by bringing the system in contact with a thermal bath. A scheme of this ensemble is shown in figure 1.2.

As can be inferred from eqn 1.6, in the canonical ensemble the probability of a given configuration Γ_i is given by:

$$\rho_{NVT}(r_i) \propto e^{-\beta U_i} \tag{1.37}$$

To generate the appropriate sequence of configurations in the canonical ensemble:

UNIVERSITAT ROVIRA I VIRGILI
IMPROVEMENT OF MONTE CARLO ALGORITHMS AND INTERMOLECULAR POTENCIALS FOR THE MODELLING OF ALKANOLS, ESTHERS, TRIOPHENES AND AROMATICS
Javier Pérez Pellitero
ISBN: 978-84-691-0377-7/DL: T.2195-2007

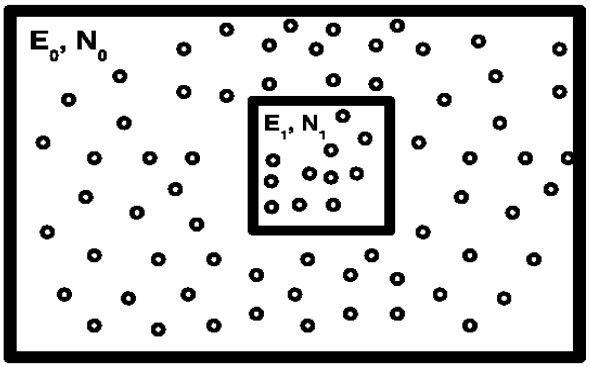

Figure 1.2: Scheme of the Canonical ensemble

- The energy U_o of the initial configuration o is calculated and then a particle of the system i is selected randomly
- A random displacement is proposed for the selected particle in the new configuration n according to:

$$r_i^n = r_i^o + \delta r_{max}(2\xi - 1) \tag{1.38}$$

where δr_{max} is the maximum displacement allowed and ξ a random number generate uniformly in the interval (0,1).

- The energy of the new configuration n is calculated and the movement accepted or rejected according to the ratio between the probabilities of both configurations. In the canonical ensemble, this ratio can be expressed as:

$$\frac{\rho_n}{\rho_o} = \frac{Q(NVT)^{-1}e^{(-\beta U_n)}}{Q(NVT)^{-1}e^{(-\beta U_o)}} = e^{[-\beta(U_n - U_o)]} = e^{(-\beta \delta U_{on})} \tag{1.39}$$

where δU_{on} is the energy difference between the old state o and the new state n.

UNIVERSITAT ROVIRA I VIRGILI
IMPROVEMENT OF MONTE CARLO ALGORITHMS AND INTERMOLECULAR POTENCIALS FOR THE MODELLING OF ALKANOLS, ESTHERS, TRIOPHENES AND AROMATICS
Javier Pérez Pellitero
ISBN: 978-84-691-0377-7/DL: T.2195-2007

1.5.2 Simulations in the Grand Canonical Ensemble

According to eqn. 1.17, in the case of the Grand Canonical ensemble the probability of a given configuration $\Gamma_{N,i}$ is:

$$\rho_{\mu VT}(\Gamma_{N,i}) \propto \frac{V^N e^{(\beta\mu N)}}{\Lambda^{3N} N!} e^{-\beta U_i} \tag{1.40}$$

The probability distribution is then sampled by means of three different movements:

- Displacement of a particle. In this case the movememt is accepted with a probabilty equal to eqn 1.39
- Destruction of a particle. In this case the ratio of the probabilities of the new state n with N particles and the old state o with $N-1$ particles is:

$$\frac{\rho_n}{\rho_o} = e^{-\beta\delta U_{on}} e^{-\beta\mu} \frac{N\Lambda^3}{V} \tag{1.41}$$

- Insertion of a particle. Now the ratio between the probabilities of the new state n with $N+1$ particles and the old state o with N particles is

$$\frac{\rho_n}{\rho_o} = e^{-\beta\delta U_{on}} e^{\beta\mu} \frac{V}{(N+1)\Lambda^3} \tag{1.42}$$

1.5.3 Simulations in the Isobaric-Isothermal (NPT) Ensemble

As can be inferred from eqn. 1.21 in the case of the isobaric-isothermal ensemble, the Metropolis method is implemented by generating a Markov chain of states which has a limiting distribution proportional to:

$$e^{-\beta(PV+U(s_i))+nlnV}$$

UNIVERSITAT ROVIRA I VIRGILI
IMPROVEMENT OF MONTE CARLO ALGORITHMS AND INTERMOLECULAR POTENCIALS FOR THE MODELLING OF ALKANOLS, ESTHERS, TRIOPHENES AND AROMATICS
Javier Pérez Pellitero
ISBN: 978-84-691-0377-7/DL: T.2195-2007

where $s = (s_1, s_2, \ldots, s_n)$ is the set of scaled coordinates:

$$s = \frac{r}{L}$$

and $L = V^{1/3}$. To generate the appropriate sequence of configurations in the isobaric-isothermal ensemble, two different moves are considered:

- Displacement of a particle. In this case the movememt is accepted with a probabilty equal to eqn 1.39
- Introduction of a volume change . In this case the ratio of the probabilities of the new state with volume V_n with N and the old state with volume V_o is:

$$\frac{\rho_n}{\rho_o} = e^{-\left[\beta[(U(s_n,V_n)-U(s_o,V_o)+P(V_n-V_o)]-Nln\left(\frac{V_n}{V_o}\right)\right]} \tag{1.43}$$

1.5.4 Simulations in the Gibbs Ensemble

To sample correctly all possible configurations of two systems that can exchange volume and particles, the next trial moves can be proposed according to equation 1.23. They are schematically shown in figure 1.3:

- Displacement of a randomly selected particle: in this case the acceptance rule is identical to that used in a conventional NVT ensemble simulation and the displacement is accepted with a probability according to eqn. 1.39
- Change of the volume of the boxes so that the total volume of the two boxes remains constant. In this case, for a change of the volume of box 1 by an amount ΔV, $V_1^n = V_1^o + \Delta V$, the ratio of the probabilities of the new state with volume V_1^n and the old state with volume V_1^o is:

$$\frac{\rho_n}{\rho_o} = e^{-\left[\beta[(U(s_n^N)-U(s_o^N)]\right]} \frac{(V_1^n)^{n_1}(V-V_1^n)^{N-n_1}}{(V_1^o)^{n_1}(V-V_1^o)^{N-n_1}} \tag{1.44}$$

UNIVERSITAT ROVIRA I VIRGILI
IMPROVEMENT OF MONTE CARLO ALGORITHMS AND INTERMOLECULAR POTENCIALS FOR THE MODELLING OF ALKANOLS, ESTHERS, TRIOPHENES AND AROMATICS
Javier Pérez Pellitero
ISBN: 978-84-691-0377-7/DL: T.2195-2007

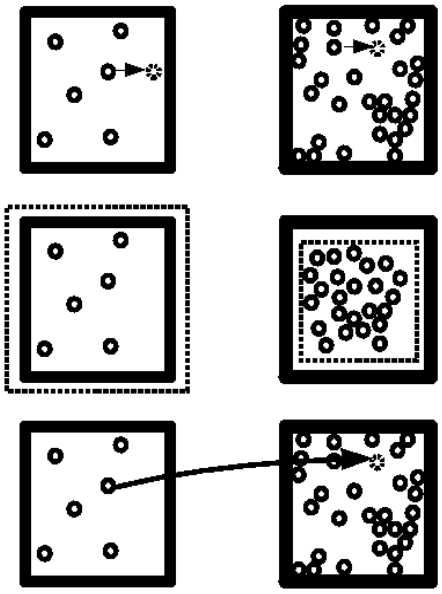

Figure 1.3: Monte Carlo steps in the Gibbs ensemble method: particle displacement, volume exchange and exchange of particles

UNIVERSITAT ROVIRA I VIRGILI
IMPROVEMENT OF MONTE CARLO ALGORITHMS AND INTERMOLECULAR POTENCIALS FOR THE MODELLING OF ALKANOLS, ESTHERS, TRIOPHENES AND AROMATICS
Javier Pérez Pellitero
ISBN: 978-84-691-0377-7/DL: T.2195-2007

- Transfer of a particle from one box to the other. When a new configuration n is generated from an old one o by removing a particle from box 1 and inserting it in box 2, the ratio between the probabilities of the states o and n is given by:

$$\frac{\rho_n}{\rho_o} = e^{-\left[\beta[(U(s_n^N)-U(s_o^N)]\right]} \frac{n_1(V-V_1)}{V_1(N-n_1+1)} \tag{1.45}$$

1.6 Histogram Reweighting

The histogram reweighting technique (HR) has been widely used to compute phase diagrams and free energies of different fluids [11]. We have used HR to calculate the VLE and also to facilitate the prediction of the critical constants by means of the FSS techniques which will be explained later in detail. The technique was introduced by Ferrenberg and Swendsen [15][16] and is based on the fact that a single simulation can give information about the properties of nearby state points. In the original formulation of the methodology, histograms at different conditions from different simulations are combined to improve the statistics extending the range of applicability of the method. During the GCMC simulation we collect information in multiple uncorrelated states by recording the potential energy U of the system as well as the number of particles of each compound $N_1$and N_2. Even though the original formulation considers the construction of multiple histograms ,as we will see later in this work, the construction of a conventional histogram can be avoided, which opens the possibility of easily extending the methodology to multicomponent systems. Histogram reweighting techniques can be divided in "single" and "multiple" histogram reweighting depending on if we are combining more than a single histogram. In the next sections, both methodologies are described:

1.6.1 Simple Histogram Reweighting

For the shake of simplicity, we start deriving the simple histogram reweighting methodology for the canonical ensemble, this means that the methodology is applied in a single dimension. Then, it will be extended to the grand canonical ensemble due to the fact that the aplication of HR methodologies to this

UNIVERSITAT ROVIRA I VIRGILI
IMPROVEMENT OF MONTE CARLO ALGORITHMS AND INTERMOLECULAR POTENCIALS FOR THE MODELLING OF ALKANOLS, ESTHERS, TRIOPHENES AND AROMATICS
Javier Pérez Pellitero
ISBN: 978-84-691-0377-7/DL: T.2195-2007

ensemble results particularly interesting for the phase equilibria calculation as well as critical point location.

While the general procedure in a MC simulation is to record the average values of the thermophisical properties of interest in the system, in this case we also construct a histogram where we record the number of times $H(E_i)$ that the system visits a given energy E_i. Because the simulation generates configurations according to the equilibrium probability distribution, a histogram $H(E_i)$ of energy values provides an estimate for the equilibrium probability distribution; this estimate becomes exact in the limit of an infinite-length simulation. For a real simulation, the histogram will suffer from statistical errors, but $H(E_i)/\mathcal{N}$, where $\mathcal{N}$ is the number of observations made, still provides an estimate for the probability over the range of energy values generated during the run. Thus, in the canonical ensemble, the probability of observing the system at a given energy for a given number of particles, temperature and volume is given by:

$$P(E_i; N, V, \beta) = \frac{\Omega(N, V, E)\exp(-\beta E_i)}{Q(N, V, \beta)} \tag{1.46}$$

where $\Omega(N, V, E)$ is the density of states. This probability can be estimated at a certain inverse temperature β_0 by constructing a histogram by means of the next expression:

$$P(E_i; N, V, \beta_0) = \frac{\overline{\Omega(N, V, E)}\exp(-\beta_0 E_i)}{Q(N, V, \beta_0)} = \frac{H(E_i)}{\mathcal{N}} \tag{1.47}$$

where $\overline{\Omega(N, V, E)}$ is an estimate for the true density of states $\Omega(N, V, E)$ obtained at β_0. Knowledge of the exact distribution at one value of β_0 is thus sufficient to determine the density of states for any different β

If we now replace $\Omega(N, V, E)$ in Eqn. 1.46 with the expression for $\overline{\Omega(N, V, E)}$ from Eqn. 1.47, and normalize the distribution, we find that the relationships between the histogram measured at $\beta = \beta_0$ and the (estimated) probability ditribution for an arbitrary β is given by:

$$P(E_i; N, V, \beta) = \frac{H(E_i)exp^{(\beta_0-\beta)E_i}}{\sum H(E_i)exp^{(\beta_0-\beta)E_i}} \tag{1.48}$$

UNIVERSITAT ROVIRA I VIRGILI
IMPROVEMENT OF MONTE CARLO ALGORITHMS AND INTERMOLECULAR POTENCIALS FOR THE MODELLING OF ALKANOLS, ESTHERS, TRIOPHENES AND AROMATICS
Javier Pérez Pellitero
ISBN: 978-84-691-0377-7/DL: T.2195-2007

From this expression, the average value of any function of E_i, denoted $f(E_i)$ can be calculated as a continuous function of β:

$$\langle f(E_i)\rangle_\beta = \sum f(E_i)P(E_i;N,V,\beta) \tag{1.49}$$

The ability to continuously vary β makes the histogram method ideal to study critical behavior.

1.6.2 Multiple Histogram Reweighting

We can write the partition function of the grand canonical ensemble Ξ as:

$$\Xi(\mu_C,V,\beta) = \sum_N \sum_U \Omega(N_C,V,U)\times \exp(\beta(\sum_C \mu_C N_C - U)) \tag{1.50}$$

being μ_c the chemical potential of each component, V the volume of the system, β the inverse temperature and $\Omega(N_i,V,T)$ the microcanonical density of states. For the case of the real components, the temperature dependance on the de Broglie wavelength does not affect neither the calculation of the vapor-liquid equilibrium nor the pressure calculation, since they are done at constant temperature. The probability of observing the system at a given state for a given temperature, volume and chemical potential is:

$$P(N_C,U;\mu_C,V,\beta) = \frac{\Omega(N_C,U)\times\exp(\beta\sum_C(\mu_C N_C-U))}{\Xi(\mu_C,V,\beta)} = \frac{H(U,N_C)}{\mathcal{N}} \tag{1.51}$$

where $H(N_c,U)$ is the value of the hypothetical histogram constructed and $\mathcal{N}$ is the total number of observations recorded during the simulation. Since the microcanonical density of states is independent of β and μ_c, simulations at different values of β and μ_c but constant total volume of the system will provide different estimates for Ω. Generally, it is not possible to cover all the

UNIVERSITAT ROVIRA I VIRGILI
IMPROVEMENT OF MONTE CARLO ALGORITHMS AND INTERMOLECULAR POTENCIALS FOR THE MODELLING OF ALKANOLS, ESTHERS, TRIOPHENES AND AROMATICS
Javier Pérez Pellitero
ISBN: 978-84-691-0377-7/DL: T.2195-2007

thermodynamic states of interest from a single simulation. Multiple simulations at different conditions are needed in order to generate data which will be reweighted according to the methodology outlined by Ferrenberg and Swendsen to form a joint probability which can be extended to the conditions of interest. This probability is given by:

$$P(N_C, U; \mu_C, V, \beta) = \frac{\sum_{j=1}^{K} H_j(N_C, U) \exp(\beta \sum_C (\mu_C N_C - U))}{\sum_{j=1}^{K} \mathcal{N}_\mathrm{j} \exp(\beta_j (\sum_c \mu_{cj} N_c - U)) \times \Xi(\mu_C, V, \beta)/\Xi(\mu_{Cj}, V, \beta_j)} \tag{1.52}$$

where K is the total number of simulations performed. To determine the values for each of the $K-1$ independent ratios Ξ_i/Ξ_j between the local Grand Partition functions we fix $\beta = \beta_i$ and $\mu_c = \mu_{ci}$ where i denotes one of the K simulations. Finally we sum Eq (3.1) over all N_c and U to obtain:

$$1 = \sum_U \sum_{N_C} \frac{\sum_{j=1}^{K} H_j(N_C, U) \exp(\beta_i (\sum_C \mu_C N_C - U))}{\sum_{j=1}^{K} \mathcal{N}_\mathrm{j} \exp(\beta_j (\sum_C \mu_{Cj} N_C - U)) \times \Xi(\mu_{Ci}, V, \beta_i)/\Xi(\mu_{Cj}, V, \beta_j)} \tag{1.53}$$

The values for the constants Ξ_i/Ξ_j are obtained by iterating Eqns. (1.52) and (1.53) specifying arbitrarily the value of Ξ at one of the K runs. As mentioned before and according to [44], the construction of a real histogram is not necessary since the previous expression can be rewritten as:

$$\begin{aligned} 1 = & \sum_{U,N_C} \frac{\sum_{j=1}^{K} H_j(N_C, U)}{\sum_{j=1}^{K} \mathcal{N}_\mathrm{j} \exp((\beta_i - \beta_j)U + \sum_C (\beta_j \mu_{Cj} - \beta_i \mu_{Ci}) N_C)) \times \Xi_i/\Xi_j} = \\ & \sum_{j=1}^{K} \sum_{,U,N_C} \frac{H_j(N_C, U)}{\sum_{j=1}^{K} \mathcal{N}_\mathrm{j} \exp((\beta_i - \beta_j)U + \sum_C (\beta_j \mu_{Cj} - \beta i \mu_{Ci}) N_C)) \times \Xi_i/\Xi_j} = \\ & \sum_{j=1}^{K} \sum_{s} \frac{1}{\sum_{j=1}^{K} \mathcal{N}_\mathrm{j} \exp((\beta_i - \beta_j)U_{js} + \sum_C (\beta_j \mu_{Cj} - \beta_i \mu_{Ci}) N_{Cs})) \times \Xi_i/\Xi_j} \end{aligned} \tag{1.54}$$

UNIVERSITAT ROVIRA I VIRGILI
IMPROVEMENT OF MONTE CARLO ALGORITHMS AND INTERMOLECULAR POTENCIALS FOR THE MODELLING OF ALKANOLS, ESTHERS, TRIOPHENES AND AROMATICS
Javier Pérez Pellitero
ISBN: 978-84-691-0377-7/DL: T.2195-2007

where the sum over s is over all the states sampled during the j^{th} simulation and U_{js} is the configurational energy of such a state. Basically, the summation first over energies and number of molecules and then over simulations is replaced with a summation over each simulation, i, and then over the states in that simulation, s. This has the advantage of allowing us to work directly with the raw data generated from the simulations making use of all the available information and avoids the need to store histograms.

In appendix Appendix-1 we show the complete derivation of the multiple histogram reweighting expression as well as the effect of the presence of the temperature in the De Broglie wavelength.

1.7 Critical Point calculation

1.7.1 Critical Point Phenomena

In this section, we provide the reader with a brief description of the near critical region. Although a wide variety of physical systems exhibit critical phenomena, we will concentrate on the liquid gas transition for the shake of simplicity.

In physical chemistry, thermodynamics, chemistry and condensed matter physics, a critical point, also called a critical state, specifies the conditions (temperature, pressure) at which the liquid state of the matter ceases to exist. In the projection onto the PT plane of the phase diagram shown schematically in figure 1.4, three separate regions can be appreciated corresponding to the three phases of matter: solid, liquid and gaseous phases. The solid and gas phases are in equilibrium along the sublimation curve, the solid and liquid phases are in equilibrium along the fusion curve, and the liquid and gaseous phase along the vapor pressure curve. Each point on these three curves represents an equilibrium state in which two or more phases can coexist. We notice however that the phase boundary between liquid and gas does not continue indefinitely. Instead, it terminates at a point on the phase diagram called the critical point, whose coordinates denoted by (P_c, ρ_c and T_c) are critical pressure, critical density and critical temperature respectively. This reflects the fact that, at extremely high temperatures and pressures, the liquid and gaseous phases become indistinguishable. As a liquid is heated, its density decreases while the pressure and density of the vapor being formed in-

UNIVERSITAT ROVIRA I VIRGILI
IMPROVEMENT OF MONTE CARLO ALGORITHMS AND INTERMOLECULAR POTENCIALS FOR THE MODELLING OF ALKANOLS, ESTHERS, TRIOPHENES AND AROMATICS
Javier Pérez Pellitero
ISBN: 978-84-691-0377-7/DL: T.2195-2007

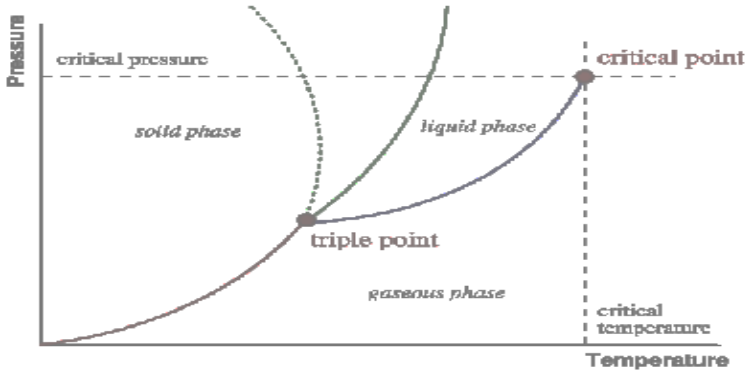

Figure 1.4: Schematical projection of the PVT surface in the PT plane

creases. The liquid and vapor densities become closer and closer to each other until the critical temperature is reached where the two densities are equal and the liquid-gas line or phase boundary disappears. Additionally, as the equilibrium between liquid and gas approaches the critical point, the heat of vaporization approaches zero, becoming zero at and beyond the critical point. More generally, the critical point is the point of termination of a phase equilibrium curve, which separates two distinct phases. At this point, the phases are no longer distinguishable. The critical point in a phase diagram is at the high-temperature extreme of the liquid-gas phase boundary. The fact that the vapor pressure curve terminates in a critical point was not appreciated until about a hundred years ago Prior to that time, scientists regarded certain gases as being "permanent" in the sense that these gases could not be made to condense no matter how much pressure was applied.

In addition to the PT projection, it is also useful to consider the projection into the $P\rho$ plane. This is shown schematically in figure 1.5 where we can appreciate that at low temperatures there is a rather large difference between the liquid and gas densities, ρ_L and ρ_G, but as the critical temperature is approached this density difference tends to zero. The existence of such a quantity will be seen to be a common feature associated with the critical points of many different physical systems. In particular, we say that $\rho_L - \rho_G$ is the *order parameter* for the liquid-gas critical point since it indicates the degree of order of the system.

The critical point in a phase diagram is at the high-temperature extreme of the liquid-gas phase boundary.

.

UNIVERSITAT ROVIRA I VIRGILI
IMPROVEMENT OF MONTE CARLO ALGORITHMS AND INTERMOLECULAR POTENCIALS FOR THE MODELLING OF ALKANOLS, ESTHERS, TRIOPHENES AND AROMATICS
Javier Pérez Pellitero
ISBN: 978-84-691-0377-7/DL: T.2195-2007

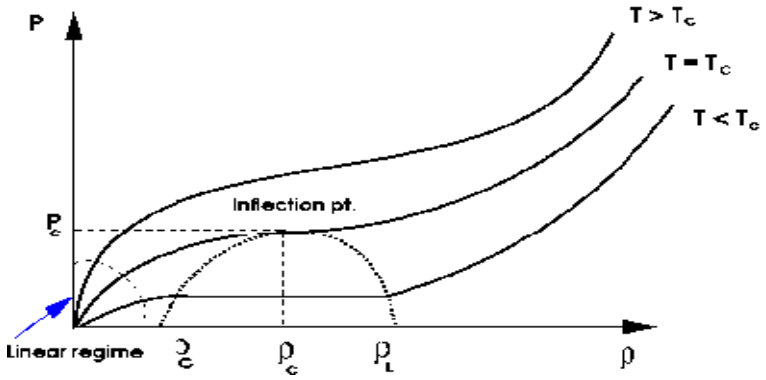

Figure 1.5: Schematical projection of the PVT surface in the $P\rho$ plane

Critical variables are useful for rewriting a equation of state into one that applies to all materials. The effect is similar to a normalizing constant.

1.7.2 The Law of Corresponding States

The equations of state of different real gases are nearly the same if expressed in reduced temperatures, pressures and volumes.

$$T_r = \frac{T}{T_c} \tag{1.55}$$

$$P_r = \frac{P}{P_c} \tag{1.56}$$

$$V_r = \frac{V}{V_c} \tag{1.57}$$

This fact is known as the "law of corresponding states". Two gases with the same value of the compressibility factor $z = P_r V_r / R T_r$ are in "corresponding" states.

This is illustrated in figure 1.6 [45] which shows the measured compressibility factor of several gases expressed in reduced temperature, pressure, and volume.

The compressibility factor plot [45] is an approximate representation of

UNIVERSITAT ROVIRA I VIRGILI
IMPROVEMENT OF MONTE CARLO ALGORITHMS AND INTERMOLECULAR POTENCIALS FOR THE MODELLING OF ALKANOLS, ESTHERS, TRIOPHENES AND AROMATICS
Javier Pérez Pellitero
ISBN: 978-84-691-0377-7/DL: T.2195-2007

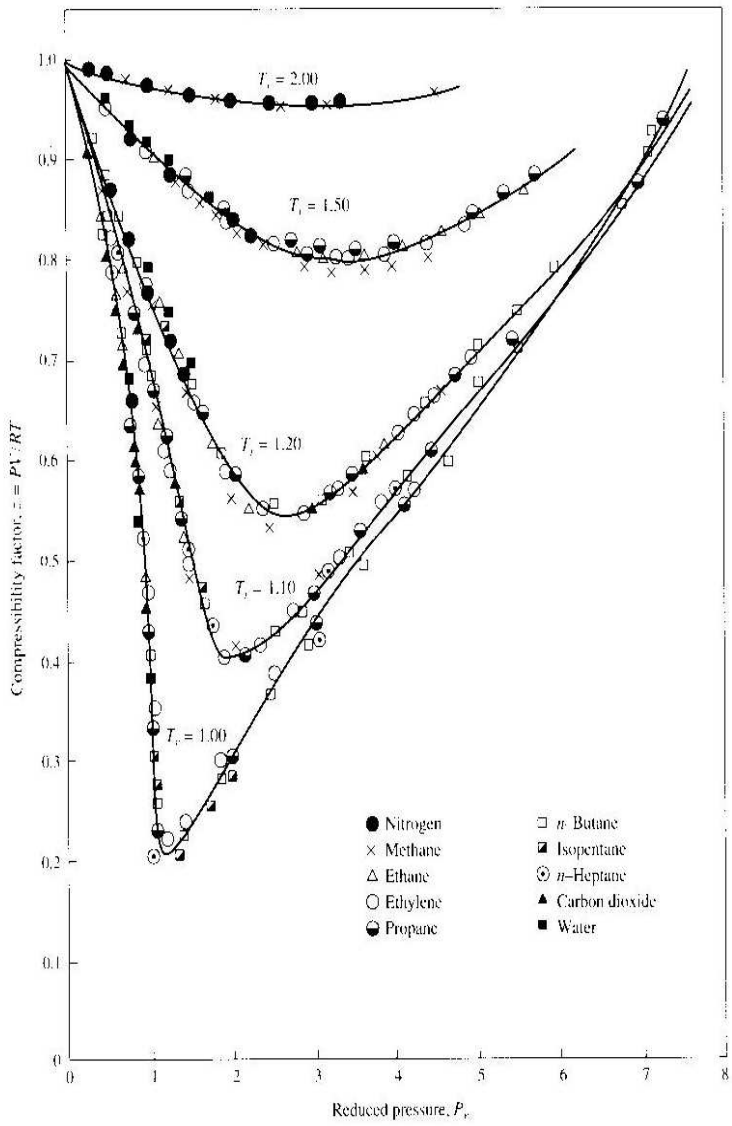

Figure 1.6: Compressibility factors $z = PV/RT$ of a variety of gases vs. reduced pressure

UNIVERSITAT ROVIRA I VIRGILI
IMPROVEMENT OF MONTE CARLO ALGORITHMS AND INTERMOLECULAR POTENCIALS FOR THE MODELLING OF ALKANOLS, ESTHERS, TRIOPHENES AND AROMATICS
Javier Pérez Pellitero
ISBN: 978-84-691-0377-7/DL: T.2195-2007

the equation of state for real gases. Suppose that the critical constants are known for a given gas Y and we want the molar volume at the temperature T and pressure P. Then we compute $T_r = T/T_c$ and $P_r = P/P_c$. Now for the isotherm at T_r on the z versus P_r plot we read the value of $z(T_c, P_c)$. Then the reduced molar volume is given by $V_c = zRT_c/P_c$, and the molar volume is given by $V = V_r V_c$. This procedure is only approximate but it is useful over a wide range of T and P.

1.7.3 Critical Exponents

The critical point theory is traditionally divided into two differents stages. The first one, called the classical era, and the recent one known as the modern era. This second starting with the consideration of the critical-point exponents. It is customary to say that the order parameter $\rho_L - \rho_G$ varies as $(-\epsilon)^\beta$ where

$$\epsilon \equiv \frac{T - T_c}{T_c} \tag{1.58}$$

and where the critical exponent β typically has a value in the range $0.3 - 0.5$. More generally we can write:

$$M = \mathcal{B}(-\epsilon)^\beta \tag{1.59}$$

where it is important to stress that it is not necessary to have a strict proportionality between the general order parameter M and $(-\epsilon)^\beta$. In practice, there exist frequently corrections terms, so that "M" might have the form $\mathcal{B}_0(-\epsilon)^\beta[1 + B(-\epsilon)^x + \ldots]$ with $x > 0$. Hence a more natural definition of the critical-point exponent β is

$$\beta \equiv \lim_{\epsilon \to 0} \frac{lnM}{ln(-\epsilon)} \tag{1.60}$$

where the corrections term will drop out on taking the limit.

Critical exponents are also observed in second-order phase transitions. They characterize the power law behavior of many physical quantities as a function of ϵ. Next we describe these relations for some of these quanti-

UNIVERSITAT ROVIRA I VIRGILI
IMPROVEMENT OF MONTE CARLO ALGORITHMS AND INTERMOLECULAR POTENCIALS FOR THE MODELLING OF ALKANOLS, ESTHERS, TRIOPHENES AND AROMATICS
Javier Pérez Pellitero
ISBN: 978-84-691-0377-7/DL: T.2195-2007

ties such as the correlation length ξ, the specific heat C or the susceptibility/compressibility χ

$$\epsilon > 0 \Rightarrow \xi \sim \epsilon^{-\nu} \qquad \epsilon < 0 \Rightarrow \xi \sim (-\epsilon)^{-\nu} \tag{1.61}$$

$$\epsilon > 0 \Rightarrow C \sim \epsilon^{-\alpha} \qquad \epsilon < 0 \Rightarrow C \sim (-\epsilon)^{-\alpha} \tag{1.62}$$

$$\epsilon > 0 \Rightarrow \chi \sim \epsilon^{-\gamma} \qquad \epsilon < 0 \Rightarrow \chi \sim (-\epsilon)^{-\gamma} \tag{1.63}$$

$$\epsilon > 0 \Rightarrow M \sim \epsilon^{\beta} \qquad \epsilon < 0 \Rightarrow M \sim (-\epsilon)^{\beta} \tag{1.64}$$

where the critical exponents are denoted by the greek letters.ν, α and γ. They fall into universality classes as is explained in the next section.

1.7.4 Universality

In statistical mechanics, universality is the observation that there are properties for a large class of systems that are independent of the dynamical details of the system. In particular, the study of phase transitions characterized by an order parameter originated the notion of universality. For systems that exhibit universality, the closer the parameter is to its critical value, the less the order parameter depends on the details of the system. The remarkable discovery made in the second half of the twentieth century was that very different systems had the same critical exponents, hence universality.

The key observation is that near a phase transition or critical point, disturbances occur at all size scales, and thus one should look for an explicitly scale-invariant theory to describe the phenomena. Universality is a by-product of the fact that there are relatively few scale-invariant theories. For any one specific physical system, the detailed description may have many scale-dependent parameters and aspects. However, as the critical point is approached, the scale-dependent parameters play less and less of an important role, and the scale-invariant parts of the physical description dominate. Thus,

UNIVERSITAT ROVIRA I VIRGILI
IMPROVEMENT OF MONTE CARLO ALGORITHMS AND INTERMOLECULAR POTENCIALS FOR THE MODELLING OF ALKANOLS, ESTHERS, TRIOPHENES AND AROMATICS
Javier Pérez Pellitero
ISBN: 978-84-691-0377-7/DL: T.2195-2007

a simplified, and often exactly solvable, model can be used to approximate the behavior of these systems near the critical point.

1.7.5 Finite Size Scaling

The accurate location of the critical point becomes extremely important in order to reliably predict thermodynamic properties either by using equations of state, contibution groups methods, molecular simulation or any other methodology. Locating the critical point with molecular simulation methods, poses a challenge to this methodology due to the appearance in this region of big fluctuations in the correlation length. This makes it impossible to apply conventional techniques such as GEMC simulation, due to the fact that the correlation length of the system will be always cut by the size of the simulation box. Instead, finite size scaling (FSS) studies, which where originally developed for spin models [46], need to be applied in order to take into account the finite size effects appearing in the vicinity of the critical locus in molecular simulation. These techniques provide an efficient way to obtain infinite volume critical parameters from simulations performed at finite size conditions. The combination of the FSS methodologies with the histogram reweighting methodology previously described in section 1.6 has proven to be an efficient tool to accurately locate the critical point The use of the histogram reweighting methodology facilitates the calculation of the vapor-liquid equilibrium as well as the location of the critical point by forming a joint density distribution calculated from the information of nearby conditions which can be extracted from a given set of simulations. The application of FSS methodologies is described in the next section

The use of finite size scaling techniques allows the bulk critical properties to be extracted from simulations of finite size. The methodology is constucted around the idea that as the critical point is approached, the correlation length diverges according to:

$$T - T_c = \xi^{-1/\nu} \tag{1.65}$$

When we are close to the critical temperature T_c, by eliminating ϵ from Eqns. 1.62, 1.63 and 1.64 and substituting the correlation length ξ by the size of the simulation box L we get:

UNIVERSITAT ROVIRA I VIRGILI
IMPROVEMENT OF MONTE CARLO ALGORITHMS AND INTERMOLECULAR POTENCIALS FOR THE MODELLING OF ALKANOLS, ESTHERS, TRIOPHENES AND AROMATICS
Javier Pérez Pellitero
ISBN: 978-84-691-0377-7/DL: T.2195-2007

$$C \propto L^{\alpha/\nu} \qquad \chi \propto L^{\gamma/\nu} \qquad M \propto L^{-\beta/\nu} \tag{1.66}$$

When a system of finite size L is considered, at the critical temperature T_c the correlation length is cut off as it approaches the system size, so that the susceptibility χ, heat capacity C and other variables will also be cutoff. This fact means that in finite size systems χ and C never diverge. This cut-off can be expressed mathematically as follows. If we continue to denote by ξ the value which the correlation length would have in an infinite system at temperature ϵ, then the cut-off takes place when $\xi > L$. As long as $\xi \ll L$ the values of χ and C should be the sames as for the infinite system. For example, we can express this for the susceptibility by writing:

$$\chi_L(\epsilon) = \xi^{\gamma/\nu}\chi_0(L/\xi) \tag{1.67}$$

where χ_0 is a dimensionlesss function of a single variable which has the following properties:

$$\chi_0(x) = constant \qquad for \;\; x \gg 1 \tag{1.68}$$

and

$$\chi_0(x) \sim x^{\gamma/\nu} \qquad as \;\; x \to 0 \tag{1.69}$$

The precise way in which the susceptibility gets cut off close to the critical temperature T_c is contained in the functional form of χ_0 Although Eqn. 1.67 contains all the information we need about the behavior of our system with varying the system size, it is not written in a very useful form, since it still contains the correlation length ξ at temperature ϵ in the infinite system, which is not known. For this reason it is more convenient to reorganize the equation defining a new dimensionless variable $\overline{\chi}$ thus:

$$\overline{\chi}(x) = x^{-\gamma}\chi_0(x^{\nu}) \tag{1.70}$$

then making again use of Eqn. 1.62 we get:

UNIVERSITAT ROVIRA I VIRGILI
IMPROVEMENT OF MONTE CARLO ALGORITHMS AND INTERMOLECULAR POTENCIALS FOR THE MODELLING OF ALKANOLS, ESTHERS, TRIOPHENES AND AROMATICS
Javier Pérez Pellitero
ISBN: 978-84-691-0377-7/DL: T.2195-2007

$$\chi_L(\epsilon) = L^{\gamma/\nu}\overline{\chi}(L^{-1/\nu}\epsilon) \tag{1.71}$$

and similarly for the heat capacity C and the order parameter M:

$$C_L(\epsilon) = L^{\alpha/\nu}\overline{C}(L^{-1/\nu}\epsilon) \tag{1.72}$$

$$M_L(\epsilon) = L^{-\beta/\nu}\overline{M}(L^{-1/\nu}\epsilon) \tag{1.73}$$

where $\overline{C}, \overline{\chi}$ and $\overline{M}$ are the so called scaling functions, which are constructed to be independent of system size, but strongly vary with the parameters T_c, ν, α, β and γ . If the correct values for the parameters are chosen, the data obtained for different system sizes will collapse onto a single curve. In the next section, the scaling relation for the susceptibility is derived showing how these expressions allow to extrapolate finite system size data to $L = \infty$ in order to obtain critical properties in the thermodynamic limit.

1.7.6 Critical Exponents Estimation

The apllication of finite size scaling methodologies allows us not only to locate the critical point, but also to determine the value of the critical exponents by extracting the information contained in the scaling functions. Although these functions are unknown, there are certain things we know about them. Eqn. 1.69 reveals that:

$$\overline{\chi}(x) \longrightarrow x^{-\gamma}(x^{\nu})^{\gamma/\nu} = constant \qquad as \quad x \longrightarrow 0 \tag{1.74}$$

for the case of the susceptibility. This fact means that close to the critical temperature the scaling functions are finite. Since, by design, all the system size dependence of these functions is contained in Eqns 1.71, 1.72 and 1.73, if we measure the scaling functions, denoted here generally by $\overline{\varphi}(x)$, dependent on the system size L and the reduced temperature ϵ, we should obtain the same result regardless of the size of the system. This fact allows us to calculate the critical exponents as well as the value of the critical temperature by

UNIVERSITAT ROVIRA I VIRGILI
IMPROVEMENT OF MONTE CARLO ALGORITHMS AND INTERMOLECULAR POTENCIALS FOR THE MODELLING OF ALKANOLS, ESTHERS, TRIOPHENES AND AROMATICS
Javier Pérez Pellitero
ISBN: 978-84-691-0377-7/DL: T.2195-2007

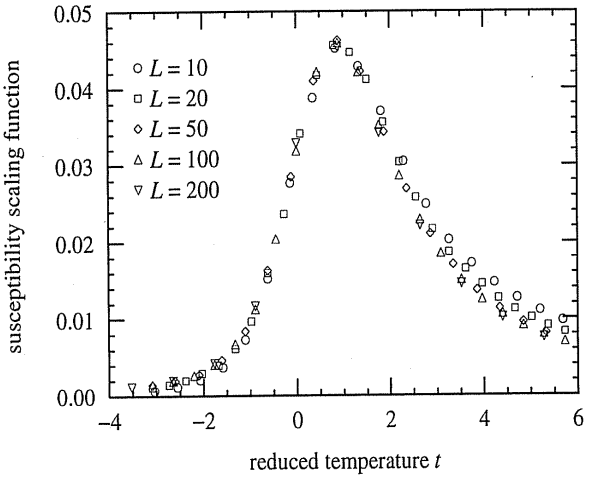

Figure 1.7: Data collapse of magnetic susceptibilty for the two dimensional Ising model. Symbols are Monte Carlo measurements of the susceptibilty for five different system sizes as indicated. From[44]

performing different calculations of the system of interest for different system sizes L close to the region where we believe the critical temperature is. It is important to remark the fact that with this methodology, we do not need to be exactly at the critical temperature, only in its vicinity.

To perform this calculation for each system, we measure the variable of interest at different temperatures ϵ obtaining in this way an estimate of the scaling function $\overline{\varphi}(x)$ for several different values of the scaling variable $x = L^{1/\nu}\epsilon$ for each system size. Recovering the fact that the scaling functions are supposed to be independent of the system size, if we use the appropriate values for the critical exponents ν, α and γ as well as the critical temperature T_c, the estimates of the scaling functions will be expected to fall on the same curve. This fact can be appreciated in figure 1.7 for the case of the magnetic susceptibility of the two dimensional Ising model.

From this collapse $\gamma = 1.76$, $\nu = 1.00$ and $T_c = 2.27J$ are found. J is the interaction energy between spins in the Ising model.

UNIVERSITAT ROVIRA I VIRGILI
IMPROVEMENT OF MONTE CARLO ALGORITHMS AND INTERMOLECULAR POTENCIALS FOR THE MODELLING OF ALKANOLS, ESTHERS, TRIOPHENES AND AROMATICS
Javier Pérez Pellitero
ISBN: 978-84-691-0377-7/DL: T.2195-2007

1.7.7 Mixed-Field Theory

The FSS technique holds that the coarse-grained properties of systems near the critical point are universal. This is true only for sufficiently large system sizes. For the small values of our simulation box length, L, the properties depend on the specific combination of L and the scaling field measuring the deviation from criticality. For asymmetric models, like the pure LJ fluid and their mixtures, mixed-field theory has to be introduced in order to take into account the effects of density and energy fields near the critical point[17] [14]. Thus, in the absence of the special symmetry prevailing in the ferromagnet Ising model leading to only one scaling field, the relevant scaling fields will be comprised of linear combinations of the dimensionless temperature and chemical potential difference,

$$\tau = T_c - T + s(\mu - \mu_c) \tag{1.75}$$
$$h = \mu - \mu_c + r(T_c - T) \tag{1.76}$$

The parameters s and r are system-specific quantities controlling the degree of field mixing. Conjugate to the two relevant scaling fields are scaling operators $\mathcal{M}$ and $\mathcal{E}$, which are comprised of linear combinations of the particle density ρ and energy density u:

$$\mathcal{M} = \frac{1}{1 - sr}[\rho - su] \tag{1.77}$$
$$\mathcal{E} = \frac{1}{1 - sr}[u - r\rho] \tag{1.78}$$

For models with Ising symmetry , $\mathcal{M}$ is the magnetization while $\mathcal{E}$ is the energy density. The joint distribution of density and energy is simply related to the joint distribution of mixed operators by:

$$P_L(\rho, u) = \frac{1}{1 - sr} P_L(\mathcal{M}, \mathcal{E}) \tag{1.79}$$

For pure fluids and their mixtures belonging to the Ising universality class, the critical behavior of the ordering operator distribution $\mathcal{M}$ assumes a scal-

UNIVERSITAT ROVIRA I VIRGILI
IMPROVEMENT OF MONTE CARLO ALGORITHMS AND INTERMOLECULAR POTENCIALS FOR THE MODELLING OF ALKANOLS, ESTHERS, TRIOPHENES AND AROMATICS
Javier Pérez Pellitero
ISBN: 978-84-691-0377-7/DL: T.2195-2007

ing form that matches the universal order parameter distribution $p_m^*(x)$ for the Ising model [47]. This means that at the finite critical point of our system, the distribution of our scaling operator $\mathcal{M}$, previously defined as a linear combination of density and energy, should coincide with the Ising model magnetization distribution. The procedure followed to determine the critical point of the finite systems according to this methodology is described next.

The probability distribution of $\mathcal{M}$ is mapped onto the variable x, which is defined as follows:

$$x = \frac{(\mathcal{M} - \langle \mathcal{M} \rangle)}{\sqrt{\langle \mathcal{M}^2 \rangle - \langle \mathcal{M} \rangle^2}} \tag{1.80}$$

This definition results in x having unit variance allowing for comparison with available data from the Ising model and has been widely used in the available literature[20] [18]:

An initial guess for the critical temperature and chemical potential is chosen either from a fit to the power law or from more accurate calculations using the cumulant methodology explained later:

The values for the critical temperature and chemical potentials as well as the values for the mixed field parameters r and s are adjusted using a "Least Squares minimization algorithm" [48] in order to obtain the same form of the universal distribution $p_m^*(x)$

1.7.8 Binder Parameter

In order to locate the critical point, an alternative methodology has been employed. The Binder cumulant parameter[23] U_L was calculated for the different volume sizes simulated and is defined as follows:

$$U_L = \frac{\langle m^4 \rangle}{\langle m^2 \rangle^2} \tag{1.81}$$

with $m = \phi - \langle \phi \rangle$ being ϕ a suitable order parameter, in our case density or composition. The Binder parameter provides a dimensionless measure of the shape of the order parameter distribution function and approaches asymptotically a value of 1 if a bimodal density distribution is found, for instance when

UNIVERSITAT ROVIRA I VIRGILI
IMPROVEMENT OF MONTE CARLO ALGORITHMS AND INTERMOLECULAR POTENCIALS FOR THE MODELLING OF ALKANOLS, ESTHERS, TRIOPHENES AND AROMATICS
Javier Pérez Pellitero
ISBN: 978-84-691-0377-7/DL: T.2195-2007

phase separation occurs. On the other hand, it asymptotically approaches a value of 3 when we deal with supercritical fluids where a Gaussian density distribution is expected. The Binder parameter is expected to have a universal value $U_L = 1.6035$ at the critical point [49] for the Ising universality class. This means that the infinite system size critical point can be identified as the point where U_L becomes system-size independent, being this point where cumulants from different sizes intersect. By taking into account the order parameter distribution based definition of the Binder parameter, we expect the universal value of this parameter to be also valid as an estimate of the apparent finite critical temperature calculated by means of the mixed-field theory. This fact allows us to propose a FSS study of this parameter in order to obtain the infinite system size critical point.

In the results section we will present both the results for estimating the infinite system size critical point either by locating the intersection for the two largest system sizes, or as a FSS extrapolation of the estimates for the finite critical temperature taken from the intersection with the Ising universal value. This combination of the Binder parameter calculation with the FSS methodology allows us to also calculate critical properties which are highly dependent on the system-size such as the composition in binary mixtures. In this work an estimate of the critical density or composition is taken from the average of the corresponding density or composition distribution. In the case of the cumulant intersection method, we use the average value of the largest system size as the estimate for these properties which tends to present significant deviations from the infinite system size value.

1.8 Force Fields

Intermolecular forces are electromagnetic forces that act between molecules or between widely separated regions of a macromolecule. These forces can be cohesive between like molecules, for example surface tension or adhesive between unlike molecules for example in capillary action. Listed in order of decreasing strength, these forces are:

- Ionic interactions
- Hydrogen bonds
- Dipole-dipole interactions
- Van der Waals' forces

UNIVERSITAT ROVIRA I VIRGILI
IMPROVEMENT OF MONTE CARLO ALGORITHMS AND INTERMOLECULAR POTENCIALS FOR THE MODELLING OF ALKANOLS, ESTHERS, TRIOPHENES AND AROMATICS
Javier Pérez Pellitero
ISBN: 978-84-691-0377-7/DL: T.2195-2007

The following functional abstraction, known as a potential function or force field in chemistry, calculates the system's potential energy in a given conformation as a sum of individual energy terms.

$$E = E_{covalent} + E_{noncovalent} \tag{1.82}$$

where the covalent term $E_{covalent}$ can be also written as a sum of the following intramolecular terms:

$$E_{covalent} = E_{bond} + E_{angle} + E_{dihedral} \tag{1.83}$$

where E_{bond} is the energy associated to the different bonds between particles, E_{angle} the bending energy, and $E_{dihedral}$ the torsion energy. The noncovalent term can also be split into:

$$E_{noncovalent} = E_{electrostatic} + E_{vanderWaals} \tag{1.84}$$

where $E_{electrostatic}$ is the energy associated with charged atoms and $E_{vanderWaals}$ accounts for the non-bonded interactions.

We can write a formal and generalistic description of a typical force field V according to the addition of the following terms:.

1. Harmonic force constant:

$$V = \sum_{l} \frac{1}{2} k_l (l - l_0)^2 \tag{1.85}$$

   where k_l are the different harmonic force constants, and l_0 the equilibrium values for the distances between the different particles.

2. Optional anharmonic force constant.

$$-\sum_{l} \frac{1}{3!} k_l^{anh} (l - l_0)^3 \tag{1.86}$$

   where k_l^{anh} are the different anharmonic constants.

UNIVERSITAT ROVIRA I VIRGILI
IMPROVEMENT OF MONTE CARLO ALGORITHMS AND INTERMOLECULAR POTENCIALS FOR THE MODELLING OF ALKANOLS, ESTHERS, TRIOPHENES AND AROMATICS
Javier Pérez Pellitero
ISBN: 978-84-691-0377-7/DL: T.2195-2007

3. Angle bending constants

$$+\sum_{\theta}\frac{1}{2}k_{\theta}(\theta-\theta_0)^2 \tag{1.87}$$

where k_θ are the bending force constants and θ_0 the equilibrium values for the different angles formed between particles. This contribution could also be expressed in terms of $cos\theta$ instead of θ.

4. Torsional potential.

$$+\sum_{n}\frac{V_n}{2}\left[1+cos(n\omega-\gamma)\right] \tag{1.88}$$

where V_n are the torsion force constants, n is the periodicity of the torsion and ω the torsion angle. An anternative but equivalent expression is

$$+\sum_{n}C_n cos(\omega)^n \tag{1.89}$$

where C_n are the torsion force constants.

5. Out of plane bending for trigonal groups.

$$+\sum_{\Gamma}\frac{1}{2}k_{\Gamma}(\Gamma-\pi)^2 \tag{1.90}$$

6. Van der Waals terms.

$$\sum_{i<j}\left\{\frac{A_{ij}}{r_{ij}^{12}}-\frac{B_{ij}}{r_{ij}^{6}}\right\} \tag{1.91}$$

where A_{ij} and B_{ij} are specific parameters to reproduce the non-bonded interactions and r_{ij} the distance between differnt particles. Other forms can also be used to account for this contribution.

7. Electrostatic interactions.

UNIVERSITAT ROVIRA I VIRGILI
IMPROVEMENT OF MONTE CARLO ALGORITHMS AND INTERMOLECULAR POTENCIALS FOR THE MODELLING OF ALKANOLS, ESTHERS, TRIOPHENES AND AROMATICS
Javier Pérez Pellitero
ISBN: 978-84-691-0377-7/DL: T.2195-2007

$$\sum_{i<j} \frac{1}{4\pi\epsilon_0} \frac{q_i q_j}{r_{ij}} \tag{1.92}$$

where q_i and q_j are the charges of the interacting particles and ϵ_0 the vacuum permittivity.

1.9 Interatomic Potentials

To reflect the physics of our systems of interest, and in particular the previously described van der Waals forces, molecular simulation techniques make use of algorithms to generate energy surfaces known as interatomic potentials. These algorithms are expected to be as simple as possible, but as complicated as they need to be to accomplish the previous condition. In general, we can write the next general expression for an interatomic potential:

$$U = \sum_i V_i(r_i) + \sum_{i<j} V_2(r_i, r_j) + \sum_{i<j<k} V_3(r_i, r_j, r_k) + \dots \tag{1.93}$$

being V_i the single atom contributions and V_2, V_3 the contributions due to the interactions between two and three particles respectively. The basic criteria to choose the type of intermolecular potential to be used are:

- Accuracy: how many decimal points of the simulation can be reliably reproduced.
- Transferability: the capacity of the potential to be extended to different systems, phases or configurations.

In general, the interatomic potentials come either from the literature, fitting to experimental data or quantum calculations of structures, or direct calculations of terms in the potential. Particularly, when fitting a potential, the availability of experimental data becomes very important for the calculation performed to include the effects we are trying to fit to.

UNIVERSITAT ROVIRA I VIRGILI
IMPROVEMENT OF MONTE CARLO ALGORITHMS AND INTERMOLECULAR POTENCIALS FOR THE MODELLING OF ALKANOLS, ESTHERS, TRIOPHENES AND AROMATICS
Javier Pérez Pellitero
ISBN: 978-84-691-0377-7/DL: T.2195-2007

1.9.1 Hard Sphere Potential

The hard sphere potential accounts for excluded volume interactions only. The potential is infinite if particles overlap and zero otherwise. Such potentials are not numerically integrable and cannot be readily used in molecular simulation techniques such as Molecular Dynamics(MD), Brownian Dynamics(BD), or Dissipative Particle Dynamics(DPD). Hard sphere potentials are typically used in Monte Carlo simulations methods or in event-based, collision dynamics methods (also called discontinuous MD).

$$U_{HS}(r_{ij}) = \begin{cases} \infty, & r_{ij} < \sigma_{ij} \\ 0, & r_{ij} \geq \sigma ij \end{cases} \tag{1.94}$$

1.9.2 Square Well Potential

In order to simplify the LJ potential calculation, a function having in a general way the same functional form of the LJ original one. This potential is obviously not realistic due to the fact that it presents two discontinuities, but on the other hand, due to its mathematical ease and flexibility, it is useful for some calculations. The concept of flexibility arises from the fact that it contains three different adjustable parameters, the previously defined diametre of the particle σ_{ij}, the well depth ϵ_{ij} and the reduced amplitude R. In general, the square well potential can be expressed as:

$$U_{SW}(r_{ij}) = \begin{cases} \infty, & r_{ij} < \sigma_{ij} \\ -\epsilon_{ij}, & \sigma_{ij} \leq r_{ij} \leq R\sigma ij \\ 0, & R\sigma_{ij} \leq r_{ij} \end{cases} \tag{1.95}$$

The square well fluid potential has an infinite repulsive slope, what prevents it predicting a maximum value for the second virial coefficient. In particular, this type of potential has been used to calculate thermodynamical properties of systems where short range interactions are considered.

UNIVERSITAT ROVIRA I VIRGILI
IMPROVEMENT OF MONTE CARLO ALGORITHMS AND INTERMOLECULAR POTENCIALS FOR THE MODELLING OF ALKANOLS, ESTHERS, TRIOPHENES AND AROMATICS
Javier Pérez Pellitero
ISBN: 978-84-691-0377-7/DL: T.2195-2007

1.9.3 Lennard-Jones Potential

The Lennard-Jones (LJ) potential (also referred to as the L-J potential, 6-12 potential or, less commonly, 12-6 potential) is a simple mathematical model, proposed in 1931 by John Lennard-Jones of Bristol University , that represents the behavior of neutral atoms and molecules. These are subject to two distinct forces in the limit of large distance and short distance: an attractive force at long ranges (van der Waals force, or dispersion force) and a repulsive force at short ranges (the result of overlapping electron orbitals, referred to as Pauli repulsion from the Pauli exclusion principle). It takes the form:

$$U(r_{ij}) = 4\epsilon_{ij}\left[\left(\frac{\sigma_{ij}}{r_{ij}}\right)^{12} - \left(\frac{\sigma_{ij}}{rij}\right)^{6}\right] \tag{1.96}$$

where $U(r_{ij})$ is the configurational potential energy, r_{ij} is the distance between the LJ particles, ϵ_{ij} is the potential well depth. and σ_{ij} the location at which the potential crosses zero. The latter two parameters can be fitted to reproduce experimental [50] data or deduced from results of accurate quantum chemistry calculations. The $\left(\frac{1}{r}\right)^{12}$ term describes repulsion while the $\left(\frac{1}{r}\right)^{6}$ term describes attraction. The LJ potential is approximate. The form of the repulsion term has no theoretical justification; the repulsion force should depend exponentially on the distance, but the repulsion term of the L-J formula is more convenient due to the ease and efficiency of computing r^{12} as the square of r^6. The attractive long-range potential, however, is derived from dispersion interactions. The LJ potential is a relatively good approximation and due to its simplicity, it is often used to describe the properties of gases, and to model dispersion and overlap interactions in molecular models. It is particularly accurate for noble gas atoms and is a good approximation at long and short distances for neutral atoms and molecules.

1.9.4 Buckingham Potential

Several formulations in which the r^{-12} repulsive term is replaced by a theoretically more realistic exponential expression have been proposed. These

UNIVERSITAT ROVIRA I VIRGILI
IMPROVEMENT OF MONTE CARLO ALGORITHMS AND INTERMOLECULAR POTENCIALS FOR THE MODELLING OF ALKANOLS, ESTHERS, TRIOPHENES AND AROMATICS
Javier Pérez Pellitero
ISBN: 978-84-691-0377-7/DL: T.2195-2007

include the Buckingham potential:

$$U_{buck} = \epsilon_{ij} \left[\frac{6}{\alpha_{ij} - 6} e^{-\alpha_{ij}\left(\frac{r_{ij}}{r_{ij}^m} - 1\right)} - \frac{\alpha_{ij}}{\alpha_{ij} - 6} \left(\frac{r_{ij}^m}{r_{ij}}\right)^6 \right] \tag{1.97}$$

where there are three adjustable parameters. The minimum energy radius r_{ij}^m, the well depth ϵ_{ij} and α_{ij} controlling the slope of the repulsive wall. A value of α between approximately 14 and 15 gives a potential that closely corresponds to the Lennard-Jones 12-6 potential in the minimum energy region. When using the Buckingham potential it is important to remember that at very short distances the potential becomes strongly attractive. This could lead to nuclei being fused during the simulation and so it is necessary to check that atoms did not become too close.

1.9.5 United Atoms(UA) and Anisotropic UA (AUA) Potential

In the last decade, potential models, have been developed for a wide range of compounds[24, 10, 25]. One of the most common approaches for modeling hydrocarbons and other flexible molecules is the use of the united-atoms (UA) model scheme, where each chemical group is represented by one Lennard-Jones center. This scheme results in a significant reduction of the computational time as compared to all-atoms models since the number of pair interactions goes as the square of the number of sites. Improvements on the standard united-atoms model, where typically a 6-12 Lennard-Jones center of force is placed on top of the most significant atom, have been proposed. For instance, Errington *et al.* have used a Buckingham exp-6 potential [26], where 3 parameters are involved in each center of force and the repulsive part of the LJ interaction is replaced by the more correct exponential term. Chen *et al.* have introduced additional sites on the centers of the C-H bonds[27]. Also, Ungerer *et al.* [28] have obtained the AUA 4 model by reparameterizing the initial Anisotropic United Atom (AUA) model proposed by Toxvaerd[29] [30]. The AUA model consists of a displacement of the Lennard-Jones centers of force towards the hydrogen atoms, converting the distance of displacement into a third adjustable parameter,see figure 1.8 for the cases of a CH_2 and a CH_3 group, while in the case of the UA model the interaction site is located over the carbon atom. The net effect of this is to consider the influence of hydrogen

UNIVERSITAT ROVIRA I VIRGILI
IMPROVEMENT OF MONTE CARLO ALGORITHMS AND INTERMOLECULAR POTENCIALS FOR THE MODELLING OF ALKANOLS, ESTHERS, TRIOPHENES AND AROMATICS
Javier Pérez Pellitero
ISBN: 978-84-691-0377-7/DL: T.2195-2007

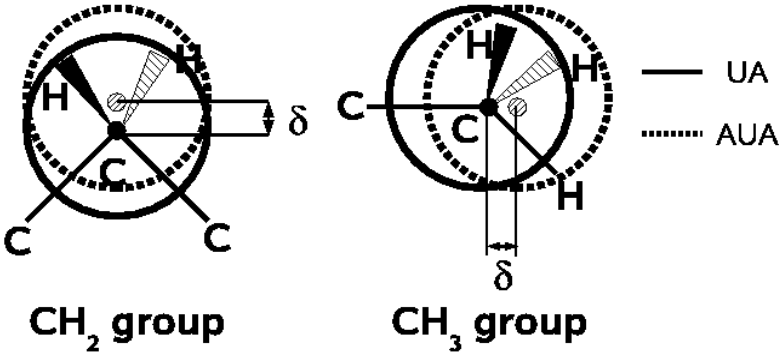

Figure 1.8: Schematic sketch of AUA model for a CH_2 and a CH_3 group. Centers of carbon atoms (used by UA model) are represented by filled circles, and the interaction centers by empty circles (AUA model)

atoms without explicitly increasing the number of interaction sites.

1.10 Simulation Techniques for Associating Fluids

1.10.1 Bias Sampling

While the accuracy of molecular simulation results depends either on the approximations done in the construction of the model or intermolecular potentials used to reproduce the interaction between different particles, the accuracy of the simulation itself depends on the sampling of the phase space performed during the simulation length. In particular, the extension of the phase space sampled in the simulations in the GCMC and GIBBS ensembles strongly depends respectively on the creation and destruction of particles and the transfer of particles between the different simulation boxes. At the same time, the acceptance probability of these MC steps depends on the structure, size and shapes of the different molecules. For instance, in the case of associating fluids some bonded configurations can result in having the system blocked due to the fact that they have energy enough to form agregates. Nonetheless these configurations represent only a small part of the phase space if we com-

UNIVERSITAT ROVIRA I VIRGILI
IMPROVEMENT OF MONTE CARLO ALGORITHMS AND INTERMOLECULAR POTENCIALS FOR THE MODELLING OF ALKANOLS, ESTHERS, TRIOPHENES AND AROMATICS
Javier Pérez Pellitero
ISBN: 978-84-691-0377-7/DL: T.2195-2007

pare it with the big amount of non bonded configurations. In this way, an efficient sample algorithm for associating flids will be one which is able to find the blocked configurations without being trapped by themselves.

Configurational Bias

Configurational bias Monte carlo, also referred to as CBMC, adresses in particular the case of long linear or branched molecules that can addopt numerous conformations. As it can be seen in figure 1.9, this method [51] [52] takes advantage of the fexibility of the molecule to grow it step by step, testing several possible random locations $r_k k = 1, 2, \ldots, k_{max}$ for the next atom. The final position of the new atom is selected among the tested locations with a probability:

$$p(r_i) = \frac{exp\left(-\beta U(r_i)\right)}{\sum_{k=1}^{K_{max}} exp\left(-\beta U(r_k)\right)} \tag{1.98}$$

where $U(r_k)$ denotes the increment of potential energy associated with the addition of a new atom in position r_k. The next process is applied to the next atom once a position r_i is selected, and so on until the end of the chain is reached. Since $U(r_k)$ includes the internal potential energy as well as the external energy, the molecule is thus reconstructed in a non-random way. Once the whole molecule has been regrown, the move is accepted according to a modified acceptance probability, so that its geometry is statistically representative at the temperature under consideration. The acceptance probability of these CBMC moves adapted for the AUA model can be found in the book by Ungerer *et al* [53]. The number of locations tested for each atom. K_{max} does not need to be the same for all atoms of the molecule. For instance, a greater number of test locations can be used for the first atom of the chain.

Reservoir Bias

Although configurational bias is applicable to flexible cyclic molecules [54], the constraint of closing the ring often makes for a poor average acceptance rate. As can be seen schematically in figure 1.10, a satisfactory way of solving this problem is to use a canonical reservoir of molecular conformations for the ring. This is a collection of molecular conformations in which the Boltzmann distribution of internal energies is respected. This means that the probability of occurrence of a given conformation in the reservoir is propor-

UNIVERSITAT ROVIRA I VIRGILI
IMPROVEMENT OF MONTE CARLO ALGORITHMS AND INTERMOLECULAR POTENCIALS FOR THE MODELLING OF ALKANOLS, ESTHERS, TRIOPHENES AND AROMATICS
Javier Pérez Pellitero
ISBN: 978-84-691-0377-7/DL: T.2195-2007

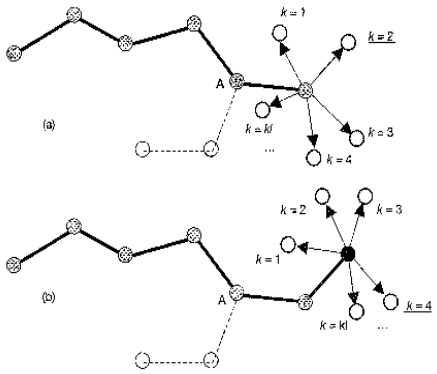

Figure 1.9: Schematic example of configurational bias applied to the regrowth of a segment of two atoms from an existing chain of six atoms (a) test of k_{max} positions to place the first new atom and selection of its position (here $k = 2$), (b) test of k_{max} positions for the second new atom and selection of its position (here $k = 4$) The dotted part of the chain is its previous configuration. From [53]

tional to $exp(-\beta U_{int})$. In practice, this reservoir is created by performing repeated internal moves in the molecules belonging to the reservoir. In the case of branched molecules, the reservoir bias results also interesting to improve the efficiency of CBMC algorithms by picking bending angles from the reservoir [55] instead of generating them repeatedly during the regrowth process. In the case of Gibbs ensemble transfers, Bourasseau [56] has also proposed the use of an additional preliminary biasing step to find suitable positions in the liquid. This methodology involves the following steps:

- In the first step, several random locations for the centre of mass r_k are tested with a very simple potential, e.g. a Lennard-Jones potential. One of these locations is selected on the basis of a similiar criterion as CBMC moves with a probability:

$$p(r_i) = \frac{exp\left(-\beta U_{LJ}(r_i)\right)}{\sum_{k=1}^{K_{max}} exp\left(-\beta U_{LJ}(r_k)\right)} \tag{1.99}$$

  where $U_{LJ}(r_k)$ is the interaction energy of the Lennard Jones centre with the system.

- in the second step, several molecular conformations c_k are randomly picked in the reservoir and tentatively inserted in the system with the

UNIVERSITAT ROVIRA I VIRGILI
IMPROVEMENT OF MONTE CARLO ALGORITHMS AND INTERMOLECULAR POTENCIALS FOR THE MODELLING OF ALKANOLS, ESTHERS, TRIOPHENES AND AROMATICS
Javier Pérez Pellitero
ISBN: 978-84-691-0377-7/DL: T.2195-2007

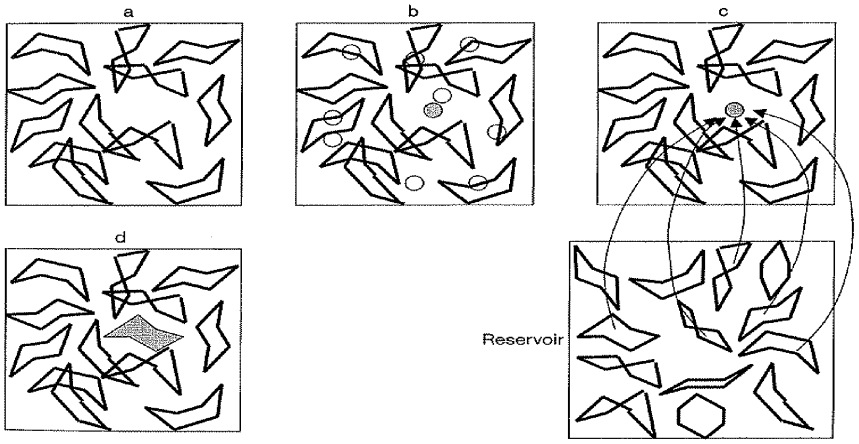

Figure 1.10: Schematic example of reservoir bias applied to the case of insertion of a new cyclohexane molecule in a box (a) initial configuration (b) test insertion of Lennard-Jones particles in several locations and selection of a favorable location (c) test of several molecular conformations taken from a canonical reservoir for insertion at the selected location (d) configuration after successful insertion. From [53]

centre of mass at the location identified in the first step, in a random orientation. One of these configurations is selected wit a probability:

$$p(c_i) = \frac{exp\left(-\beta U_{ext}(c_i)\right)}{\sum_{k=1}^{K_{max}} exp\left(-\beta U_{ext}(c_k)\right)} \tag{1.100}$$

- the move is accepted or rejected with an acceptance criterion which corrects for the bias introduced for the two first steps.[53]

The use of the reservoir bias move affords significant savings in computer time for cyclic molecules in condensed phases as well as for small flexible molecules with a limited number of different conformation such as short alcohols. In the case of rigid molecules, the reservoir bias is completely useless but the two-step procedure above described provides a very significant improvement compared with the unbiased moves.

UNIVERSITAT ROVIRA I VIRGILI
IMPROVEMENT OF MONTE CARLO ALGORITHMS AND INTERMOLECULAR POTENCIALS FOR THE MODELLING OF ALKANOLS, ESTHERS, TRIOPHENES AND AROMATICS
Javier Pérez Pellitero
ISBN: 978-84-691-0377-7/DL: T.2195-2007

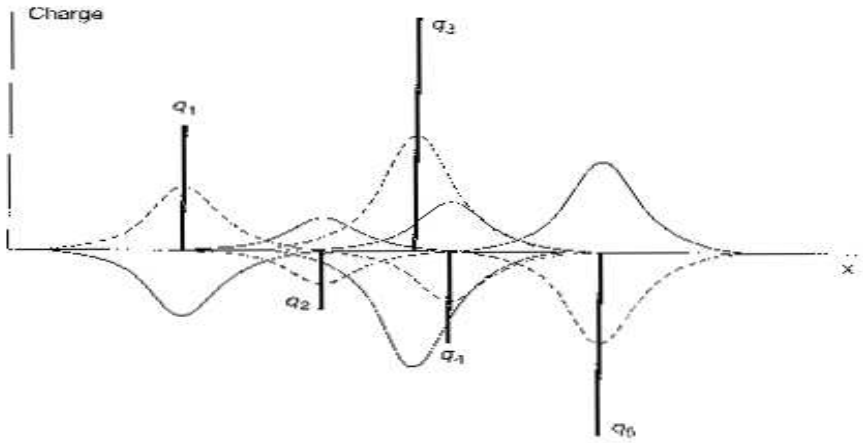

Figure 1.11: Electrostatic charge decomposition used in the Ewald summation method. Every point charge q_i (vertical bars) is associated with a screening gaussian distribution of opposite charge $q_i^{gauss}(r)$(full line). The distribution of point charges is expressed as the sum of screened charges ($q_i + q_i^{gauss}(r)$) which converges fast and the opposite distributions (-$q_i^{gauss}(r)$) (dotted lines) which is integrated by Fourier analysis. From [53]

1.10.2 Ewald Summation

The Ewald summation is a commonly used method in molecular simulation to compute the electrostatic energy with periodic boundary conditions. Basically, the problem arises from the fact that the electrostatic energy of an elementary charge with another charge is infinite when periodic boundary conditions are applied. The method works by splitting the lattice summation into a short-range part and a long-range part, where the long-range part is evaluated in a fast converging Fourier representation. The short range-part on the other hand works in real space and calculates particle-particle interactions of a Coulomb potential, originating from a Gausssian charge distribution, which results from the splitting procedure. Finally, a self-energy correction is applied, taking into account summation over all particles in Fourier space. Since The Ewald summation has been widely treated in the literature [57] [58] only a simplified acount will be provided here.

As is schematically shown in figure 1.11, the Ewald summation involves adding a Gaussian distribution of screening charges around every point charge q_i located at position r_i according to:

UNIVERSITAT ROVIRA I VIRGILI
IMPROVEMENT OF MONTE CARLO ALGORITHMS AND INTERMOLECULAR POTENCIALS FOR THE MODELLING OF ALKANOLS, ESTHERS, TRIOPHENES AND AROMATICS
Javier Pérez Pellitero
ISBN: 978-84-691-0377-7/DL: T.2195-2007

$$q_i^{gauss}(r) = -q_i \left(\frac{\alpha}{\sqrt{\pi}}\right)^3 exp\left(-\alpha^2|r - r_i^2\right) \tag{1.101}$$

so that the screened charges q_i^{sc} can be defined as:

$$q_i^{sc}(r) = q_i + q_i^{gauss}(r) \tag{1.102}$$

The whole charge of the Gaussian distribution is exactly opposite to the related point charge. The interaction energy U_j of any point charge q_j with the other charges may be computed from the electrostatic potential $\Phi(r)$ through:

$$U_j = q_j \Phi(r_j) \tag{1.103}$$

where the total electrostatic potential $\Phi(r_j)$ can be written using the general principle of superimposing states in electrostatics as the sum of the next terms:

- the contribution $\Phi^{'}(r_j)$ due to screened charges $q_i^{sc}(r_j)$
- the contribution $\Phi^{''}(r_j)$ due to Gaussian distributions $q_i^{gauss}(r_j)$ opposite in sign to the screening charges
- a correction factor for the screening charges of the point charge q_j itself

The first term $\Phi^{'}(r_j)$ is obtained by summing the contributions of all screened charges within a spherical cut-off which is generally taken as half the box length. This contibution converges faster because the screened charges $q_i^{sc}(r_j)$ are neutrally charged entities. It can be computed rather simply from standard library functions, making the computation of $\Phi^{'}(r_j)$ somewhat similar to LJ interactions. The second term $\Phi^{''}(r_j)$ is obtained after careful derivation using Fourier transformation. Its final expression involves a summation of terms in Fourier space, i.e. a summation over vectors $\overrightarrow{k} = \left(\frac{2\pi}{L_x}k_x, \frac{2\pi}{L_y}k_y, \frac{2\pi}{L_z}k_z\right)$:

$$\Phi^{''}(r_j = \sum_{k_x=-k_{ewmax}}^{k_{ewmax}} \sum_{k_y=-k_{ewmax}}^{k_{ewmax}} \sum_{k_z=-k_{ewmax}}^{k_{ewmax}} \phi^{''}(k_x, k_y, k_z) \tag{1.104}$$

UNIVERSITAT ROVIRA I VIRGILI
IMPROVEMENT OF MONTE CARLO ALGORITHMS AND INTERMOLECULAR POTENCIALS FOR THE MODELLING OF ALKANOLS, ESTHERS, TRIOPHENES AND AROMATICS
Javier Pérez Pellitero
ISBN: 978-84-691-0377-7/DL: T.2195-2007

where $\phi^{''}$ includes contributions for all screening charges $-q_i^{gauss}(r)$, and k_{ewmax} is an integer defining a cutoff distance in Fourier space.

The accuracy of the method depends on the approximations, made in short- and long-range parts of the method, which are characterized by α, the width of the Gaussian charge distribution, R_c, the cutoff-radius in the real-space part and k_{max}, the maximum wave number in the Fourier space part. For instance, in the case of liquid water, when a small simulation box is used $(20 - 25\mathring{A})$, the optimal α is approximately $0.3\mathring{A}^{-1}$, and $k_{ewmax} = 6 - 7$ proves sufficient to make the energy converge.

UNIVERSITAT ROVIRA I VIRGILI
IMPROVEMENT OF MONTE CARLO ALGORITHMS AND INTERMOLECULAR POTENCIALS FOR THE MODELLING OF ALKANOLS, ESTHERS, TRIOPHENES AND AROMATICS
Javier Pérez Pellitero
ISBN: 978-84-691-0377-7/DL: T.2195-2007

Chapter 2

Critical point estimation of the LJ pure fluid and binary mixtures

UNIVERSITAT ROVIRA I VIRGILI
IMPROVEMENT OF MONTE CARLO ALGORITHMS AND INTERMOLECULAR POTENCIALS FOR THE MODELLING OF ALKANOLS, ESTHERS, TRIOPHENES AND AROMATICS
Javier Pérez Pellitero
ISBN: 978-84-691-0377-7/DL: T.2195-2007

2.1 INTRODUCTION

The Lennard-Jones (LJ) fluid has been the subject of many numerical studies principally due to its widespread use as a model for nonpolar molecules. For example, atomistic fluids such as Argon are well represented by means of this model. The application of Monte Carlo simulation permits the calculation of the equilibrium properties of any LJ fluid. In particular, algorithms such as the Gibbs ensemble (GEMC) greatly simplifies the calculation of the phase equilibria[7]. Despite the simplicity of these methodologies, they generally have difficulties in the accurate location of critical points due to the appearance of long range density fluctuations. Instead, finite size scaling (FSS) studies, which were originally developed for spin models[46], need to be applied in order to take into account the finite-size effects appearing in the vicinity of the critical locus. These techniques provide an efficient way to obtain infinite volume critical parameters from simulations performed at finite-size conditions. For off-lattice systems, difficulties arise due to the asymmetry of the coexisting phases. In the absence of the particle-hole symmetry, the scaling fields are not identical with the physical fields. In the simplest asymmetric-fluid scaling description, the scaling fields are assumed to be combinations of the temperature and the chemical potential [59][17]. Recently[60], however, it has been found that a more complete scaling description of the fluid critical point should also involve the pressure in addition to the temperature and chemical potential. Several systems have been studied using the field mixing theory such as the square-well fluid[61] or the restricted-primitive model[49]. The combination of the FSS methodologies with histogram reweighting methods (HR) has proven to be an efficient tool to accurately locate the critical point. The use of the histogram reweighting methodology facilitates the calculation of the vapor-liquid equilibrium and critical point location by forming a joint density distribution calculated from the information of nearby conditions which can be extracted from a given set of simulations.

The location of the critical point of the pure LJ fluid has received considerable attention. For instance, critical values have been obtained for the reduced critical temperature T_c^* and the reduced critical density ρ_c^* by fitting GEMC data at subcritical temperatures to a scaling law using Ising universality class exponents and the Law of Rectilinear Diameters [62]. [63]. In their FSS studies Bruce and Wilding [14],[17] calculated the critical constants of the truncated LJ potential. More recently Caillol applied the same procedure to the full LJ potential on the surface of a four-dimensional hypersphere[18]. Potoff et al[20] considered the same case with conventional boundary conditions. However,

UNIVERSITAT ROVIRA I VIRGILI
IMPROVEMENT OF MONTE CARLO ALGORITHMS AND INTERMOLECULAR POTENCIALS FOR THE MODELLING OF ALKANOLS, ESTHERS, TRIOPHENES AND AROMATICS
Javier Pérez Pellitero
ISBN: 978-84-691-0377-7/DL: T.2195-2007

little work has been carried out for binary mixtures, although particular mention can be made of the aforementioned work by Potoff et al[20] where they extended the same calculations to LJ mixtures.

In the present chapter, we compare the combination of mixed-field theory with FSS studies for the full pure LJ fluid and LJ binary mixtures, with the fourth order cumulant calculation, also known as the Binder parameter. In the case of the Binder parameter two possibilities are considered, either the intersection of the Binder parameter for two different system sizes or the intersection of the Binder parameter with the known value for the system universality class combined with a FSS study. The Binder parameter provides an alternative route to estimating critical pressures and temperatures in a straightforward and direct way. Furthermore, Kim and Fisher [64] [65] have recently shown the possibility of performing a detailed near- critical coexistence study by means of the Binder parameter analysis. It should be stressed that the main goal of this work is not to improve on the already accurate predictions of the critical properties of the LJ systems, but rather to present and contrast the alternative methodology based on the Binder parameter with a view to the future application of these techniques to models for real mixtures. These models may include several Lennard Jones interaction sites in each molecule as well as electrostatic interactions and hence require considerably larger computational resources than the systems studied in this work. In addition, an alternative strategy for the histogram reweighting will be presented that is particularly suited for mixtures since it avoids the construction of histograms, a particularly costly operation in terms of computer memory when more than one component is present. We also estimate the line of critical points for a Lennard Jones system using the proposed Binder intersection method with FSS.

2.2 THEORY

In this section, a brief overview is given of histogram reweighting, mixed-field theory, Binder parameter and Finite Size Scaling methodologies.

UNIVERSITAT ROVIRA I VIRGILI
IMPROVEMENT OF MONTE CARLO ALGORITHMS AND INTERMOLECULAR POTENCIALS FOR THE MODELLING OF ALKANOLS, ESTHERS, TRIOPHENES AND AROMATICS
Javier Pérez Pellitero
ISBN: 978-84-691-0377-7/DL: T.2195-2007

2.2.1 Histogram Reweighting

The histogram reweighting technique (HR) has been widely used to compute phase diagrams and free energies of different fluids. In this work HR has been used to calculate the VLE and also to facilitate the prediction of the critical constants by means of the FSS techniques which was explained in detail in chapter 1. The technique was introduced by Ferrenberg and Swendsen [15][16] and is based on the fact that a single simulation can give information about the properties of nearby state points. In the original formulation of the methodology, histograms at different conditions from different simulations are combined to improve the statistics, thus extending the range of applicability of the method. During the simulation we collect information in multiple uncorrelated states by recording the total energy of the system as well as the number of particles of each compound $N_1$and N_2.

2.2.2 VLE calculation

To determine vapor-liquid equilibrium, equality of chemical potentials, temperature and pressure must be imposed in the system. In the GCMC ensemble the pressure is related to the partition function of the grand canonical ensemble, Ξ, as follows,

$$pV = kT \ln \Xi' + constant \tag{2.1}$$

where Ξ' is the partition function determined from the simulations with histogram reweighting, where an arbitrary constant is included.

When phase coexistence occurs, a bimodal distribution of densities is expected where the area under each peak is the same indicating equality of pressures in each phase. VLE is hence determined for a given temperature by tuning the chemical potentials until equality of pressures is obtained between the phases. To determine VLE, we take advantage of a simulation in the criticla region in order to bridge the liquid and vapor regions. Furthermore, this critical simulation will allow us to directly estimate the critical locus using either the mixed field theory or the Binder parameter to be described later.

Finally, to deal with the binary systems of interest, the absolute value of the grand partition function must be evaluated in order to determine the absolute pressure. To allow for the calculation of the constant present in Eqn. 2.1, an

UNIVERSITAT ROVIRA I VIRGILI
IMPROVEMENT OF MONTE CARLO ALGORITHMS AND INTERMOLECULAR POTENCIALS FOR THE MODELLING OF ALKANOLS, ESTHERS, TRIOPHENES AND AROMATICS
Javier Pérez Pellitero
ISBN: 978-84-691-0377-7/DL: T.2195-2007

extrapolation to low density is carried out taking as reference the ideal gas[20] [66].

2.2.3 Mixed-Field Theory

As is described in detail in section 1.7.5, the FSS technique holds that the coarse-grained properties of systems near the critical point are universal. The concept of universality can be characterized through the probability distribution functions of observables such as density and energy if the system sizes are large enough. In the case of small system sizes, the critical properties are function of the box length if the system sizes are large enough. In the case of small systems, the critical properties depends on the box length L as well as on the scaling field measuring the deviation from criticality. For asymmetric models, like the pure LJ fluid and their mixtures, the mixed-field theory described in section1.7.7 must be introduced in order to take into account the effect of the density and energy fields.

In this work we adopted the simple scaling description of Bruce and Wilding [17] and ignored the effects of pressure in the scaling fields. The parameters s and r are system-specific quantities taking into account the contributions of temperature and chemical potential to each of the fields. Conjugate to the two relevant scaling fields are scaling operators $\mathcal{M}$ and $\mathcal{E}$, which are comprised of linear combinations of the particle density ρ and energy density u:

$$\mathcal{M} = \frac{1}{1-sr}[\rho - su] \tag{2.2}$$

$$\mathcal{E} = \frac{1}{1-sr}[u - r\rho] \tag{2.3}$$

For models with Ising symmetry , $\mathcal{M}$ is the magnetization while $\mathcal{E}$ is the energy density. The joint distribution of density and energy is simply related to the joint distribution of mixed operators by:

$$P_L(\rho, u) = \frac{1}{1-sr} P_L(\mathcal{M}, \mathcal{E}) \tag{2.4}$$

For pure fluids and their mixtures belonging to the Ising universality class,

UNIVERSITAT ROVIRA I VIRGILI
IMPROVEMENT OF MONTE CARLO ALGORITHMS AND INTERMOLECULAR POTENCIALS FOR THE MODELLING OF ALKANOLS, ESTHERS, TRIOPHENES AND AROMATICS
Javier Pérez Pellitero
ISBN: 978-84-691-0377-7/DL: T.2195-2007

the critical behavior of the ordering operator distribution $\mathcal{M}$ assumes a scaling form that matches the universal order parameter distribution $p_m^*(x)$ for the Ising model [47]. This means that at the finite critical point of our system, the distribution of our scaling operator $\mathcal{M}$, previously defined as a linear combination of density and energy, should coincide with the Ising model magnetization distribution. The procedure followed to determine the critical point of the finite systems according to this methodology was previously described in section 1.7.7.

2.2.4 Binder parameter

In order to locate the critical point, an alternative methodology has been employed. The Binder cumulant parameter[23] U_L was calculated for different volume sizes using an equal area construction for both phases in equilibrium and is defined as follows:

$$U_L = \frac{\langle m^4 \rangle}{\langle m^2 \rangle^2} \tag{2.5}$$

with $m = \phi - \langle \phi \rangle$ being ϕ a suitable order parameter, in our case density or composition. As it is explained in more detail in section 1.7.8the Binder parameter provides a dimensionless measure of the shape of the order parameter distribution function and approaches asymptotically either a value of 1 if a bimodal density distribution is found or a value of 3 when we deal with supercritical fluids. In the critical point, the Binder parameter is expected to have a universal value $U_L = 1.6035$ at the critical point [49] for the Ising universality class. This means that the infinite system size critical point can be identified as the point where U_L becomes system-size independent, being this point where cumulants from different sizes intersect. This is the first method that we use in order to estimate the infinite size critical point from the Binder parameter.

In this work we propose a second method for estimating the critical point. By taking into account the order parameter distribution based definition of the Binder parameter, we expect the universal value of this parameter to be also valid as an estimate of the apparent finite critical temperature. This fact allows us to propose a FSS study of this parameter in order to obtain the infinite system size critical point in a similar way to the finite critical temperature estimated by mixed-field theory.

In the results section we will present both methods for estimating the in-

UNIVERSITAT ROVIRA I VIRGILI
IMPROVEMENT OF MONTE CARLO ALGORITHMS AND INTERMOLECULAR POTENCIALS FOR THE MODELLING OF ALKANOLS, ESTHERS, TRIOPHENES AND AROMATICS
Javier Pérez Pellitero
ISBN: 978-84-691-0377-7/DL: T.2195-2007

finite system size critical point. That is, either by locating the intersection for several system sizes, or as a FSS extrapolation of the estimates for the finite critical temperature taken from the intersection with the Ising universal value.

2.2.5 Finite Size Scaling

After determining the apparent critical conditions for each of the system sizes, either by using where the Binder parameter intersects the universal parameter or by a mixed field study, the critical constants are expected to follow known scaling laws. [14] For instance, the temperature of the finite system is expected to vary near the critical point with system size as:

$$\langle T\rangle_c(L) - \langle T\rangle_c(\infty) \sim L^{-(\theta+1)/\nu} \tag{2.6}$$

where $\Theta = 0.54$ and $\nu = 0.629$ [67] [68].

The critical density of the finite system is expected to vary near the critical point with system size as:

$$\langle \rho\rangle_c(L) - \langle \rho\rangle_c(\infty) \sim L^{-(d-1/\nu)} \tag{2.7}$$

where d is the dimensionality of the system.

For a mixture, [20] a similar scaling behavior is seen for the critical mole fraction:

$$\langle x\rangle_{1c}(L) - \langle x\rangle_{1c}(\infty) \sim L^{-(d-1/\nu)} \tag{2.8}$$

Since the pressure can be defined in terms of energy density, we scale it in the same way as the energy like operator [20]:

$$\langle p\rangle_c(L) - \langle p\rangle_c(\infty) \sim L^{-(d-1/\nu)} \tag{2.9}$$

By plotting the finite critical values using these functions, an extrapolation can be made to estimate the infinite system size value, as shown in the results

UNIVERSITAT ROVIRA I VIRGILI
IMPROVEMENT OF MONTE CARLO ALGORITHMS AND INTERMOLECULAR POTENCIALS FOR THE MODELLING OF ALKANOLS, ESTHERS, TRIOPHENES AND AROMATICS
Javier Pérez Pellitero
ISBN: 978-84-691-0377-7/DL: T.2195-2007

section.

2.3 Model and simulation details

The intermolecular interaction between non-bonded pairs of particles was calculated using the full LJ potential given by Eqn. 1.96:

The LJ parameters were used to obtain reduced quantities $T^* = k_bT/\epsilon$, $\rho^* = \sigma^3/\rho$ and $p^* = p\sigma^*/\epsilon$. In the present work, we have studied the properties of the untruncated potential. To approximate infinite thermodynamic systems with finite-size systems we employed periodic boundary conditions with long-range corrections (LRC). A cutoff radius of half the box length was used.[57]

In the case of binary mixtures, the Lorentz-Berthelot combining rules [11] were used to calculate the cross potential parameters for the mixture. For the binary LJ mixture we chose a mixture having $\sigma_1 = \sigma_2 = 1.0$ and $\epsilon_1 = 1.0, \epsilon_2 = 0.5$ to allow for comparison with the only previous study where FSS has been applied. [20]

In the case of the pure LJ fluid, different sets of GCMC simulations were performed in order to sample phase space. The calculation of the phase diagram was extended to subcritical temperatures only for the smaller systems with reduced volume $V^* = 100, 250, 750$, while in the case of the bigger systems $V^* = 1000, 1500, 3000$ the computational effort was centered only near the critical point. During the simulation, we stored the number of particles and the configurational energy every 500 MC. Applying the cumulant intersection calculation to the two smaller system sizes results in a very fast and straightforward location of the critical point. For the smaller systems, runs around 100 million MC steps were enough to obtain accurate statistics, while for the larger systems runs were extended up to 900 million MC steps.

For the selected binary LJ mixture, the systems considered were not as large as in the case of the pure LJ fluid due to the higher computational time required. The systems considered were $V^* = 150, 250, 350, 500, 1000$. The phase diagram was extended down in pressure by adding simulations near the predicted coexistence chemical potentials when the density distributions obtained became unreliable. For the smaller systems $V^* = 150, 250, 350$ the length of the runs was 100 million MC steps while in the case of $V^* = 500, 1000$ it was set to 250 million MC steps. During the simulation we stored the number of particles and the configurational energy every 1000 MC steps.

UNIVERSITAT ROVIRA I VIRGILI
IMPROVEMENT OF MONTE CARLO ALGORITHMS AND INTERMOLECULAR POTENCIALS FOR THE MODELLING OF ALKANOLS, ESTHERS, TRIOPHENES AND AROMATICS
Javier Pérez Pellitero
ISBN: 978-84-691-0377-7/DL: T.2195-2007

2.4 Results and Discussion

2.4.1 Pure Fluid

In the case of the untruncated LJ potential, different estimates are found for the critical point depending on the applied methodology, see Table 2.1. The first studies are based on GEMC data which were extrapolated by means of scaling laws to the critical point. Following this procedure, Smit [13] reported in 1992 $T_c^* = 1.316(6)$ and $\rho_c^* = 0.304(6)$ while Lotfi [69] also in 1992 gave $T_c^* = 1.310$ and $\rho_c^* = 0.314$. Three more FSS studies can be found in the bibliography. The work by Potoff and Panagiotopoulos [20] in 1998 reported $T_c^* = 1.3120(6)$ and $\rho_c^* = 0.316(1)$ considering periodic boundary conditions. Shi and Johnson [19] performed a FSS study for the long-range corrected fluid with a cutoff radius $r_c = 5.0\sigma$ They predicted $T_c^* = 1.3145(2)$ and $\rho_c^* = 0.316(1)$. The other existing FSS work by Caillol [18] in 1998 considers the full LJ potential on the surface of a four- dimensional hypersphere. This technique does not require long-range corrections. Finally, in another work, Potoff and Panagiotopoulos[70] predicted $T_c^* = 1.311(2)$ and $\rho_c^* = 0.316(2)$ using a methodology based on the calculation of the surface tension.

After determining the apparent critical conditions for each of the system sizes, either by using where the Binder parameter intersects the universal parameter or by a mixed field study, the critical constants are expected to follow known scaling laws. [14]

In the present study we have compared mixed-field theory with the cumulant intersection calculation.

In figure 2.1 we present the phase diagram of the pure LJ fluid calculated with a system volume $V^* = 250$. We have computed coexistence densities from the equal area construction. The results agrees with the GEMC data of Smit [63] as well as with the GCMC data from [70]. It should be noted that in the case of ref. [70] a much larger system size is used which permits the authors to approach more closely the critical point. Away from the critical region we do not observe any significant difference between the results obtained at different system sizes.

Figure 2.2 shows the matching between the order operator distribution for $V^* = 1500$ at the apparent critical point and the universal distribution for the

UNIVERSITAT ROVIRA I VIRGILI
IMPROVEMENT OF MONTE CARLO ALGORITHMS AND INTERMOLECULAR POTENCIALS FOR THE MODELLING OF ALKANOLS, ESTHERS, TRIOPHENES AND AROMATICS
Javier Pérez Pellitero
ISBN: 978-84-691-0377-7/DL: T.2195-2007

Source	T_c^*	ρ_c^*	**Type**
Wei and Johnson[19]	1.3145(2)	0.316(1)	Mixed-Field Th. + FSS
Potoff and Panagiotopoulos[20]	1.3120(7)	0.316(1)	Mixed-Field Th. + FSS
Caillol[18]	1.326(2)	0.316(2)	Mixed-Field Th. + FSS
Potoff and Panagiotopoulos[70]	1.311(2)	0.316(2)	Surface tension + FSS
Lotfi et al. [69]	1.310	0.314	Power Law
Smit [13]	1.316(6)	0.304 (6)	Power Law
This work	1.3123(6)	0.3174 (6)	Mixed-Field Th. + FSS
This work	1.3126(6)	0.3174 (6)	Cumulant + FSS
This work	1.313(1)	0.317 (1)	Cumulant Intersection

Table 2.1: **Critical constants estimations of the pure LJ fluid**

Ising three dimensional universality class[47]. The agreement obtained between our simulation results and the reference Ising model data is excellent, as observed in previous works for this system. It should be noted, however, that there exists a small deviation between the two curves, as can also be seen in previous works. This difference could be due to the fact that pressure mixing has not been incorporated in the scaling fields [71]

We have calculated the critical temperature by extrapolating to infinite volume the apparent critical temperatures found for different system sizes. The results are shown in figure 2.3. We obtain $T_c^* = 1.3123(6)$ and $\rho_c^* = 0.3174(6)$. Our estimate of the critical temperature is in very good agreement with Potoff and Panagiotopoulos [20] who predicted $T_c^* = 1.3120(6)$ and $\rho_c^* = 0.316(1)$. As was expected, the prediction of the critical temperature of Shi and Johnson [19] $T_c^* = 1.3145(2)$ and $\rho_c^* = 0.316(1)$ is slightly higher due to the fact that they considered a cutoff radius $r_c = 5.0\sigma$ instead of half the simulation box. Meanwhile, the prediction of Caillol $T_c^* = 1.326(2)$ on the surface of a four-dimensional hypersphere differs significantly from our results.

As can be observed, in the case of the critical density, the dependence on the system size is lower than in the case of the temperature. This fact can be attributed to a lower degree of mixing in the corresponding field.

We have also determined the critical temperature and density $T_c^* = 1.313(1)$ and $\rho_c^* = 0.317(1)$ using the cumulant intersection methodology or Binder parameter. The critical density has been determined by taking the average from the simulation box at the largest system size. The validity of this calculation is supported by the weak dependence of the critical density observed in the FSS studies. As will be seen later, this is not true in the case of the binary mixture.

UNIVERSITAT ROVIRA I VIRGILI
IMPROVEMENT OF MONTE CARLO ALGORITHMS AND INTERMOLECULAR POTENCIALS FOR THE MODELLING OF ALKANOLS, ESTHERS, TRIOPHENES AND AROMATICS
Javier Pérez Pellitero
ISBN: 978-84-691-0377-7/DL: T.2195-2007

In figure 2.4 we show the intersection of the Binder parameter for different system sizes. As can be seen, due to the finite size of our simulations we have observed a slight dependence in the intersections as the volume of the system is increased. This fact is attributed to the correction terms present in the formulation of U_L when the size is too small [72]. As a consequence, the value of $U_L$is slightly shifted from the universal value obtained for the Ising model $U_L = 1.6035$[73], this value is approached when the system size is increased. [73]. The higher dependence of this value if compared with other models like the restrictive primitive model [49] or the square well fluid [74] where a value of $U_L \approx 1.6875$ is obtained, can likely be attributed to the higher asymmetry of the Lennard-Jones model [61].

In figure 2.3 are plotted estimates for the finite system size critical temperature taken from the intersection of the Binder parameter with the Ising universal value.We have found for the different system sizes that the values for the temperature corresponding to the universal value of the Binder parameter agree very well with the apparent finite critical temperatures obtained by means of the mixed-field theory. This correspondence could be expected taking into account that the value of U_L provides a dimensionless measure of the shape of the order parameter distribution function analogous to the mixed-field calculation. The scaling of the former locates the critical point at $T_c^* = 1.3126(6)$ and $\rho_c^* = 0.3174(6)$, values which are in complete agreement with the mixed-field theory. Since we use the same set of Monte Carlo data in both the mixed-field FSS as well as the Binder parameter intersection with FSS, the resulting statistical uncertainties are indicative of the relative efficiency of each method. As can be seen from the results, the statistical errors are comparable hence suggesting that the efficiency of both techniques is also comparable. In other words, the proposed intersection method provides the same statistical efficiency as the mixed-field theory and at the same time is simpler to apply.

Despite the fact that the cumulant intersection methodology provides slightly shifted values for the critical parameters when not large enough systems are used, this methodology allows a much more straightforward way to locate the critical temperature with a very reasonable level of accuracy $\approx 0.2\%$.

2.4.2 Binary mixture

We have extended our analysis to LJ binary mixtures, where to our knowledge there only exists one previous FSS study[20] . We have selected the same conditions as used in this work in order to be able to directly compare results.

UNIVERSITAT ROVIRA I VIRGILI
IMPROVEMENT OF MONTE CARLO ALGORITHMS AND INTERMOLECULAR POTENCIALS FOR THE MODELLING OF ALKANOLS, ESTHERS, TRIOPHENES AND AROMATICS
Javier Pérez Pellitero
ISBN: 978-84-691-0377-7/DL: T.2195-2007

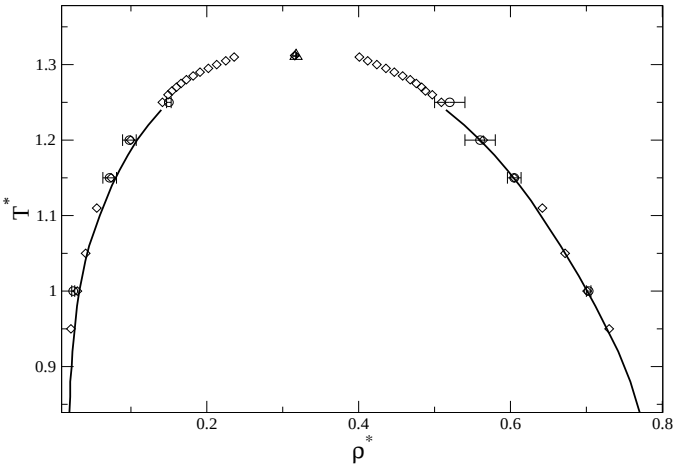

Figure 2.1: LJ pure phase diagram $V^* = 250$ HR GCMC results of this work (solid line), HR data from [70] and GEMC literature results (circles)[63] The triangle represents our estimate of the critical point of the infinite system. Unless shown, errors are smaller than the symbol size.

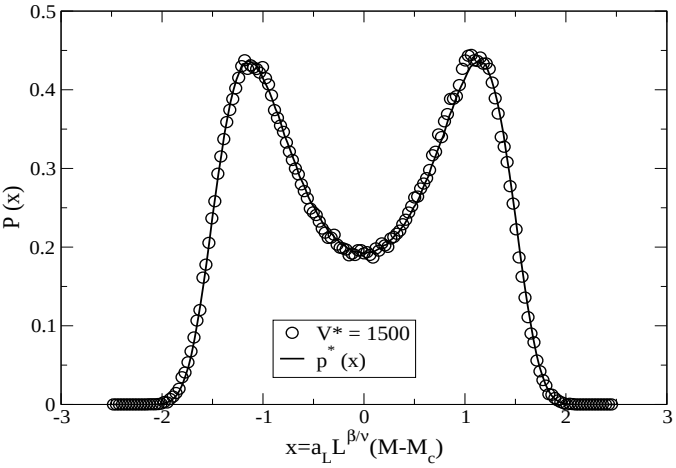

Figure 2.2: Ordering operator distribution at the apparent critical conditions for $V^* = 1500$

UNIVERSITAT ROVIRA I VIRGILI
IMPROVEMENT OF MONTE CARLO ALGORITHMS AND INTERMOLECULAR POTENCIALS FOR THE MODELLING OF ALKANOLS, ESTHERS, TRIOPHENES AND AROMATICS
Javier Pérez Pellitero
ISBN: 978-84-691-0377-7/DL: T.2195-2007

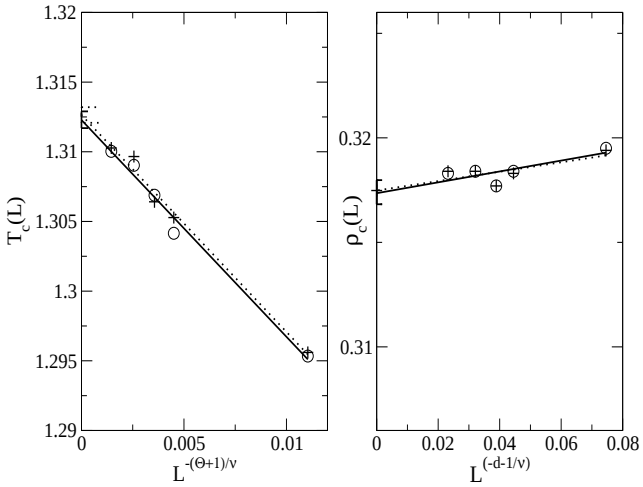

Figure 2.3: Apparent critical temperature $T_c^*(L)$ expressed as a function of $L^{-(\Theta+1)/\nu}$ and apparent critical density $\rho_c^*(L)$ expressed as a function of $L^{-(d-1/\nu)}$ Empty circles are mixed-field results, crosses are cumulant results. Solid lines represent least- squares fits of the mixed-field data, dotted lines represent least-squares fits of the Binder parameter data.

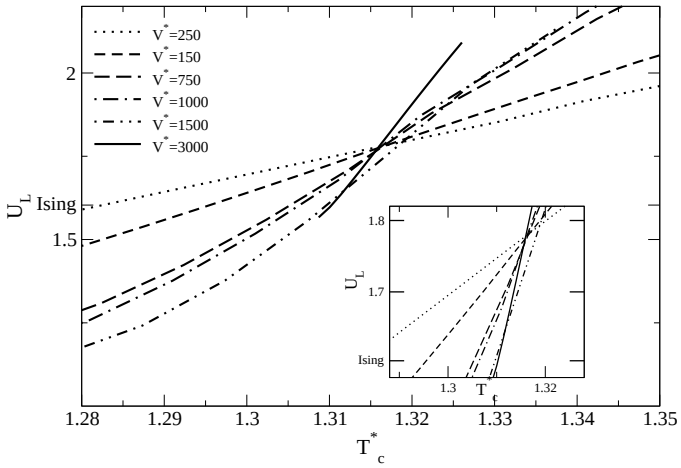

Figure 2.4: Critical temperature determination using the Binder cumulant intersection method

UNIVERSITAT ROVIRA I VIRGILI
IMPROVEMENT OF MONTE CARLO ALGORITHMS AND INTERMOLECULAR POTENCIALS FOR THE MODELLING OF ALKANOLS, ESTHERS, TRIOPHENES AND AROMATICS
Javier Pérez Pellitero
ISBN: 978-84-691-0377-7/DL: T.2195-2007

The use of histogram reweighting techniques allows us to extend the calculation of the pressure-composition diagrams to nearby temperatures from a given set of simulations at some fixed temperature. In figure 2.5 we show the diagram calculated at $T^* = 1.00$ for the system $V^* = 250$ where we compare with GEMC data. In figure 2.6 we have extended the calculation of the phase diagrams to temperatures $T^* = 0.86$ and $T^* = 1.14$ using the same set of original simulations at $T^* = 1.00$ for the smallest system $V^* = 150$, which implies an important advantage if compared with the GEMC methodology. In this case it is interesting to remark that the use of this methodology allows us to calculate in a straightforward way the line of critical points applying a FSS study of the finite critical parameters determined with the cumulant methodology from the systems $V^* = 150$ and $V^* = 250$, see figure 6. The critical locus is determined until we reach the limit of the fluctuations for the larger system used in the calculations, in this case $V^* = 250$, then additional simulations in the critical region are required in order to cover the full range of temperatures.

We have calculated critical parameters by applying both, mixed-field theory and cumulant intersection calculations. As in the case of the pure LJ fluid, for the mixed field theory we have calculated the apparent critical parameters by tuning the chemical potential until the ordering operator distribution collapses onto the universal distribution $p_m^*(x)$. We have found $p_c^* = 0.152(1)$, $\rho_c^* = 0.401(3)$ and $x_c^* = 0.458(2)$ in good agreeement with the work of Potoff and Panagiotopoulos. As can be seen in figure 2.7, the dependence of the apparent critical composition and density is stronger than in the case of the pure fluid. Potoff and Panagiotopoulos attributed this fact to the presence of larger-field mixing contributions from the energy-like operator in the mixture. Regarding the critical pressure, we find that it appears to scale in the same way as the density and the composition, since we have obtained what appears to be a linear dependence of $p_c^*(L)$ vs $L^{-(d-1/\nu)}$, see figure 2.7, although the relatively large errors as compared to the pure systems make it difficult to be conclusive. As can be seen in figure 2.8 we have also calculated the critical parameters using the cumulant intersection methodology. Critical pressure $p_c^* = 0.151(1)$ has been determined from the intersection of the different curves calculated at different system sizes. The values of the critical density and composition calculated from the average of the box of the larger system size present a higher deviation due to the previously mentioned stronger system-size dependence of these values. In this case, the accuracy of the intersection is lower due to the large increase in the configurational space.

The critical point has been located using the Binder cumulant methodology. As in the case of the pure Lennard-Jones fluid, we have also scaled the apparent critical pressures found at the Ising universal value of the Binder parameter. We have determined $p_c^* = 0.1512(9)$, $\rho_c^* = 0.399(4)$ and $x_c^* = 0.458(2)$, which are in excellent agreement with mixed field theory and show a similar

UNIVERSITAT ROVIRA I VIRGILI
IMPROVEMENT OF MONTE CARLO ALGORITHMS AND INTERMOLECULAR POTENCIALS FOR THE MODELLING OF ALKANOLS, ESTHERS, TRIOPHENES AND AROMATICS
Javier Pérez Pellitero
ISBN: 978-84-691-0377-7/DL: T.2195-2007

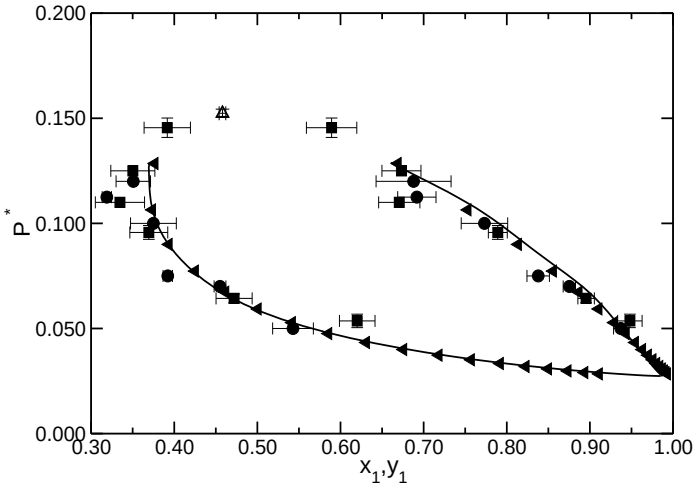

Figure 2.5: P-xy diagram for the binary LJ mixture. HR data from this work (solid line). HR data from [20] (filled triangles) GEMC data [20](circles). GEMC data [75](squares). The open triangle represents the prediction of the critical point of this work.

statistical error as for the mixed-field theory showing a similar efficiency for both techniques.

The results are, as in the case of the pure LJ fluid, in good agreement with the study by Potoff [20] who predicted $p_c^* = 0.1522(9)$, $\rho_c^* = 0.406(2)$ and $x_c^* = 0.459(3)$ with the use of the mixed-field theory. The results obtained using the mixed-field theory suggests, as stated in section 1.7.7, that the mixture belongs to the same universality class as the pure fluid. This fact is shown by the good fits obtained for the universal fixed point ordering operator distributions. We have also found the expected linear dependence of the aparent critical pressure as a function of $L^{-(d-1/\nu)}$. In the case of the critical density, the dependence of $\rho_c^*(L)$ is in this case slightly higher. The aparent critical composition also exhibits a linear dependence with $L^{-(d-1/\nu)}$. Finally, regarding the intersections of the Binder parameter they seem to approach again the universal Ising value.

2.4.3 H_2S/n-hexane mixtures

After testing the methodology with the LJ fluid, the calculations have been extended to the $H_2S/n-hexane$ mixture. As mentioned before, due to the

UNIVERSITAT ROVIRA I VIRGILI
IMPROVEMENT OF MONTE CARLO ALGORITHMS AND INTERMOLECULAR POTENCIALS FOR THE MODELLING OF ALKANOLS, ESTHERS, TRIOPHENES AND AROMATICS
Javier Pérez Pellitero
ISBN: 978-84-691-0377-7/DL: T.2195-2007

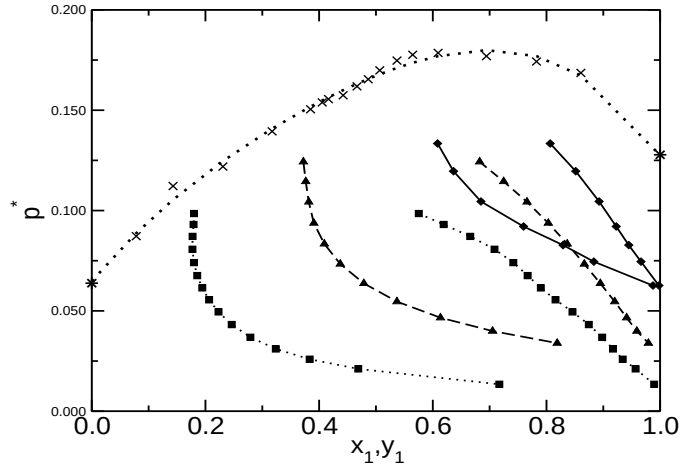

Figure 2.6: P-xy diagram for the binary LJ mixture at $T^* = 1.00$(triangles) and $T^* = 1.14$(diamonds), $T^* = 0.86$(squares). The crosses represent the critical points calculated from the FSS study for different temperatures. The stars are the predictions for the pure fluid critical pressure obtained in [20] while the dotted line is the regression of the data.

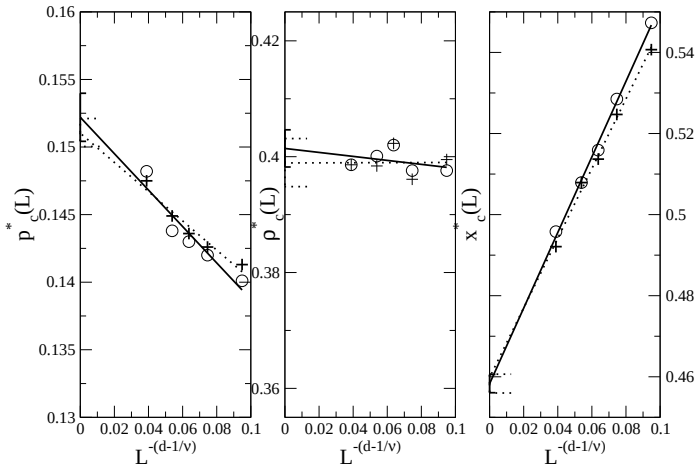

Figure 2.7: Apparent critical pressure $p_c^*(L)$, apparent critical density $\rho_c^*(L)$, and apparent critical composition $x_c^*(L)$ expressed as a function of $L^{-(d-1/\nu)}$. The lines represent least-squares fits of the data

UNIVERSITAT ROVIRA I VIRGILI
IMPROVEMENT OF MONTE CARLO ALGORITHMS AND INTERMOLECULAR POTENCIALS FOR THE MODELLING OF ALKANOLS, ESTHERS, TRIOPHENES AND AROMATICS
Javier Pérez Pellitero
ISBN: 978-84-691-0377-7/DL: T.2195-2007

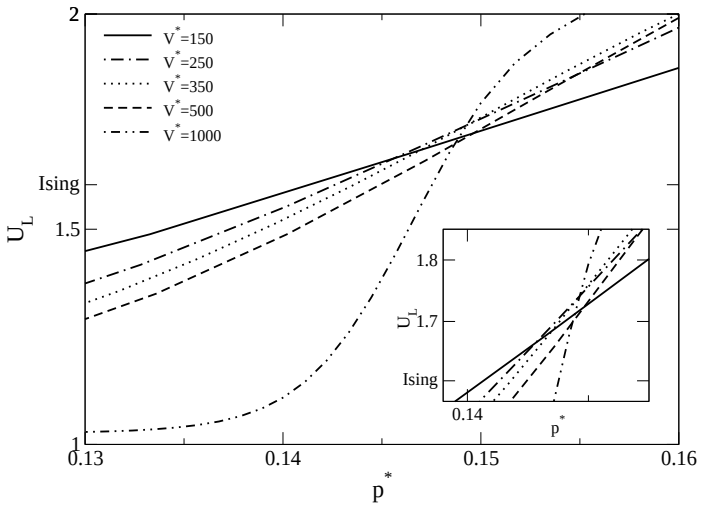

Figure 2.8: Critical pressure determination using the Binder cumulant intersection method

Source	p_c^*	ρ_c^*	x_c^*	**Type**
Potoff and Panag.[20]	0.1522(9)	0.406(2)	0.459(3)	Mixed-Field Th.
This work	0.152(1)	0.401(3)	0.458(2)	Mixed-Field Th. + FSS
This work	0.1512(9)	0.399(4)	0.458(2)	Cumulant + FSS
This work	0.151(1)	0.39(1)	0.49(1)	Cumulant Intersection

Table 2.2: **Critical constants estimations of the binary LJ mixture**

UNIVERSITAT ROVIRA I VIRGILI
IMPROVEMENT OF MONTE CARLO ALGORITHMS AND INTERMOLECULAR POTENCIALS FOR THE MODELLING OF ALKANOLS, ESTHERS, TRIOPHENES AND AROMATICS
Javier Pérez Pellitero
ISBN: 978-84-691-0377-7/DL: T.2195-2007

high acidity and toxicity of H_2S, little is known about the physichochemical properties of hydrogen sulfide at the required conditions. Data on phase equilibria can be found from estimates derived from only a few experimental data combined with correlations and equations of state [76] [77]. Using the Kristof&Liszi [78] intermolecular potential, previous works have been done with molecular simulation obtaining good results for pure H_2S [79]. The phase diagram has been determined at $T = 423.15K$ to allow for comparison with previous GEMC data [53]. As in the case of the binary mixture, the P-xy phase diagram of the binary LJ mixture has been determined from the smallest system sizes, while for the bigger systems computational effort was put only near the critical point in order to complete the FSS study. In this case, special attention must be paid to the system sizes taking into account the increase of computational time due to the higher complexity of the real model. To reflect this increase,for the smallest system $V^* = 250$, simulations performed in the liquid phase required approximately 1 CPU hour per 10 million MC steps in a 2800 MHz AMD processor. The results are shown in figure 2.9 for the system $V^* = 250$. The critical pressure was determined from the cumulant intersection (figure 2.10). Once the critical pressure is known critical density and composition can be calculated. The mixed field theory has also been used to confirm the result obtained with the cumulant intersection methodology (figure2.11). In table 2.3, comparison is given between the results obtained using both methodologies.

Work	**Type**	P_c^***[Mpa]**	ρ_c^***[kg/m$_3$]**	$\mathbf{x}_{H_2S_c}$
This work	Cumulant	9.7(2)	305(3)	0.80(1)
This work	Mixed Field	9.86(9)	309(3)	0.820(9)
GEMC data	Power Law	9.79	304.8	0.845

Table 2.3: **Critical parameters of H_2S/n-hexane mixture**

2.4.4 Conclusions

We have estimated the critical point of the pure Lennard Jones fluid. To determine the critical parameters we applied the fourth order cumulant or Binder parameter intersection method as well as , the Binder parameter intersection with the universal value and mixed-field theory combined with Finite Size Scaling. We find excellent agreement between the results obtained with all three methods and also with previous Finite Size Scaling Studies of the LJ crit-

UNIVERSITAT ROVIRA I VIRGILI
IMPROVEMENT OF MONTE CARLO ALGORITHMS AND INTERMOLECULAR POTENCIALS FOR THE MODELLING OF ALKANOLS, ESTHERS, TRIOPHENES AND AROMATICS
Javier Pérez Pellitero
ISBN: 978-84-691-0377-7/DL: T.2195-2007

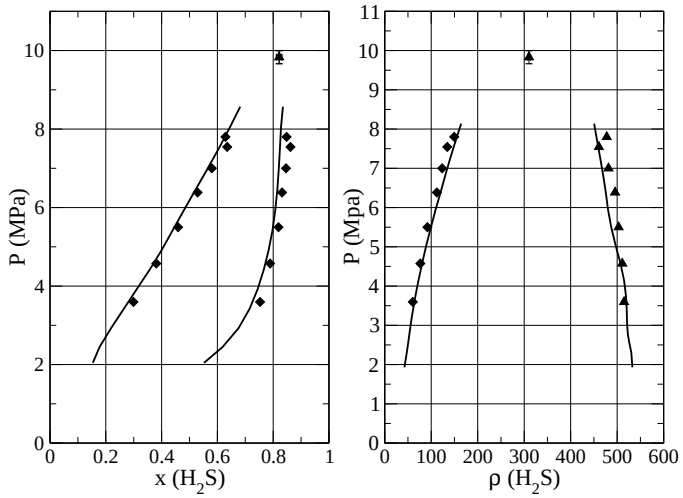

Figure 2.9: Pressure composition and Pressure-density diagram for H_2S/n-hexane mixture obtained for the system $V^* = 250$. Histogram reweighting (solid lines). GEMC (diamonds). The triangles represents the critical point prediction.

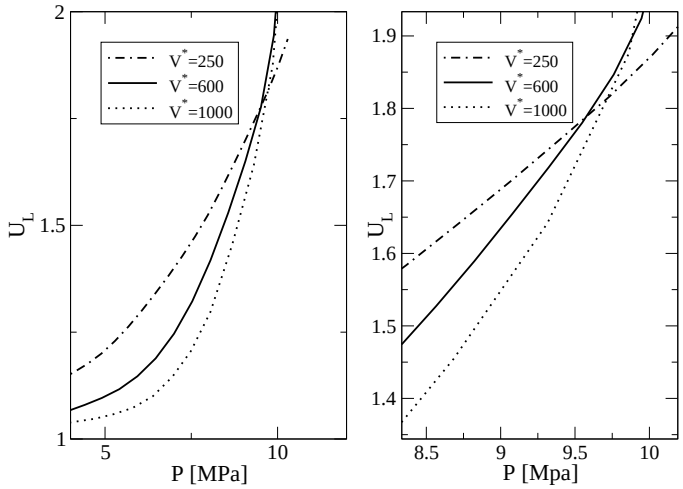

Figure 2.10: Critical pressure determination using the Binder cumulant method

UNIVERSITAT ROVIRA I VIRGILI
IMPROVEMENT OF MONTE CARLO ALGORITHMS AND INTERMOLECULAR POTENCIALS FOR THE MODELLING OF ALKANOLS, ESTHERS, TRIOPHENES AND AROMATICS
Javier Pérez Pellitero
ISBN: 978-84-691-0377-7/DL: T.2195-2007

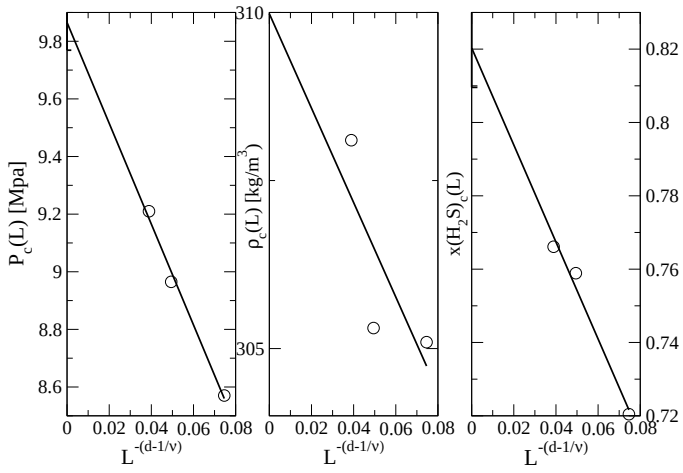

Figure 2.11: Apparent critical pressure $P_c^*(L)$, apparent critical density $\rho_c^*(L)$, and apparent critical composition $x_c^*(L)$ expressed as a function of $L^{-(d-1/\nu)}$. The lines represent least-squares fits of the data. L is expressed in reduced units.

ical point. In addition, we have extended the calculation to binary mixtures interacting with the LJ potential where we have again applied successfully both mixed field and Binder parameter methodologies with a finite size scaling study as well as the Binder parameter intersection method. Once more, we find excellent agreement with literature values.

In addition, we have shown that all the applied methodologies are affected by the use of finite size simulation cells. Furthermore, we have shown the agreement of the apparent critical temperatures calculated from the cumulant intersection with the result provided by the mixed field theory. Although the intersections found for the different system sizes appear to approach the universal Ising value of the Binder parameter, the increasing numerical error committed when increasing the size of the system makes it difficult to see a clear trend. This is particularly true in the case of the binary mixture.

Finally, real mixtures have been successfully attempted despite the increase of computational time due to the complexity of the models. The results obtained present a slight deviation for the composition when compared with GEMC data. The critical point has also been predicted using HR and FSS techniques.

To summarize, we have shown that the combination of histogram reweighting techniques with the Binder fourth order cumulant calculation is completely equivalent to the mixed field methods and can be employed in a finite

UNIVERSITAT ROVIRA I VIRGILI
IMPROVEMENT OF MONTE CARLO ALGORITHMS AND INTERMOLECULAR POTENCIALS FOR THE MODELLING OF ALKANOLS, ESTHERS, TRIOPHENES AND AROMATICS
Javier Pérez Pellitero
ISBN: 978-84-691-0377-7/DL: T.2195-2007

size scaling study in order to estimate the critical parameters with the same precision as for the mixed field studies.

The main advantage of this method compared with the mixed-field theory is that no matching of the Ising universal distribution is required and the estimation of the finite critical point is straightforward. In addition, recent works have shown that the Binder parameter can also be used to estimate the coexistence properties close to the critical point.

UNIVERSITAT ROVIRA I VIRGILI
IMPROVEMENT OF MONTE CARLO ALGORITHMS AND INTERMOLECULAR POTENCIALS FOR THE MODELLING OF ALKANOLS, ESTHERS, TRIOPHENES AND AROMATICS
Javier Pérez Pellitero
ISBN: 978-84-691-0377-7/DL: T.2195-2007

Chapter 3

An Anisotropic United Atoms (AUA) intermolecular potential optimization for thiophenes

UNIVERSITAT ROVIRA I VIRGILI
IMPROVEMENT OF MONTE CARLO ALGORITHMS AND INTERMOLECULAR POTENCIALS FOR THE MODELLING OF ALKANOLS, ESTHERS, TRIOPHENES AND AROMATICS
Javier Pérez Pellitero
ISBN: 978-84-691-0377-7/DL: T.2195-2007

3.1 Introduction

Due to the increasing requirements for sulfur removal from fuel, there has been a constant growth of interest in these compounds in the petroleum industry. The reason for lowering sulfur level include the environmental effects of acid rain so produced when sulfur compounds are emitted to the atmosphere, oxidized to sulfur oxides, and later scavenged by atmospheric precipitation as sulfuric acid. Sulfur containing molecules must either be removed or converted into hydrocarbons and H_2S in order to accomplish the strict limits in sulfur emissions imposed by the environmental laws. Since the family of thiophenes is much more resistant than thiols or sulfides to known conversion processes, adsorption is currently being considered as an alternative. In particular, the most difficult compounds to remove from liquid fuels are typically dibenzothiophene(DBT) and its derivatives[31]. Hence, there is a strong need for thermodynamic data for this compound for which only limited vapor-equilibrium data can be found in the literature. For example, experimental data of vapor-liquid equilibrium (VLE) for mixtures containing thiophene + alkanes + CO_2 have been published recently[80]. In addition, mixtures of ethanol+thiophene have also been considered[81]. A much older study for systems consisting of aromatic hydrocarbons and thiophene in polar solvents also exists [82, 83]. Finally, a review on the critical point determination of organic sulfur compounds can also be found[84]. It should be noted that available experimental data is sometimes based on extrapolation and empirical adjustments rather than purely on direct measurement and hence care should be taken when comparing to such data.

Molecular simulation is rapidly becoming an alternative way to predict equilibrium thermodynamic properties of pure fluids and mixtures. Of course, the accuracy of the predictions is intimately related with the intermolecular potentials used to reproduce the interactions between molecules. In the last decade, potential models, also referred to as force fields, have been developed for a wide range of compounds[24, 10, 25]. One of the most common approaches for modeling hydrocarbons and other flexible molecules is the use of the united-atoms model scheme, where each chemical group is represented by one Lennard-Jones center. This scheme results in a significant reduction of the computational time as compared to all-atoms models since the number of pair interactions goes as the square of the number of sites. Improvements on the standard united-atoms model, where typically a 6-12 Lennard-Jones center of force is placed on top of the most significant atom, have been proposed. For instance, Errington *et al.* have used a Buckingham exp-6 potential [26],

UNIVERSITAT ROVIRA I VIRGILI
IMPROVEMENT OF MONTE CARLO ALGORITHMS AND INTERMOLECULAR POTENCIALS FOR THE MODELLING OF ALKANOLS, ESTHERS, TRIOPHENES AND AROMATICS
Javier Pérez Pellitero
ISBN: 978-84-691-0377-7/DL: T.2195-2007

where 3 parameters are involved in each center of force and the repulsive part of the LJ interaction is replaced by an exponential term. Chen *et al.* have introduced additional sites on the centers of the C-H bonds[68]. Also, Ungerer *et al.* [28] have obtained the AUA 4 model by reparameterizing the initial Anisotropic United Atom (AUA) model proposed by Toxvaerd[29] [30]. The AUA model consists of a displacement of the Lennard-Jones centers of force towards the hydrogen atoms, converting the distance of displacement into a third adjustable parameter.

In this chapter, we obtain an optimized intermolecular potential for the sulfur group of the thiophene family aimed at giving a quantitative description of both liquid and coexistence properties, based on an extension of the AUA 4 intermolecular potentials already given in previous works[32, 28]. To guarantee the transferability of the parameters to the different compounds of the family, we used the experimental values of density, vaporization enthalpy and saturation pressure of both thiophene and benzothiophene. As a starting point for the procedure, we have taken the parameters for sulfur of sulfides and thiols by Delhommelle[85]. We have then fitted the Lennard-Jones parameters to experimental results of thiophene and benzothiophene according to the methodology described by Bourasseau et al[86]. These optimized parameters have then been used to calculate the properties of 2-methylthiophene, 2,5-dimethylthiophene and dibenzothiophene in order to demonstrate the transferability of the resulting parameters to other members of the thiophene family.

3.2 Model

3.2.1 Intermolecular Interactions

To describe the dispersion interactions, the different molecules are represented by a set of interacting Lennard-Jones sites for each CH_3, CH_2, C or S group. The interaction between two different united atoms, i and j, from different molecules is calculated according to:

UNIVERSITAT ROVIRA I VIRGILI
IMPROVEMENT OF MONTE CARLO ALGORITHMS AND INTERMOLECULAR POTENCIALS FOR THE MODELLING OF ALKANOLS, ESTHERS, TRIOPHENES AND AROMATICS
Javier Pérez Pellitero
ISBN: 978-84-691-0377-7/DL: T.2195-2007

$$U^{LJ}(r_{ij}) = 4\epsilon_{ij}\left[\left(\frac{\sigma_{ij}}{r_{ij}}\right)^{12} - \left(\frac{\sigma_{ij}}{r_{ij}}\right)^{6}\right] \tag{3.1}$$

To calculate the parameters between unlike united atoms, we use the Lorentz-Berthelot combining rules:

$$\epsilon_{ij} = \sqrt{\epsilon_{ii}\epsilon_{jj}} \tag{3.2}$$

$$\sigma_{ij} = \frac{\sigma_{ii} + \sigma_{jj}}{2} \tag{3.3}$$

To model the aromatic rings we have taken the AUA 4 CH intermolecular potential for aromatic compounds by Contreras *et al.* [21], and the aromatic C group by Ahunbay *et al.* [32] optimized for polyaromatic compounds. The choice of the latter set of parameters is discussed in section 3.3 where we have tested the influence of the use of C parameters based either on alkylbenzenic or polyaromatic compounds. The methylene group was taken from the work of Ungerer *et al.*[28] and finally we have fitted the parameters for the sulfur atom, ϵ_S and σ_S. Note that in this case, since there is only one atom present, there is no anisotropy and hence the displacement parameter is set equal to zero. The parameters for the different potentials are shown in table 3.1. In table 3.2 we show the bond angles and distances used for the different bonds. These parameters have been taken from the experimental geometry of thiophene[87] as well as from *ab initio* calculations at the Density Functional Theory level. All the models have been assumed to be rigid, as for the AUA 4 model for aromatics. Due to the moderate dipolar moment of the thiophene molecule, $\mu = 0.54D$ [88] we have considered that a simple model without charges should be able to reproduce accurately the vapor-liquid equilibrium properties, at least of pure systems. Previously, the AUA 4 model has already been successfully implemented for molecules such as orthoxylene which has a dipole moment similar to thiophene [21].

UNIVERSITAT ROVIRA I VIRGILI
IMPROVEMENT OF MONTE CARLO ALGORITHMS AND INTERMOLECULAR POTENCIALS FOR THE MODELLING OF ALKANOLS, ESTHERS, TRIOPHENES AND AROMATICS
Javier Pérez Pellitero
ISBN: 978-84-691-0377-7/DL: T.2195-2007

Group	$\sigma(\mathring{A})$	$\epsilon/k(K)$	$\delta(\mathring{A})$
CH_3[28]	3.607	120.15	0.216
CH[21]	3.246	89.42	0.407
C[32]	3.246	37.73	—
S	3.493	179.2	—

Table 3.1: **Lennard-Jones parameters**

bond	length $(\mathring{A})$	angle	$\Sigma(deg)$
$C-C$[89](functional groups)	1.53	$C_{ar}-C_{ar}-C_{ar}$	112.7
$C_{ar}-C_{ar}$ (aromatic ring)	1.39	$C_{ar}-S-C_{ar}$	92.2
$C_{ar}-S$	1.72	$C_{ar}-C_{ar}-S$	111.2

Table 3.2: **Bond lengths and angles**

3.3

Evaluation of the AUA 4 intermolecular potentials for alkylbenzenes and polyaromatic hydrocarbons

Due to the aromatic character of thiophene compounds the aromatic groups CH and C are particularly relevant before a new intermolecular potential for the sulphur atom can be developed. These groups were optimized for benzene[90] while in later works [21] [32] the C group was reparametrized to better account for both alkylbenzene and polyaromatic compounds respectively. With this in mind, in the first work p-xylene was used as a reference alkylbenzene to calibrate the parameters of the aromatic carbon C group to which the alkyl substituents are attached. The model was then tested on alkylbenzenes that were not used to optimize the potential parameters. In this thesis GEMC simulations were carried out for styrene to test the transferability of the LJ parameters. In table 3.4 are shown the LJ parameters used to model

Group	$\sigma(\mathring{A})$	$\epsilon/k(K)$	Estimated F
S (based on thiophene and benzothiophene)	3.493	179.2	2.668
S(based on thiophene only)	3.518	176.9	1.814
S(based on benzothiophene only)	3.416	184.57	3.036

Table 3.3: **Lennard-Jones parameters and error criterion as a function of the target molecules**

UNIVERSITAT ROVIRA I VIRGILI
IMPROVEMENT OF MONTE CARLO ALGORITHMS AND INTERMOLECULAR POTENCIALS FOR THE MODELLING OF ALKANOLS, ESTHERS, TRIOPHENES AND AROMATICS
Javier Pérez Pellitero
ISBN: 978-84-691-0377-7/DL: T.2195-2007

the π-bounded CH and CH_2 groups of the vinyl radical and in table 3.5 are shown the results obtained using the alkylbenzene optimized LJ parameters.

Group	σ [$\dot{A}$]	ε/k **[K]**	δ [$\dot{A}$]
CH (olefins) [86]	3.32	90.6	0.414
CH_2 (olefins) [86]	3.48	111.1	0.295

Table 3.4: **LJ parameters of the vinyl group**

T (K)	Property	Calc. Property	Exptl. Property	% dev
360	P_{sat}	21.4(0.8)	15.94	34.3
	H_{vap}	40.7	40.8	-0.2
	ρ_{liq}	843.3(1.8)	843	0.0
383	P_{sat}	31.9(0.6)	35.8	-10.9
	H_{vap}	39.3	39.4	-0.3
	ρ_{liq}	821.6(1.6)	820.7	0.1
418	P_{sat}	120(5)	99.7	20.4
	H_{vap}	36.7	37.1	-1.1
	ρ_{liq}	783.2(1.5)	784.8	-0.2
500	P_{sat}	676(2)	575	17.7
	H_{vap}	30.4	30.6	-0.7
	ρ_{liq}	689.7(2)	689.8	0.0
540	P_{sat}	1345(20)	1096	22.8
	H_{vap}	26.2	26.6	-1.5
	ρ_{liq}	632.9(2.2)	634.1	-0.2
580	P_{sat}	2369(33)	1921	23.3
	H_{vap}	23.4	21.4	9.3
	ρ_{liq}	554.2(3.8)	565.7	-2.0

Table 3.5: **Comparison of predicted and experimental equilibrium properties of styrene using alkylbenzene based AUA 4 parameters. Vapor pressure (P_{sat}) is expressed in kPa, vaporization enthalpies (H_{vap}) is in kJ/mol, and liquid density (ρ_{liq}) is in kg/m^3.**

As can be seen in figures 3.1-3.2, the proposed parameter set for the C group of alkylsubstituted aromatics obtained from the optimization of p-xylene properties appear to provide good predictions for styrene alkylbenzenes and styrene investigated in the present study. Heats of vaporization, liquid densities, and normal boiling temperatures are predicted with an average accuracy of approximately 2%. confirming the good transferability of the AUA intermolecular potential. In particular, the benzene-based parameters for the aromatic CH group and the π alkene based parameters for the CH and CH2

UNIVERSITAT ROVIRA I VIRGILI
IMPROVEMENT OF MONTE CARLO ALGORITHMS AND INTERMOLECULAR POTENCIALS FOR THE MODELLING OF ALKANOLS, ESTHERS, TRIOPHENES AND AROMATICS
Javier Pérez Pellitero
ISBN: 978-84-691-0377-7/DL: T.2195-2007

vinyl groups have been used without modification. This transferability is considered to be the result of the good physical sense of the potential parameters, which were shown to reproduce correctly the liquid structure of benzene.

Since we plan to develop an intermolecular potential valid also for polythiophenes, we have also tested the behavior of the polyaromatics based parameters of [32] by repeating some of the simulations done for styrene. The purpose of these parameters is to extend the AUA potential to polycyclic aromatic hydrocarbons, without reconsidering, as in the case of alkylbenzene compounds, the parametrization of the aromatic CH nor the parametrization of the $CH2$ and $CH3$ groups of alkanes nor the CH and CH_2 groups for π bounded alkenes. For this purpose, naphthalene was used as a reference to calibrate the parameters of the aromatic carbon that connects the aromatic cycles to each other. The results obtained using these parameters are presented in table 3.6 as well as in figures 3.1-3.2. The results obtained for the saturated liquid densities as well as for the heats of vaporization are almost equal to those obtained using the alkylbenzene based parameters. Despite the fact that in the case of the saturation pressure, the use of the polyaromatics based parameters slightly increases the overestimation of this property, we think that the adoption of this set of parameters for the thiophenes models is well justified, in particular for the modeling of polythiophenes.

T (K)	Property	Calc. Property	Exptl. Property	% dev
383	P_{sat}	33.7(0.7)	35.8	-5.9
	H_{vap}	38.6	39.4	-2.0
	ρ_{liq}	812.1(1.9)	820.7	-1.0
418	P_{sat}	128(7)	99.7	28.3
	H_{vap}	36.7	37.1	-1.1
	ρ_{liq}	782(4)	784.8	-0.3
500	P_{sat}	724(2)	575	25.9
	H_{vap}	30.4	30.6	-0.7
	ρ_{liq}	689.4(2)	689.8	0.0
540	P_{sat}	1366(23)	1096	24.6
	H_{vap}	25.7	26.6	-3.4
	ρ_{liq}	628.3(2.5)	634.1	-0.9

Table 3.6: **Comparison of predicted and experimental equilibrium properties of styrene using polyaromatics based AUA 4 parameters. Vapor pressure (P_{sat}) is expressed in kPa, vaporization enthalpies (H_{vap}) is in kJ/mol, and liquid density (ρ_{liq}) is in kg/m^3.**

UNIVERSITAT ROVIRA I VIRGILI
IMPROVEMENT OF MONTE CARLO ALGORITHMS AND INTERMOLECULAR POTENCIALS FOR THE MODELLING OF ALKANOLS, ESTHERS, TRIOPHENES AND AROMATICS
Javier Pérez Pellitero
ISBN: 978-84-691-0377-7/DL: T.2195-2007

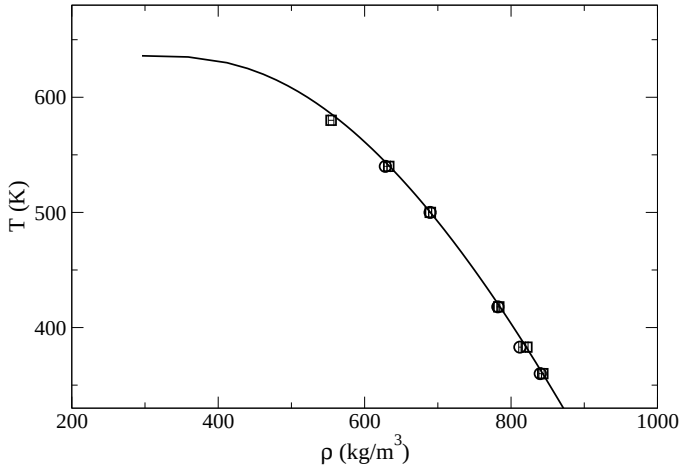

Figure 3.1: Saturated liquid densities of styrene. Solid line represents experimental results data[88]. Squares and circles represent the simulation results for the alkylbenzene based [21] and polyaromatics based AUA 4 parameters [32] respectively.

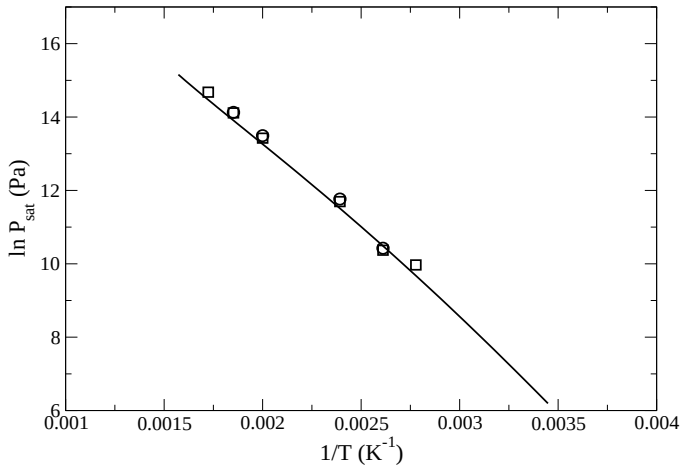

Figure 3.2: Saturation pressures of styrene. Legend as in figure 3.1.

UNIVERSITAT ROVIRA I VIRGILI
IMPROVEMENT OF MONTE CARLO ALGORITHMS AND INTERMOLECULAR POTENCIALS FOR THE MODELLING OF ALKANOLS, ESTHERS, TRIOPHENES AND AROMATICS
Javier Pérez Pellitero
ISBN: 978-84-691-0377-7/DL: T.2195-2007

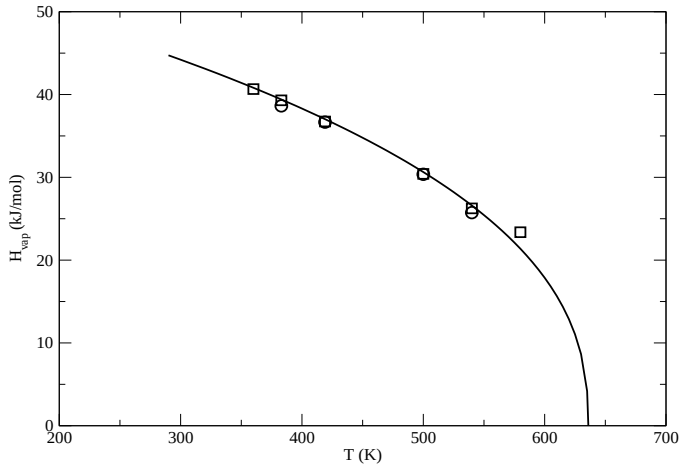

Figure 3.3: Vaporization enthalpies of styrene. Legend as in figure 3.1

3.4 Simulation details

3.4.1 Fitting procedure

To determine the coexistence properties at the conditions selected to fit the Lennard-Jones parameters, we have used the Gibbs ensemble Monte Carlo (GEMC)[7] method due to the straightforward and easiness of the methodology when a single point is involved. GEMC has been combined with a configurational bias scheme[56] and an additional bias for the insertion of the center of mass of the molecules[91]. The selected probabilities for the different moves were generally set to 0.245 for rigid body translation, 0.25 for rigid body rotation, 0.5 for transfer and 0.005 for volume change. A total of 250 molecules have been considered in all the simulations, using a cutoff radius equal to half of the box with standard long range Lennard-Jones corrections [57]. Coexistence densities, average pressure (calculated through the virial) and enthalpies of vaporization (computed as the difference in enthalpy between the two simulation boxes) were calculated from the different simulations.

UNIVERSITAT ROVIRA I VIRGILI
IMPROVEMENT OF MONTE CARLO ALGORITHMS AND INTERMOLECULAR POTENCIALS FOR THE MODELLING OF ALKANOLS, ESTHERS, TRIOPHENES AND AROMATICS
Javier Pérez Pellitero
ISBN: 978-84-691-0377-7/DL: T.2195-2007

To calculate liquid properties under atmospheric conditions, we have used simulations in the isothermal-isobaric (NPT) ensemble by fixing the external pressure at 1 atm while temperatures close to the experimental normal boiling temperatures have been chosen: 340 K in the case of thiophene, 400 K in the case of benzothiophene. The molar enthalpy of vaporization is given by:

$$\Delta H_{vap} = -\langle E_{liq(inter)} \rangle + RT \tag{3.4}$$

where $\langle E_{liq(inter)} \rangle$ is the average molar intermolecular potential energy in the simulation. This expression assumes that (i) the molar volume of the liquid is negligible compared with that of the vapor, (ii) the vapor is close enough to an ideal gas, and (iii) the difference between the intramolecular energies of the two phases is negligible. In the case of the Lennard-Jones models used in this work, these assumptions are indeed justified for reduced temperatures T/T_c lower than 0.6, which corresponds to vapor pressures significantly lower than atmospheric pressure.

3.4.2 Liquid-Vapor Phase Equilibria

Once the parameters were determined as described in the next section, the coexistence curves and vapor-pressures of the different compounds considered were obtained using Grand Canonical Monte Carlo (GCMC) simulations combined with histogram reweighting[15][16]. As for the Gibbs ensemble, a configurational bias scheme[56] and an additional bias for the insertion of the center of mass of the molecules[91] were implemented to enhance the acceptance rate of insertions. The probabilities of the different moves used in the simulations were 0.15 for translation, 0.15 for rotation, and 0.7 for insertion or deletion. A simulation box of size $L = 32\mathring{A}$ was used in all cases. Systems were allowed to equilibrate for at least one million MC steps followed by the production run. In the case of a liquid phase, the length of the production run was set normally to 25 million MC steps. Standard deviations of the ensemble averages were calculated by breaking the production runs into three blocks. Due to the limited number of particles present in the box for the vapor phase at low temperatures, we have applied the assumptions of Eqn. 3.4. In this way, the enthalpy can be calculated in a much more reliable way, since the vapor molar volume of the gas is estimated through the ideal gas law, not being affected in this way by the error committed due to the low number of molecules in the vapor phase. In this way the pressure at low temperatures can be determined by applying thermodynamic integration [86]

UNIVERSITAT ROVIRA I VIRGILI
IMPROVEMENT OF MONTE CARLO ALGORITHMS AND INTERMOLECULAR POTENCIALS FOR THE MODELLING OF ALKANOLS, ESTHERS, TRIOPHENES AND AROMATICS
Javier Pérez Pellitero
ISBN: 978-84-691-0377-7/DL: T.2195-2007

using the enthalpies calculated with the aforementioned approximations. We have checked this proposed method by comparing the results with additional NPT simulations in order to ensure that the energy and density of the liquid phase are not affected by these approximations as will be shown in the results section.

3.5 Determination of the Lennard-Jones parameters

In order to optimize the Lennard Jones parameters for the S group, we have selected thiophene and benzothiophene experimental results as reference data. Thiophene was chosen as being the most representative compound of the family, and benzothiophene in order to improve the transferability of the parameters to polyaromatic rings such as dibenzothiophene. For the two compounds, we have used the vaporization enthalpy, pressure and liquid density at a temperature near to the normal boiling point and at a reduced temperature of about 0.8 as reference data. The selection of the vaporization enthalpy and liquid density allows the predictions to be reliable over a large range of temperature since they control the temperature dependence of the vapor pressure through the Clapeyron equation. To optimize the Lennard-Jones parameters, a GEMC simulation was carried out at a reduced temperature of 0.8 and a NPT simulation at a temperature near to the normal boiling point. This set of simulations optimizes the behavior of the parameters over a total of 10 different properties of thiophene and benzothiophene.

Once the simulations have been carried out, an optimization procedure is applied until the error has been minimized. The optimization methodology has already been described in detail[86] and is thus only briefly described here.

The normalized error criterion selected to drive the optimization procedure is given by the following expression:

$$F = \frac{1}{n}\sum_{i=1}^{n}\frac{\left(X_i^{mod} - X_i^{exp}\right)^2}{s_i^2} \tag{3.5}$$

where n is the total number of reference data, X_i^{mod} is the value of the

UNIVERSITAT ROVIRA I VIRGILI
IMPROVEMENT OF MONTE CARLO ALGORITHMS AND INTERMOLECULAR POTENCIALS FOR THE MODELLING OF ALKANOLS, ESTHERS, TRIOPHENES AND AROMATICS
Javier Pérez Pellitero
ISBN: 978-84-691-0377-7/DL: T.2195-2007

i^{th} property calculated in the simulations, X_i^{exp} is the experimental value of the i^{th} property and s_i is the statistical uncertainty of the computed variable X_i^{mod} (estimated from the standard block averaging technique[57]). F is a function of the different y_i Lennard-Jones parameters to be optimized, in this case $y_1 = \epsilon_S$ and $y_2 = \sigma_S$. The condition for minimizing F implies that:

$$\frac{\partial F}{\partial y_j} = \sum_{i=1}^{n} \frac{2\left(X_i^{mod} - X_i^{exp}\right)\frac{\partial X_i^{mod}}{\partial y_j}}{s_i^2} = 0 \tag{3.6}$$

Eqn.3.6 have been obtained by considering a Taylor expansion around an initial point y^0 corresponding to the initial selection of the Lennard-Jones set of parameters:

$$X_i^{mod}(y^0 + \Delta y) = X_i^{mod}(y^0) + \sum \frac{\partial X_i^{mod}}{\partial y_k)} \Delta y_k \tag{3.7}$$

Then the minimum condition of Eqns. 3.6 can be expressed as:

$$\sum_{i=1}^{n} \frac{\left(X_i^{mod}(y_0) - X_i^{exp} + \sum_k \frac{\partial X_i^{mod}}{\partial y_k}\Delta y_k\right)\frac{\partial X_i^{mod}}{\partial y_j}}{s_i^2} = 0 \tag{3.8}$$

where the derivatives $\frac{\partial X_i^{mod}}{\partial y_k}$ have been evaluated by using statistical fluctuations [86], which are known to provide good results in the estimation of thermodynamic derivative properties [92] instead of the statistically less reliable and more time consuming finite difference evaluations [93]. The minimum of F is then obtained by solving a system of linear equations $A\Delta y = B$ with n unknowns Δy_k. The optimized parameters y_k are obtained with $y_k = y_k^0 + \Delta y_k$.

The initial set of parameters, $\sigma_0 = 3.60\mathring{A}$ and $\epsilon_0 = 190.0K$ have been taken from the S of the sulfide group optimized by Delhommelle[85]. Although these parameters were not optimized for thiophene, we find that they provide a relatively good level of agreement with experimental results for the liquid density, vaporization enthalpy and vapor pressure when evaluated at ambient

UNIVERSITAT ROVIRA I VIRGILI
IMPROVEMENT OF MONTE CARLO ALGORITHMS AND INTERMOLECULAR POTENCIALS FOR THE MODELLING OF ALKANOLS, ESTHERS, TRIOPHENES AND AROMATICS
Javier Pérez Pellitero
ISBN: 978-84-691-0377-7/DL: T.2195-2007

temperatures as well as at a reduced temperature of 0.8. Despite the reasonable results obtained, the liquid density and vaporization enthalpy of thiophene were overestimated while the vapor pressure was underestimated. The critical point of thiophene was also overestimated by $\approx 25K$. After the aforementioned optimization process, the Lennard-Jones parameters obtained for the sulfur atom were $\sigma = 3.493\mathring{A}$ and $\epsilon = 179.2K$. We have also considered the possibility of optimizing the parameters based only on thiophene or benzothiophene separately. In table 3.3 are given the different sets of parameters obtained according to the different selections of target properties as well as the estimated normalized errors committed according to the target molecules chosen on applying these parameters. It may be noticed that compared with the original S parameters of organic sulfides, both ϵ and σ are smaller, whatever the reference molecules used.

3.6 Calculation of the critical point

In order to accurately locate the critical point, we have applied a recently implemented[94] methodology based on the calculation of a fourth order cumulant (Binder parameter) combined with the use of finite size scaling[14] techniques. The Binder parameter U_L is defined as follows:

$$U_L = \frac{\langle m^4 \rangle}{\langle m^2 \rangle^2} \tag{3.9}$$

where m is an appropriate order parameter, in our case density. The procedure is as follows: system size dependent critical conditions are determined for different system sizes by locating the temperature at which the system takes on the "universal" Ising value of the system. Once these values are calculated, the critical constants are expected to change as a function of the system size according to known scaling laws[14]. For instance, the temperature of the finite system is expected to vary near the critical point with system size as:

$$\langle T \rangle_c(L) - \langle T \rangle_c(\infty) \sim L^{-(\theta+1)/\nu} \tag{3.10}$$

where $\Theta = 0.54$ and $\nu = 0.629$ [67][68].

UNIVERSITAT ROVIRA I VIRGILI
IMPROVEMENT OF MONTE CARLO ALGORITHMS AND INTERMOLECULAR POTENCIALS FOR THE MODELLING OF ALKANOLS, ESTHERS, TRIOPHENES AND AROMATICS
Javier Pérez Pellitero
ISBN: 978-84-691-0377-7/DL: T.2195-2007

In the same way, the critical density of the finite system is expected to vary with system size as:

$$\langle\rho\rangle_c(L) - \langle\rho\rangle_c(\infty) \sim L^{-(d-1/\nu)} \tag{3.11}$$

where d is the dimensionality of the system.

By plotting the finite size critical values according to these functions, an extrapolation can be made to estimate the corresponding infinite system size value.

3.7 Performance of the optimized parameters

The transferability of the optimized parameters has been tested over the two reference compounds as well as three other thiophenes: 2-methylthiophene, 2,5-dimethylthiophene and dibenzothiophene (DBT). DBT has been selected in order to test the performance of the optimized parameters for polyaromatic molecules.

3.7.1 Thiophene and alkylthiophenes

In figure 3.4 and table 3.7 the vapor-liquid coexistence density curve of thiophene is given. The results are compared with the TraPPE model proposed by Lubna *et al.* [95]. Also shown in figure 3.4 is a comparison between the histogram reweighting results obtained by applying the assumptions of section 3.4.2 and NPT simulations. Below a temperature of 0.65 T_c the results shown from HR are estimated by applying the new methodology. As can be seen, the proposed method for calculating the coexistence densities at low temperatures is consistent with the NPT simulations. The liquid density is found to be reproduced on average within 1% of the experimental value while the critical temperature is predicted within less than 1% improving considerably the 3% and 4.5 % obtained respectively by the TraPPE model. In the case of the critical densities, both predictions are almost equivalent being in good agreement with the experimental value. The set of calculated critical parameters for the rest of the molecules are presented in table 3.8. To determine the finite size critical values, additional simulations in the critical region have been done for

UNIVERSITAT ROVIRA I VIRGILI
IMPROVEMENT OF MONTE CARLO ALGORITHMS AND INTERMOLECULAR POTENCIALS FOR THE MODELLING OF ALKANOLS, ESTHERS, TRIOPHENES AND AROMATICS
Javier Pérez Pellitero
ISBN: 978-84-691-0377-7/DL: T.2195-2007

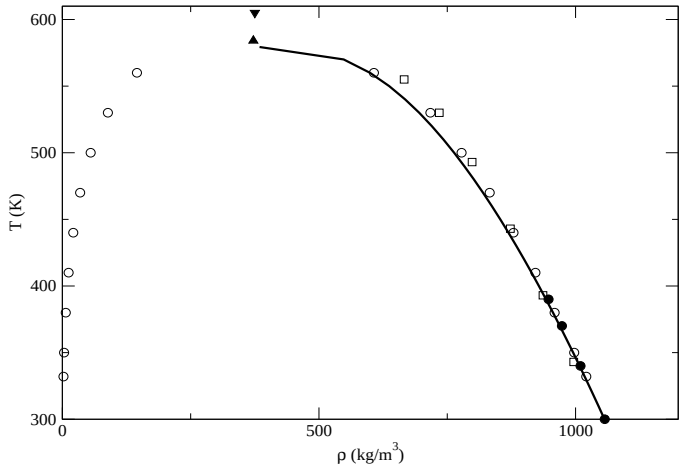

Figure 3.4: Coexistence curve of thiophene. The straight line represents experimental data [88], open circles are the HR results of the new model. Squares are GEMC simulation results of the TraPPE model from ref. [95]. The up triangle represents the critical point of this model while the down triangle represents the critical point of the TraPPE model. Filled symbols represent NPT simulations results.

the different molecules using system sizes ranging from $L = 25\mathring{A}$ in the case of alkylthiophenes up to $L = 42\mathring{A}$ in the case of polythiophenes. As is shown in figure 3.5, the Binder parameter has been calculated along the equilibrium line for different system sizes. The intersections of the Binder parameter with the Ising universal value have been used as estimations for the apparent critical points, which have then been scaled according to Eqns. (3.10) and (3.11) as shown in figure 3.6. The coexistence density curves and the saturated liquid densities of the alkylthiophenes are presented in figure 3.7.

A good agreement has been obtained for the 2-methylthiophene coexistence densities, and the critical point is underestimated by approximately 1%. The deviations are larger in the case of 2,5-dimethylthiophene, but in this case the reliability of the experimental data is poor. Indeed, the DIPPR properties for this compound are mostly based on extrapolation, the quoted uncertainty being of 10% for all the properties calculated. In the case of thiophene, these values are 1% for the liquid density and 3% for the saturation pressure and the vaporization enthalpy. The saturation pressures, as plotted in figure 3.8, reveal a slight overestimation of this property; despite the fact that for thiophene the target values have been well reproduced within a reasonable mean error of 9% for the absolute value of the saturation pressure. In the case of the other alkylthiophenes the deviations are slightly higher but al-

UNIVERSITAT ROVIRA I VIRGILI
IMPROVEMENT OF MONTE CARLO ALGORITHMS AND INTERMOLECULAR POTENCIALS FOR THE MODELLING OF ALKANOLS, ESTHERS, TRIOPHENES AND AROMATICS
Javier Pérez Pellitero
ISBN: 978-84-691-0377-7/DL: T.2195-2007

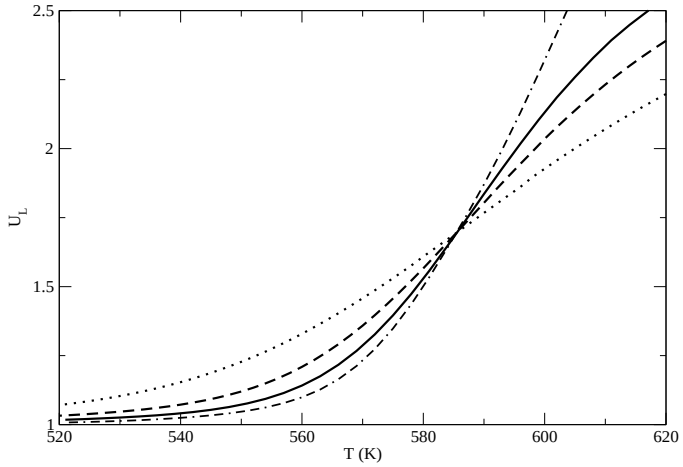

Figure 3.5: Binder parameter intersections for different system sizes for thiophene.

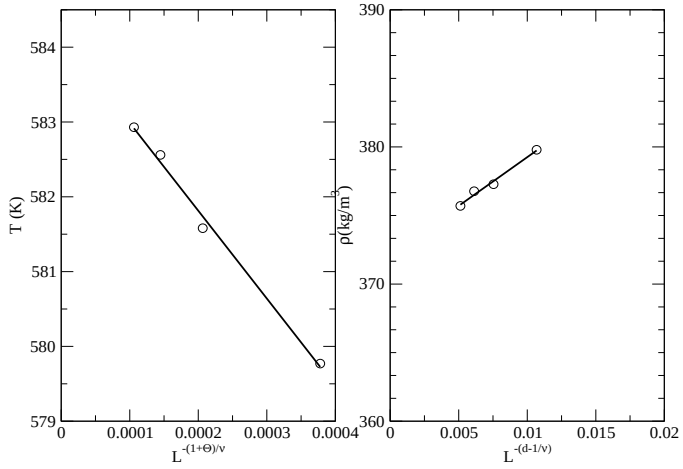

Figure 3.6: Finite size scaling for the critical temperature and density of thiophene.

UNIVERSITAT ROVIRA I VIRGILI
IMPROVEMENT OF MONTE CARLO ALGORITHMS AND INTERMOLECULAR POTENCIALS FOR THE MODELLING OF ALKANOLS, ESTHERS, TRIOPHENES AND AROMATICS
Javier Pérez Pellitero
ISBN: 978-84-691-0377-7/DL: T.2195-2007

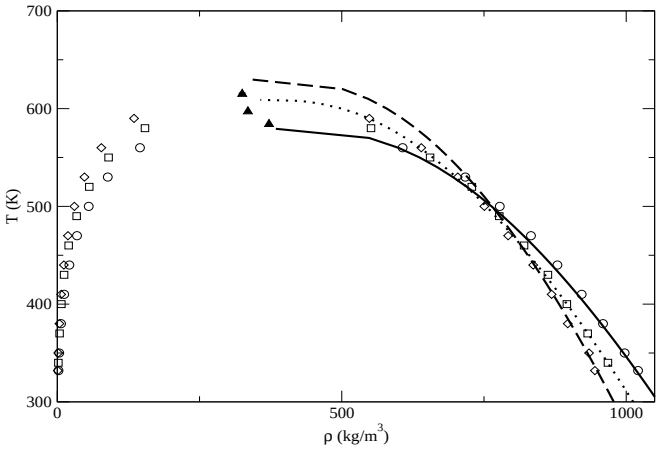

Figure 3.7: Coexistence curves of alkylthiophenes. Solid, dashed and dotted lines represent experimental data[88] for thiophene, 2-methylthiophene and 2,5-dimethylthiophene respectively. Circle, square, and diamond symbols represent the simulation results for thiophene, 2-methylthiophene and 2,5-dimethylthiophene respectively. Filled triangles denote estimates of the critical points of this model.

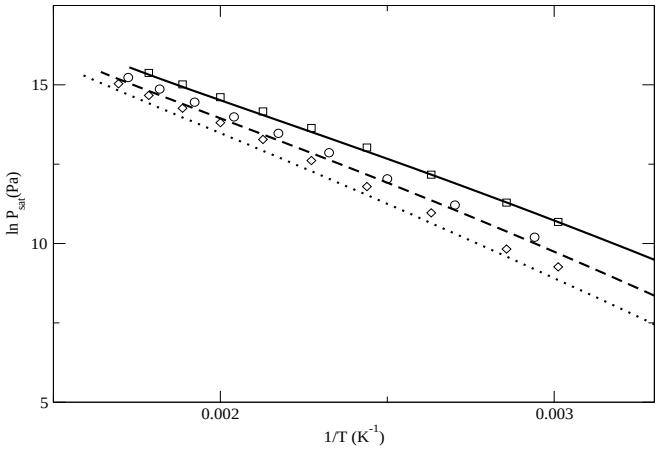

Figure 3.8: Saturation pressures of alkylthiophenes. Solid, dashed and dotted lines represent experimental data[88] for thiophene, 2-methylthiophene and 2,5-dimethylthiophene respectively. Symbols represent the simulation results.

UNIVERSITAT ROVIRA I VIRGILI
IMPROVEMENT OF MONTE CARLO ALGORITHMS AND INTERMOLECULAR POTENCIALS FOR THE MODELLING OF ALKANOLS, ESTHERS, TRIOPHENES AND AROMATICS
Javier Pérez Pellitero
ISBN: 978-84-691-0377-7/DL: T.2195-2007

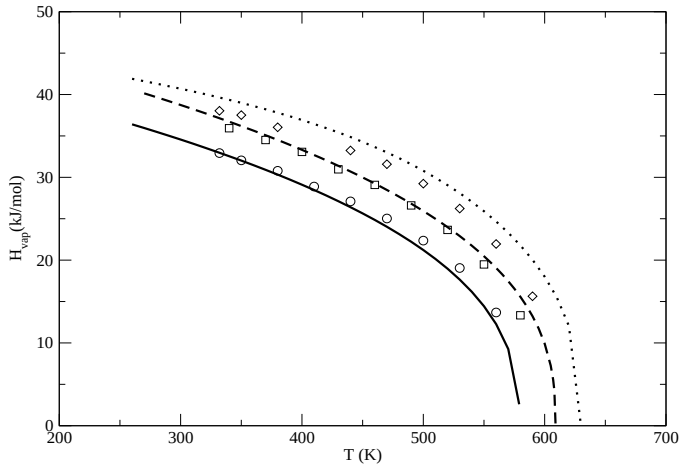

Figure 3.9: Enthalpies of vaporization of alkylthiophenes. Solid, dashed and dotted lines represent experimental data[88] for thiophene, 2-methylthiophene and 2,5-dimethylthiophene respectively. Symbols represent the simulation results.

ways within a reasonable error. The calculated normal boiling temperatures are also presented in table 3.7. A larger deviation, 2%, has once more been obtained for 2,5-dimethylthiophene, while in the case of thiophene less than a 1% error has been found. Finally, in figure 3.9, we present the results for the enthalpy of vaporization. A good agreement has been obtained for thiophene and 2-methylthiophene, while higher deviations have been obtained for 2,5-dimethylthiophene. This deviation can again be attributed to the low reliability of the experimental data reported for this molecule, and also to the fact that the model slightly underestimates the decrease in P_{sat} and the increase in ΔH_{vap} due to the presence of the methyl substituents

3.7.2 Polythiophenes

Simulations for benzothiophene and dibenzothiophene have been conducted to test the behavior of the optimized parameters for polyaromatic rings. The vapor-liquid coexistence density curve is shown in figure 3.10 and in table 3.9. In the case of benzothiophene, the liquid density is well reproduced as expected since the experimental properties of this molecule have been selected as target values in the optimization process. The critical temperature has been underestimated by approximately 2%. In the case of dibenzothio-

UNIVERSITAT ROVIRA I VIRGILI
IMPROVEMENT OF MONTE CARLO ALGORITHMS AND INTERMOLECULAR POTENCIALS FOR THE MODELLING OF ALKANOLS, ESTHERS, TRIOPHENES AND AROMATICS
Javier Pérez Pellitero
ISBN: 978-84-691-0377-7/DL: T.2195-2007

phene the liquid density is also well reproduced although larger deviations are observed than for benzothiophene. Critical temperature is underestimated by 3.5%. As in the case of 2,5-dimethylthiophene, the accuracy of the experimental data is limited for this molecule. An uncertainty of 10% has beeBinder parameter intersections for different system sizes for dimethyl, ethylmethyl and diethylether]Binder parameter intersections for different system sizes for dimethyl, ethylmethyl and diethylethen reported in the case of the density and vaporization enthalpy while 5% is given for the saturation pressure. In figure 3.11, saturation pressures are compared with experimental results. In both cases the simulation results give a slight overestimation of this property as could be expected from the results obtained for benzothiophene after the optimization process. Despite this overestimation, the error committed in the evaluation of the normal boiling temperatures is only approximately 2%. The enthalpies of vaporization are plotted in figure 3.12. In the case of both benzothiophene and dibenzothiophene this property is reproduced satisfactorily, with again a higher deviation in the case of dibenzothiophene.

3.8 Conclusions

The AUA4 potential has been successfully extended to alkyl and polythiophenes. Despite the simplicity of the model, no charges have been introduced and a rigid geometry is considered, reparametrizing only the one center of force for the sulfur group has allowed the vapor-liquid equilibrium properties to be reproduced satisfactorily. The optimization of the LJ parameters has been carried out based on target properties of both thiophene and benzothiophene, the most significant compounds of the families of alkyl and polythiophenes respectively. Although the behavior of the model could be improved individually by optimizing different sets of LJ parameters for only thiophene or only benzothiophene, our goal is to produce parameters that are transferable to other molecules. We have hence decided to develop only a single centre of force based on the simultaneous optimization of both molecules. Saturated liquid densities have been calculated with mean errors of 1.5% in the case of alkylthiophenes. Slightly larger deviations have been obtained for polythiophenes as was expected from the fact that the experimental data is reported with high errors. Although the model tends to overestimate saturation pressures, the normal boiling points have been calculated within 1-2% in all cases. Vaporization enthalpies have also been reproduced with a good level of agreement. The calculation of the critical points has been made through the recently implemented [94] methodology based on the calculation of a fourth order cu-

UNIVERSITAT ROVIRA I VIRGILI
IMPROVEMENT OF MONTE CARLO ALGORITHMS AND INTERMOLECULAR POTENCIALS FOR THE MODELLING OF ALKANOLS, ESTHERS, TRIOPHENES AND AROMATICS
Javier Pérez Pellitero
ISBN: 978-84-691-0377-7/DL: T.2195-2007

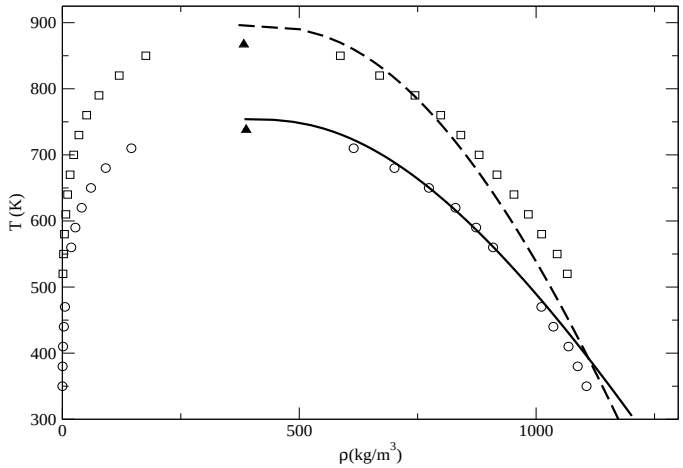

Figure 3.10: Coexistence curves of polythiophenes. Solid and dashed lines represent experimental data[88] for benzothiophene and dibenzothiophene respectively. Symbols represent the simulation results. Triangles denote estimates of the critical points of this model.

mulant (Binder parameter) combined with the use of finite size scaling[14] techniques. This method allows the critical points to be located in a straightforward and accurate way. Critical parameters have been thereby calculated in general within a 0.05% statistical error for the critical temperature and at most 1.5% for the critical density. The model critical temperature of thiophene is found to be within 1% of the experimental value. The lack of charges in the model implies that although it should be reliable for both pure systems of other molecules of the same family as well as non-polar mixtures, care should be taken when applying it to situations where charges play an important role such as adsorption in cation-exchanged zeolites or the computation of dynamical properties such as viscosity or diffusion. In addition, attention should be paid to the reliability of these models for the prediction of non-equilibrium properties. Indeed, recent work using the AUA model for benzene[96] shows that an accurate agreement with experiment for transport properties is more demanding in terms of the intermolecular potential and charges were required in order to provide a better account of the viscosity[97].

UNIVERSITAT ROVIRA I VIRGILI
IMPROVEMENT OF MONTE CARLO ALGORITHMS AND INTERMOLECULAR POTENCIALS FOR THE MODELLING OF ALKANOLS, ESTHERS, TRIOPHENES AND AROMATICS
Javier Pérez Pellitero
ISBN: 978-84-691-0377-7/DL: T.2195-2007

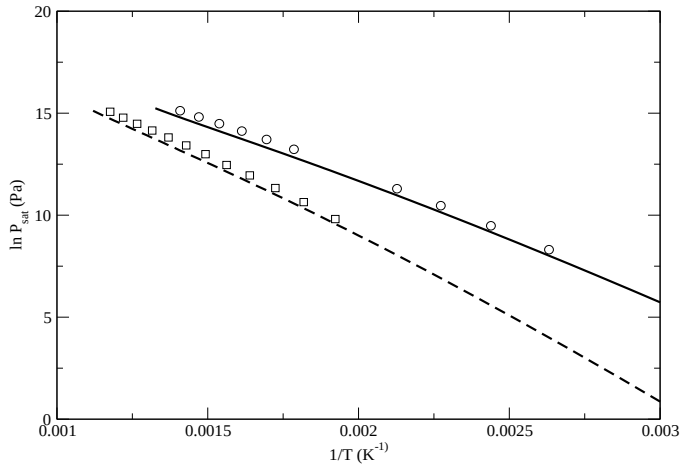

Figure 3.11: Saturation pressures of polythiophenes. Solid and dashed lines represent experimental data[88] for benzothiophene and dibenzothiophene respectively. Symbols represent the simulation results.

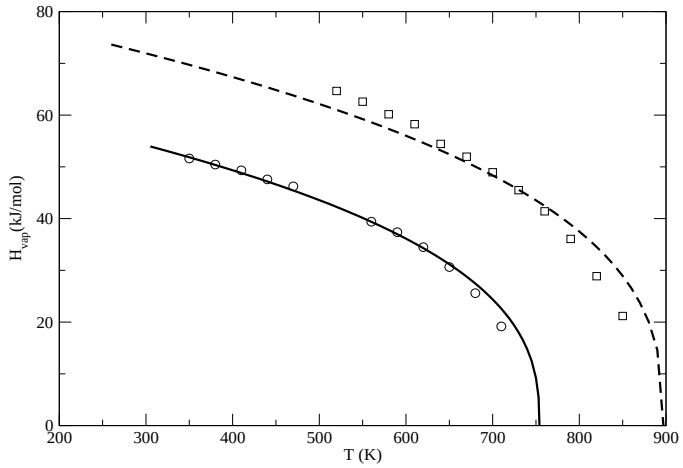

Figure 3.12: Enthalpies of vaporization of polythiophenes. Solid and dashed lines represent experimental data[88] for benzothiophene and dibenzothiophene respectively. Symbols represent the simulation results.

UNIVERSITAT ROVIRA I VIRGILI
IMPROVEMENT OF MONTE CARLO ALGORITHMS AND INTERMOLECULAR POTENCIALS FOR THE MODELLING OF ALKANOLS, ESTHERS, TRIOPHENES AND AROMATICS
Javier Pérez Pellitero
ISBN: 978-84-691-0377-7/DL: T.2195-2007

	$\rho_{liquid}(kg/m^3)$			$\Delta H_{vap}(kJ/mol)$			$P_{sat}(kPa)$		
T(K)	AUA	exptl	% dev	AUA	exptl	% dev	AUA	exptl	% dev
				Thiophene					
560	607.0±3.7	599.3	1.29	13.6±0.1	12.3	11.3	4754±11	4511.	5.38
530	717.1±2.6	695.3	3.15	19.0±0.1	17.7	7.91	3318±17	3067.	8.15
500	777.8±1.4	763.3	1.9	22.3±0.1	21.2	5.32	2213±12	2013	9.92
470	832.7±1.1	819.7	1.59	25.0±0.05	24.0	4.17	1414±9	1259	12.25
440	879.1±0.5	869.2	1.13	27.0±0.05	26.4	2.63	839±7	739	13.4
410	921.8±1.8	914.3	0.82	28.8±0.1	28.5	1.45	453±4	399	13.36
380	959.2±2.1	956.0	0.34	30.2±0.1	30.3	-0.41	214±3	193	11.27
350	997.3±1.7	995.2	0.21	31.9±0.05	32.0	-0.37	91.6±2	80.3	14.05
332	1020.7±7.4	1017.8	0.30	32.9±0.3	33.0	-0.15	50.0±1	43.3	15.64
				2-methylthiophene					
580	551.5±8.6	582.8	-5.38	13.3±0.2	15.6	-14.3	4118±29	3471	18.63
550	655.3±2.0	660.1	-0.74	19.5±0.1	20.5	-4.88	2860±31	2361	21.09
520	728.6±3.4	719.4	+1.27	23.6±0.05	24.0	-1.42	1893±29	1548	22.22
490	776.9±2.4	770.0	+0.90	26.6±0.05	26.8	-0.78	1189±25	968	22.82
460	820.4±0.6	815.3	+0.63	29.1±0.05	29.2	-0.57	708±17	568	24.56
430	862.4±0.9	856.9	+0.64	30.9±0.05	31.4	-1.36	385±13	307	25.16
400	895.6±1.2	895.7	-0.01	33.1±0.1	33.3	-0.74	168±7	149	12.86
370	932.3±1.2	932.5	-0.03	34.5±0.1	35.1	-1.64	74.0±5	63.2	17.02
340	967.9±4.8	967.5	+0.04	35.9±0.2	36.7	-2.15	26.9±2	22.2	21.21
				2,5-dimethylthiophene					
590	548.5±8.1	606.3	-9.53	15.6±0.05	20.0	-22.0	3381±41	2729	23.8
560	639.7±3.4	670.3	-4.56	21.9±0.05	24.7	-11.0	2339±61	1825	28.1
530	703.9±4.8	720.9	-2.35	26.2±0.1	28.1	-6.61	1562±52	1172	33.1
500	750.6±1.9	764.3	-1.79	30.0±0.1	30.8	-2.47	992±26	715	38.6
470	792.5±1.4	803.0	-1.31	31.6±0.1	33.0	-4.33	584±15	408	42.9
440	836.6±1.7	838.5	-0.23	33.2±0.2	34.9	-4.66	300±12	214	39.7
410	868.9±1.2	871.4	-0.29	33.5±0.2	36.4	-7.94	132±8	101	30.1
380	897.2±2.6	902.5	-0.58	36.0±0.2	37.8	-4.67	57.8±2	41.9	38.0
350	934.6±4.1	931.9	+0.29	37.5±0.3	39.0	-3.81	18.4±0.8	14.5	26.7
332	945.0±5.3	948.9	-0.41	38.0±0.3	39.6	-4.07	10.5±0.2	6.98	51.1

Table 3.7: **Equilibrium properties of thiophene, 2-methylthiophene and 2,5-dimethylthiophene**

UNIVERSITAT ROVIRA I VIRGILI
IMPROVEMENT OF MONTE CARLO ALGORITHMS AND INTERMOLECULAR POTENCIALS FOR THE MODELLING OF ALKANOLS, ESTHERS, TRIOPHENES AND AROMATICS
Javier Pérez Pellitero
ISBN: 978-84-691-0377-7/DL: T.2195-2007

Molecule	Type	$T_c(K)$	$\rho_c(kg/m^3)$	$T_b(K)$
Thiophene	This model	584.1(2)	372.1(4)	356.6
	Experiment	579	384	357.3
	TraPPE-UA	605	375	357.4
Benzothiophene	This model	737.9(2)	388(5)	481.8
	Experiment	754	384	493.0
2-methylthiophene	This model	597.1(3)	335(1)	380.3
	Experiment	609	357	385.7
2,5-dimethylthiophene	This model	615(1)	325(5)	399.9
	Experiment	630	342	409.9
Dibenzothiophene	This model	867.0(3)	383(4)	590.9
	Experiment	897(9)	360	604.6

Table 3.8: **Critical properties of the different compounds**

UNIVERSITAT ROVIRA I VIRGILI
IMPROVEMENT OF MONTE CARLO ALGORITHMS AND INTERMOLECULAR POTENCIALS FOR THE MODELLING OF ALKANOLS, ESTHERS, TRIOPHENES AND AROMATICS
Javier Pérez Pellitero
ISBN: 978-84-691-0377-7/DL: T.2195-2007

	$\rho_{liquid}(kg/m^3)$			$\Delta H_{vap}(kJ/mol)$			$P_{sat}(kPa)$		
T(K)	AUA	exptl	% dev	AUA	exptl	% dev	AUA	exptl	% dev
				Benzothiophene					
710	614.9±11	650.8	-5.52	19.2±0.4	22.6	-15.1	3681±38	2658	38.4
680	701.0±8.1	718.8	-2.48	25.6±0.4	27.4	-6.81	2718±50	1919	41.5
650	773.8±4.2	774.8	-0.14	30.6±0.4	31.2	-1.77	1955±29	1351	44.6
620	829.8±4.0	824.1	0.69	34.5±0.1	34.3	0.56	1358±18	921	47.3
590	873.5±1.3	869.0	0.51	37.4±0.1	37.0	1.04	900±16	602	49.2
560	909.1±3.6	910.7	-0.18	39.4±0.1	39.4	0.03	556±15	374	48.3
470	1011±2.6	1023	-1.19	46.2±0.2	45.4	1.75	82.0±3	58.1	41.1
440	1036±6.8	1058	-2.04	47.6±0.2	47.2	0.86	36.3±1.4	25.4	42.8
410	1068±6.4	1091	-2.13	49.3±0.3	48.8	1.05	13.7±0.3	9.61	42.5
380	1087±7.9	1124	-3.24	50.4±0.4	50.4	0.16	4.33±0.1	3.03	43.0
350	1106±8.5	1156	-4.29	51.6±0.4	51.8	-0.44	1.08±0.05	0.76	43.03
				Dibenzothiophene					
850	586.8±2.1	637.5	-7.96	21.2±0.2	28.9	-26.8	3497±38	2540	37.7
820	669.7±4.5	695.2	-3.68	28.9±0.2	34.5	-16.4	2633±45	1899	38.7
790	744.3±2.0	741.8	+0.34	36.1±0.1	38.8	-7.16	1940±48	1392	39.4
760	798.6±3.3	782.2	+2.11	41.4±0.1	42.4	-2.44	1402±39	997	40.6
730	841.1±3.4	818.3	+2.79	45.5±0.1	45.6	-0.15	990±27	696	42.4
700	879.7±3.4	851.4	+3.31	48.9±0.05	48.4	+1.25	675±18	470	43.8
670	917.4±2.6	882.3	+3.98	51.9±0.01	50.9	+2.15	436±11	305	43.1
640	953.2±1.3	911.3	+4.6	54.4±0.05	53.2	+2.34	257±6	160	35.9
610	983.7±3.8	938.9	+4.77	58.2±0.3	55.3	+5.26	154±3	112	38.6
580	1012±4.8	965.2	+4.82	60.2±0.3	57.3	+4.93	83.3±1.4	61.7	35.0
550	1044±7.2	990.4	+5.45	62.9±0.4	59.2	+5.69	41.8±0.9	31.5	32.4
520	1066±5.1	1015	+5.03	64.7±0.4	61.0	+5.98	18.2±0.3	14.7	24.0

Table 3.9: **Equilibrium properties of benzothiophene and dibenzothiophene**

UNIVERSITAT ROVIRA I VIRGILI
IMPROVEMENT OF MONTE CARLO ALGORITHMS AND INTERMOLECULAR POTENCIALS FOR THE MODELLING OF ALKANOLS, ESTHERS, TRIOPHENES AND AROMATICS
Javier Pérez Pellitero
ISBN: 978-84-691-0377-7/DL: T.2195-2007

Chapter 4

An Anisotropic United Atoms (AUA) potential for alcohols

UNIVERSITAT ROVIRA I VIRGILI
IMPROVEMENT OF MONTE CARLO ALGORITHMS AND INTERMOLECULAR POTENCIALS FOR THE MODELLING OF ALKANOLS, ESTHERS, TRIOPHENES AND AROMATICS
Javier Pérez Pellitero
ISBN: 978-84-691-0377-7/DL: T.2195-2007

4.1 Introduction

The increasing popularity of the use of oxygenated compounds in the field of biocombustibles has given rise to an increased interest in the family of alcohols in the petroleum industry. In particular, the simplest and most commonly used alcohols in the elaboration of biodiesels are methanol (common name methyl alcohol) and ethanol (ethyl alcohol). Alcohols are polar molecules due to the presence of the hydroxyl group in the "head" of the alkyl flexible chain which gives the molecule a nonpolar character. Alcohols, like water, can show either acidic or basic properties at the O-H group. With a pKa of around 16-19 they are generally slightly weaker acids than water, but they are able to react with strong bases. On the other hand, the nonbonded pair of electrons of the oxygen gives these compounds a basic character in the presence of strong acids. Since alcohols are also widely used as solvents, the thermodynamic properties of this family and its mixtures has been widely investigated either experimentally, theoretically or by means of molecular simulation. [98][39]

In the case of the shorter alcohols, as in the case of methanol, several models have been proposed to investigate its behaviour [33][34][35] mainly at ambient temperature and density. Vapor-liquid coexistence curves from methanol to hexanol have been obtained[36] by combining the charges of the OPLS (optimized potential for liquid simulation) force field with the Lennard-Jones (LJ) hydroxyl group parameters derived by Van Leeuwen in [37] and the alkyl groups of the Siepmann-Karaborni-Smit(SKS) [38] force field. The OPLS force field was found to be unreliable at high temperatures and longer chains. Although the model of Van Leeuwen behaves much better, it requires the methyl groups of the different alcohols to be specifically readjusted. More recently, in 2001 Chen *et al* [39] have extended the TraPPE [25](Transferable Potentials for Phase Equilibria) force field to several primary, secondary and tertiary alcohols trying to introduce as few as possible new "pseudo-atoms" to account for the difference in electronegativity between an alkane $C-C$ bond or a $C-O$ bond. In general they obtained a good agreement for a variety of alcohols and they were also able to reproduce correctly the azeotropic compositions of binary n-hexane/methanol mixtures.

In this work, we use an optimized intermolecular potential for the hydroxyl group of the family of alcohols aimed at giving a quantitative description of both liquid and coexistence properties, based on an extension of the AUA 4 intermolecular potentials already given in previous works[32, 28]. The

UNIVERSITAT ROVIRA I VIRGILI
IMPROVEMENT OF MONTE CARLO ALGORITHMS AND INTERMOLECULAR POTENCIALS FOR THE MODELLING OF ALKANOLS, ESTHERS, TRIOPHENES AND AROMATICS
Javier Pérez Pellitero
ISBN: 978-84-691-0377-7/DL: T.2195-2007

optimisation of the potential forms part of the works done by Bourasseau [99] in his thesis, while here we have extended his work to further compounds of the family and the calculation of Henry constants of different gases in alkanols. In contrast with the TraPPE approach,the aim of this optimisation was to use the same set of LJ parameters for the alkyl chain previously optimized for alkanes, without the need of defining new "pseudo-atoms". The coulombic charges have been then parameterized to reproduce the electronic structure of ethanol and methanol obtained from *ab initio* calculations. In a second step, the LJ parameters of the OH group have been fitted to reproduce selected equilibrium properties of methanol and ethanol, where the influence of the hydroxyl group is higher.

4.2 Model

4.2.1 Intermolecular Interactions

To describe the dispersion interactions, the different molecules are represented by a set of interacting Lennard-Jones sites for each CH_3, CH_2, C aromatic C and CH or OH and the respective Coulombic interactions. The energy between two different particles, i and j is calculated according to:

$$U^{LJ}(r_{ij}) = 4\epsilon_{ij}\left[\left(\frac{\sigma_{ij}}{r_{ij}}\right)^{12} - \left(\frac{\sigma_{ij}}{r_{ij}}\right)^{6}\right] + \left[\frac{q_i q_j}{4\pi\epsilon_0 r_{ij}}\right] \tag{4.1}$$

where r_{ij} is the separation between a given pair of particles i and j, ϵ_{ij} the LJ well depth, σ_{ij} the LJ size of particles, q_i and qj the partial charges and ϵ_0 the permittivity of space.

To calculate the parameters between unlike united atoms, we use the Lorentz-Berthelot combining rules:

$$\epsilon_{ij} = \sqrt{\epsilon_{ii}\epsilon_{jj}} \tag{4.2}$$

UNIVERSITAT ROVIRA I VIRGILI
IMPROVEMENT OF MONTE CARLO ALGORITHMS AND INTERMOLECULAR POTENCIALS FOR THE MODELLING OF ALKANOLS, ESTHERS, TRIOPHENES AND AROMATICS
Javier Pérez Pellitero
ISBN: 978-84-691-0377-7/DL: T.2195-2007

$$\sigma_{ij} = \frac{\sigma_{ii} + \sigma_{jj}}{2} \tag{4.3}$$

The different alkanols considered in this work have been modelled by using the AUA 4 the CH_3, CH_2 and C groups from Ungerer *et al.*[28]. In the case of the aromatic ring of phenol, we have used the CH intermolecular potential for polyaromatic compounds of Contreras *et al.* [21], and the aromatic C group of Ahunbay *et al.* [32]. The AUA parameters for the different potentials are shown in table 4.1. In table 4.3 we give the bond distances as well as the bond angles of the aromatic ring. The $\widehat{COH}$ angle and the lengths of the bonds $C-O$ and $O-H$ have been determined from *ab initio* calculations.

The bending angle is modelled by means of the following expression:

$$U_{bend}/k = \frac{1}{2} k_{bend} \left[cos(\theta) - cos(\theta_0)\right]^2 \tag{4.4}$$

where k_0 is the bending constant and θ, θ_0 the bending and equlibrium angles respectively. While the $\widehat{COH}$ angle has been considered to be rigid, as will be explained in more detail in the following section, the values for the $\widehat{CCO}$ bending angles have been taken, as in the case of Chen *et al*, from the AMBER94 force field[100]. The different values of the bending parameters are listed in table 4.2. The torsional potentials are taken from the OPLS-UA force field [101][24]:

$$U_{tors}(\phi) = c_0 + \frac{1}{2}c_1(1 + cos\phi) + \frac{1}{2}c_2(1 - cos2\phi) + \frac{1}{2}c_3(1 + cos3\phi) \tag{4.5}$$

where ϕ is the dihedral angle and the Fourier coefficients are listed in table 4.4.

4.2.2 Charge Optimization

To determine the values and positions of the electrostatic charges in the hydroxyl group of the different compounds as well as of the neighboring carbons, we have tried to reproduce the electrostatic potential of an isolated molecule determined from *ab initio* calculations. We have decided to optimize

UNIVERSITAT ROVIRA I VIRGILI
IMPROVEMENT OF MONTE CARLO ALGORITHMS AND INTERMOLECULAR POTENCIALS FOR THE MODELLING OF ALKANOLS, ESTHERS, TRIOPHENES AND AROMATICS
Javier Pérez Pellitero
ISBN: 978-84-691-0377-7/DL: T.2195-2007

Group	$\sigma(\AA)$	$\epsilon/k(K)$	$\delta(\AA)$
CH_3[28]	3.607	120.15	0.216
CH_2[28]	3.461	86.29	0.384
C	2.44	15.04	—
CH_{ar}[21]	3.246	89.42	0.407
C_{ar}[32]	3.246	37.73	—
OH	3.034	85.27	0.0951

Table 4.1: **Lennard-Jones parameters and distances of anisotropy**

bond	length $(\AA)$	angle	$\Sigma(deg)$
$C-C$	1.53	C_{ar}-C_{ar}-C_{ar}	112.7
$C_{ar}-C_{ar}$ (aromatic ring)	1.39	$C_{ar}-O-H$	108.9
$C-O$	1.425		
$O-H$	0.96		

Table 4.2: **Bond lengths and angles**

the charges to reproduce the potential calculated in a grid placed over the envelope created by spheres centered on the different atoms of the molecule. These spheres have been selected to have a radius twice the *van der Waals* radius, and they have been constructed according to the methodology proposed by Singh *et al* [102]. The methodology used is described next:

- The geometry of the molecule is optimized and the potential energy calculated for the given geometry over the N points of the chosen grid.
- The values of the partial charges are optimized so that they reproduce the potential energy over the surface. We let $\{q\} = q_i, \ldots, q_M$ be a distribution of M charges placed over the molecule. The electrostatic potential created by this set of charges over the different points p of the surface can be written as:

$$V_{q,p} = \frac{1}{4\pi\epsilon_0} \sum_{i=1}^{M} \frac{q_i}{r_{ip}} \tag{4.6}$$

  where r_{ip} is the distance between the charge i and the point over the grid p.
- We now define χ so that:

UNIVERSITAT ROVIRA I VIRGILI
IMPROVEMENT OF MONTE CARLO ALGORITHMS AND INTERMOLECULAR POTENCIALS FOR THE MODELLING OF ALKANOLS, ESTHERS, TRIOPHENES AND AROMATICS
Javier Pérez Pellitero
ISBN: 978-84-691-0377-7/DL: T.2195-2007

Angle	$\theta_0[deg]$	$k_0/k[K]$
$CH_x - CH_2 - O$	109.47	59800
$CH_x - CH_2 - CH_y$	114	74900
$CH_x - CH - CH_y$	112	72700
$CH_x - C - CH_y$	109.47	70311

Table 4.3: **Bending parameters**

Torsion	$c_0/k[K]$	$c_1/k[K]$	$c_2/k[K]$	$c_3/k[K]$
$CH_x - CH_2 - CH_2 - CH_y$	0	670.06	-136.38	1582.64
$CH_x - CH_2 - CH_2 - OH$	0	353.24	-106.68	1539.86
$CH_x - CH_2 - O - H$	0	419.64	-58.34	375.86
$CH_x - C_{ar} - O - H$	0	0	0	327.12

Table 4.4: **Torsion potential constants**

$$\chi^2 = \sum_{p=1}^{N} \left(V_{q,p} - V_p^{ref}\right)^2 \tag{4.7}$$

where V_p^{ref} represents the potential value at the point p obtained from *ab initio* calculations. The value of χ^2 must now be minimized to obtain the optimized values of the partial charges. This requires that the derivatives of χ^2 with respect to the charges $\{q\}$ must be equal to zero, so we can write:

$$\forall i \in \{1, M\}, \qquad \sum_{p=1}^{N} \frac{2}{r_{ip}} \left(\sum_{j=1}^{M} \frac{q_j}{r_{jp}} - V_p^{ref} \right) = 0 \tag{4.8}$$

An additional equation is introduced to account for the restriction that the molecule must be neutral:

$$\sum_{j=1}^{M} q_j = 0 \tag{4.9}$$

So we obtain:

UNIVERSITAT ROVIRA I VIRGILI
IMPROVEMENT OF MONTE CARLO ALGORITHMS AND INTERMOLECULAR POTENCIALS FOR THE MODELLING OF ALKANOLS, ESTHERS, TRIOPHENES AND AROMATICS
Javier Pérez Pellitero
ISBN: 978-84-691-0377-7/DL: T.2195-2007

$$\sum_{j=1}^{M}\frac{q_j}{r_{jp}}=\sum_{j=1}^{M-1}\left(\frac{q_j}{r_{jp}}+\frac{0-\sum_{j=1}^{M-1}q_j}{r_{Mp}}\right)=\sum_{j=1}^{M-1}q_j\left(\frac{1}{r_{jp}}-\frac{1}{r_{Np}}\right) \quad (4.10)$$

Substituting into equation 4.8 we obtain:

$$\forall i\in\{1,M\},\qquad \sum_{p=1}^{N}\frac{1}{r_{ip}}\left(\sum_{j=1}^{M-1}q_j\left(\frac{1}{r_{jp}}-\frac{1}{r_{Np}}\right)-V_p^{ref}\right)=0 \quad (4.11)$$

or:

$$\forall i\in\{1,M\},\qquad \sum_{j=1}^{M-1}\sum_{p=1}^{N}\left(\frac{1}{r_{ip}r_{jp}}-\frac{1}{r_{ip}r_{Np}}\right)q_j=\sum_{p=1}^{N}\frac{V_p^{ref}}{r_{ip}} \quad (4.12)$$

The problem reduces finally to solve a system of M equations with $M-1$ unknowns.

- Once the values have been determined, we can calculate the $RRMS$ (Relative Root Mean Square) deviation of the charge distribution which will give us information about the accuracy of the optimized set of charges:

$$RRMS=\frac{\sqrt{\sum_{p=1}^{N}\left(V_p^{calc}-V_p^{ref}\right)^2}}{\sqrt{\sum_{p=1}^{N}\left(V_p^{ref}\right)^2}} \quad (4.13)$$

The lower the $RRMS$ deviation, the higher the accuracy obtained in the representation of the electrostatic potential over the van der Waals surface.

This method presents the inconvenience of optimizing the charges only with respect to a single conformation of the molecule, so we are assuming the charge distribution to be valid for the different conformations adopted by the flexible molecule. The second assumption has to do with the fact that the charges have been determined for an isolated molecule, so we are assuming that the electrostatic potential created by a molecule in a vapor or liquid phase is equivalent to that created by an isolated molecule. This approximation is equivalent to neglecting the induction term created by the surrounding

UNIVERSITAT ROVIRA I VIRGILI
IMPROVEMENT OF MONTE CARLO ALGORITHMS AND INTERMOLECULAR POTENCIALS FOR THE MODELLING OF ALKANOLS, ESTHERS, TRIOPHENES AND AROMATICS
Javier Pérez Pellitero
ISBN: 978-84-691-0377-7/DL: T.2195-2007

molecules.

In the particular case of this work, we wish to obtain a single optimized set of charges which can be extended to a wide variety of alcohols, either rigid or flexible. The aforementioned methodology has been applied to different conformations of methanol and ethanol, in order to find the distribution of charges that most accurately respresents these two alcohols, which are taken to be representative of the other molecules to be studied. This assumption is made based on the fact that these two alcohols have the highest influence of the electrostatic energy with respect to the total energy, so that if the set of charges is able to reproduce correctly these target molecules, it will be expected also to reproduce correctly further compounds. In figure 4.1 we can see the two different charge distributions that have been investigated. The first one, referred from now on as distribution $\mathcal{A}$, having three charges, two of them placed over the hydrogen and the neighbour carbon, and the third one on the bisector of the $\widehat{COH}$ angle. The second distribution has four charges, two of them placed over the hydrogen and the neighbour carbon while the third one is placed on the bond between the carbon and the oxygen and the last one on the bisector of the $\widehat{COH}$ angle. The first distribution is analogous to the one commonly used for water [103], so it is interesting to test the behavior of this type of distribution for the alcohols. The reason of adding a fourth charge in distribution $\mathcal{B}$ is to improve the poor description of the dipolar moment obtained using distribution $\mathcal{A}$. Although these types of distributions are novel for alcohols in the literature, they are well justified to describe such a compounds.

The optimization of both distributions has been made according to three different configurations: methanol, ethanol-*trans*, and ethanol-*gauche* where the dihedral angles are 180° and 60° respectively. These last two configurations correspond to those found to be more stable experimentally. Table 4.5 gives the values of the $RRMS$ deviations obtained for the six optimizations according to the different distributions of charges and conformations.

We can see the important effect of adding the fourth charge in the bisector of the $\widehat{COH}$ angle. The average deviation obtained for the distribution $\mathcal{A}$ is around 25% while for distribution $\mathcal{B}$ this value is only about 12% Although the three optimizations for the distribution $\mathcal{B}$ present much improved $RRMS$ values, we have selected the set of charges optimized for the ethanol-*gauche* since this is the one presenting more constant $RRMS$ values for the three different considered conformations. The values of the charges obtained in this case are shown in table 4.6

UNIVERSITAT ROVIRA I VIRGILI
IMPROVEMENT OF MONTE CARLO ALGORITHMS AND INTERMOLECULAR POTENCIALS FOR THE MODELLING OF ALKANOLS, ESTHERS, TRIOPHENES AND AROMATICS
Javier Pérez Pellitero
ISBN: 978-84-691-0377-7/DL: T.2195-2007

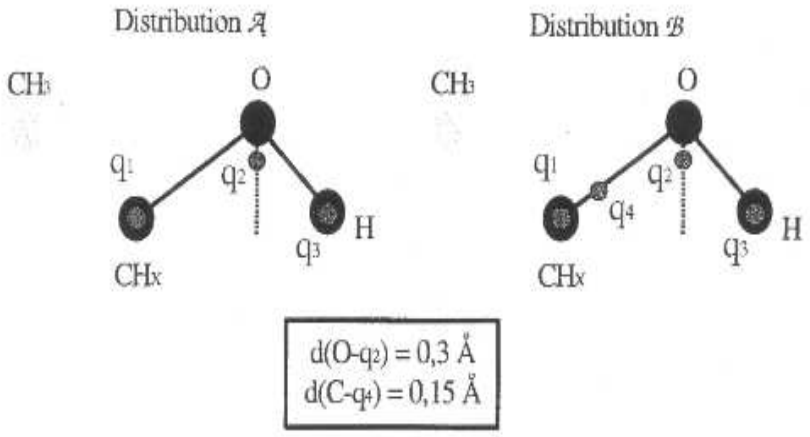

Figure 4.1: Schematic representation of the two different proposed charge distributions for alcohols.

4.3 Simulation details

To determine the coexistence properties we have used the Gibbs ensemble Monte Carlo (GEMC) combined with a configurational bias scheme[56] and an additional bias for the insertion of the center of mass of the molecules[91]. The selected probabilities for the different moves were generally set to 0.245 for rigid body translation, 0.25 for rigid body rotation, 0.5 for transfer and 0.005 for volume change. A total of 250 molecules have been used in all the simulations, using a cutoff radius equal to half of the box length with standard finite-size Lennard-Jones corrections [57]. Coexistence densities, average pressure (calculated through the virial) and enthalpies of vaporization (computed as the difference in enthalpy between the two simulation boxes) were calculated from the different simulations.

To investigate the critical region we have used Grand Canonical Monte Carlo (GCMC) simulations combined with histogram reweighting[15][16]. As for the Gibbs ensemble, a configurational bias scheme[56] and an additional bias for the insertion of the center of mass of the molecules[91] were implemented to enhance the acceptance rate of insertions. The probabilities of the

UNIVERSITAT ROVIRA I VIRGILI
IMPROVEMENT OF MONTE CARLO ALGORITHMS AND INTERMOLECULAR POTENCIALS FOR THE MODELLING OF ALKANOLS, ESTHERS, TRIOPHENES AND AROMATICS
Javier Pérez Pellitero
ISBN: 978-84-691-0377-7/DL: T.2195-2007

Distribution	methanol	ethanol-*trans*	ethanol-*gauche*
$\mathcal{A}$ optimized for methanol	**25.9**	24.9	24.3
$\mathcal{A}$ optimized for ethanol-*trans*	26.1	**24.8**	23.7
$\mathcal{A}$ optimized for ethanol-*gauche*	26.8	25.2	**23.4**
$\mathcal{B}$ optimized for methanol	**10.9**	11.9	12.9
$\mathcal{B}$ optimized for ethanol-*trans*	12.91	**10.2**	13.9
$\mathcal{B}$ optimized for ethanol-*gauche*	11.5	12.0	**12.4**

Table 4.5: $RRMS$ **values in** $\%$ **obtained after the optimization according to the different charge distributions and conformations**

-	charge q_1	charge q_2	charge q_3	charge q_4
Distribution $\mathcal{B}$ optimized for ethanol-*gauche*	-1.99	-1.49	0.70	2.78

Table 4.6: **Charges values obtained for the selected optimization**

different moves used in the simulations were 0.15 for translations, 0.15 for rotations, 0,1 for internal rotations and 0.6 for insertion or deletion. Simulation boxes of sizes between $L = 16 - 32\mathring{A}$ were used depending on the molecule. Systems were allowed to equilibrate for at least one million MC steps followed by the production run. In the case of a liquid phase, the length of the production run was set normally to 25 million MC steps.

4.4 Determination of the Lennard-Jones parameters

In order to optimize the Lennard Jones parameters for the OH group, we have selected ethanol and methanol experimental results as the reference data. These two compounds have been selected because of being the molecules where the effect of the hydroxyl group is expected to be higher. In addition, including both compounds in the optimization method takes into account the effect of both CH_3 and CH_2 as adjacent groups. To optimize the Lennard-Jones parameters, a GEMC simulation was carried out at a reduced temper-

UNIVERSITAT ROVIRA I VIRGILI
IMPROVEMENT OF MONTE CARLO ALGORITHMS AND INTERMOLECULAR POTENCIALS FOR THE MODELLING OF ALKANOLS, ESTHERS, TRIOPHENES AND AROMATICS
Javier Pérez Pellitero
ISBN: 978-84-691-0377-7/DL: T.2195-2007

ature close to the critical temperature, (450 K) for each of the compounds as well as an NPT simulation at a temperature near to the normal boiling point, (300 K). This set of four simulations optimizes the behavior of the parameters over a total of 10 different properties of ethanol and methanol.

Once the simulations have been carried out, the optimization procedure already described in section 3.4.1 is applied until the error has been minimized.

4.5 Calculation of the critical point

In order to accurately locate the critical point, and as in the case of thiophenes in chapter 3 we have applied the methodology based on the calculation of a fourth order cumulant (Binder parameter) combined with the use of finite size scaling[14] techniques described in chapter 2. The methodology is then very briefly described here. The Binder parameter U_L is defined as follows:

$$U_L = \frac{\langle m^4 \rangle}{\langle m^2 \rangle^2} \tag{4.14}$$

where m is an appropriate order parameter, in our case density. The procedure is as follows: system size dependent critical conditions are determined for different system sizes by locating the temperature at which the system takes on the "universal" Ising value of the system. Once these values are calculated, the critical constants are expected to change as a function of the system size according to known scaling laws[14]. For instance, the temperature of the finite system is expected to vary near the critical point with system size as:

$$\langle T \rangle_c(L) - \langle T \rangle_c(\infty) \sim L^{-(\theta+1)/\nu} \tag{4.15}$$

where $\Theta = 0.54$ and $\nu = 0.629$ [67][68].

In the same way, the critical density of the finite system is expected to vary with system size as:

UNIVERSITAT ROVIRA I VIRGILI
IMPROVEMENT OF MONTE CARLO ALGORITHMS AND INTERMOLECULAR POTENCIALS FOR THE MODELLING OF ALKANOLS, ESTHERS, TRIOPHENES AND AROMATICS
Javier Pérez Pellitero
ISBN: 978-84-691-0377-7/DL: T.2195-2007

$$\langle\rho\rangle_c(L) - \langle\rho\rangle_c(\infty) \sim L^{-(d-1/\nu)} \tag{4.16}$$

where d is the dimensionality of the system.

By plotting the finite size critical values according to these functions, an extrapolation can be made to estimate the corresponding infinite system size value.

4.6 Performance of the optimized parameters

The developed force field has been tested for several alcohols including methanol and ethanol which were involved in the fitting procedure. In figure 4.2 the vapor-liquid coexistence curves are presented for the density of the three shorter alcohols considered: methanol, ethanol and propanol. Saturated vapour pressures and heats of vaporization are compared to experimental data [88] in figures 4.3 and 4.4 respectively. The numerical values obtained for the different properties are presented as well in table 4.7. The liquid densities compare well with the experimental results, particularly in the case of methanol. The deviations are slightly higher in the cases of ethanol and propanol. In comparison with the UA model, we can state that our model better reproduces the critical point while the UA model describes better the coexistence curve at low temperatures. In general, it appears that both models are unable to reproduce exactly the shape of the liquid-vapor phase coexistence curve, failing either in the near-critical region or at low temperatures. Further improvements in the model, such as taking into account the flexibility of the COH angle or considering polarization in the model, would most likely be necessary to reproduce more accurately the shape of the diagram.

The saturation pressures of methanol and ethanol are found to be in very good agreement with the experimental results, while propanol is slightly overestimated. In the case of methanol, where the influence of the hydroxyl group is highest, the heats of vaporization present significant deviations from the experimental results. As could be expected, this effect becomes less important when we consider longer chains. Once more, following the behavior observed in the case of the saturated liquid densities, the AUA4 model reproduces better the critical region while it presents deviations at low temperatures. In the case of the UA model, it reproduces better the low temperatures while it presents higher deviations near the critical region. The fact that both models present the same trend for the vaporization enthalpies reinforces the hypoth-

UNIVERSITAT ROVIRA I VIRGILI
IMPROVEMENT OF MONTE CARLO ALGORITHMS AND INTERMOLECULAR POTENCIALS FOR THE MODELLING OF ALKANOLS, ESTHERS, TRIOPHENES AND AROMATICS
Javier Pérez Pellitero
ISBN: 978-84-691-0377-7/DL: T.2195-2007

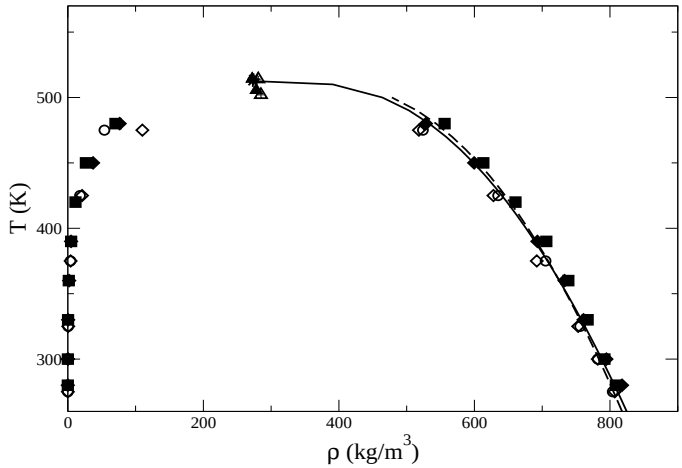

Figure 4.2: Coexistence curves of ethanol and methanol. Solid and dashed and dotted lines represent experimental data[88] for methanol and ethanol respectively. Square and circle symbols represent the simulation results for methanol and ethanol respectively. Up triangles denote critical point predictions. Stars depict experimental critical points. Open symbols denote UA model results from ref. [39] with GEMC while filled symbols are AUA4 model + HR results

esis that the incorporation of polarization to the model should be considered to better describe this property. The critical points of the different alcohols predicted with the AUA4 model are presented in table 4.8. The estimations of the UA model are also shown although a direct comparison is not possible due to the fact that in the work of Chen *et al* [39] the scaling exponent β has been fitted in order to give a better description of the critical region. In this case, the critical exponent has been fitted to reproduce the experimental critical temperatures and densities. They obtain in all cases significantly smaller values than the universal Ising value of 0.325. As can be observed in figure 4.8 we have not observed for the different alcohols any evidence that this model belongs to a different universality class. The intersections take place close to the universal Ising value of $U_L = 1.6035$ as in the case of the LJ fluid in chapter 2 or the thiophene compounds in chapter 3. In figure 4.9 we show the results obtained for the Finite Size Scaling of the intersections with universal values of the Binder parameter for the case of methanol.

In figure 4.10 the coexistence liquid densities for octanol and phenol are presented. The predicitions of the AUA4 model compare well with the available experimental results, particularly at low temperatures. As in the case of the UA model, the critical point of octanol is underpredicted. This behavior is accentuated as compared with the shorter alcohols. This effect can be

UNIVERSITAT ROVIRA I VIRGILI
IMPROVEMENT OF MONTE CARLO ALGORITHMS AND INTERMOLECULAR POTENCIALS FOR THE MODELLING OF ALKANOLS, ESTHERS, TRIOPHENES AND AROMATICS
Javier Pérez Pellitero
ISBN: 978-84-691-0377-7/DL: T.2195-2007

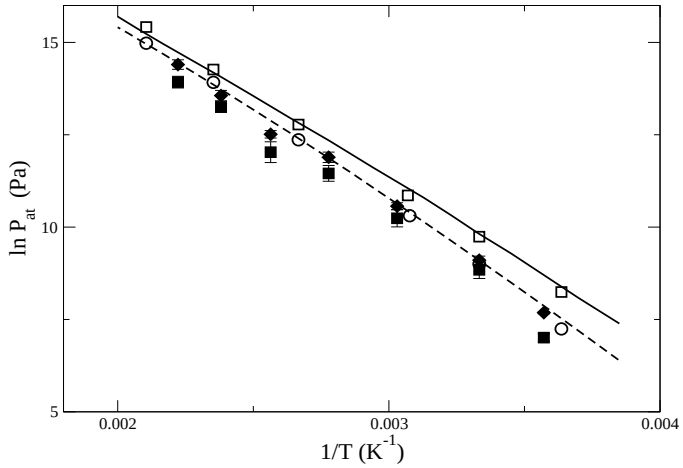

Figure 4.3: Saturated vapour pressures of ethanol and methanol. Linestyles for experimental data and symbols as in figure 4.2

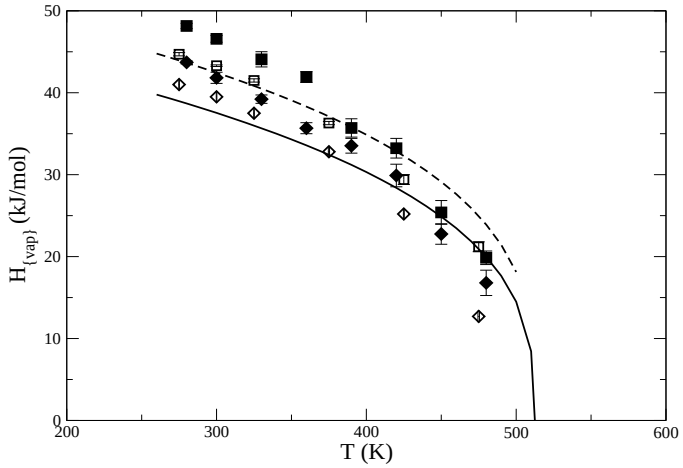

Figure 4.4: Heats of vaporization of ethanol and methanol. Linestyles for experimental data and symbols as in figure 4.2

UNIVERSITAT ROVIRA I VIRGILI
IMPROVEMENT OF MONTE CARLO ALGORITHMS AND INTERMOLECULAR POTENCIALS FOR THE MODELLING OF ALKANOLS, ESTHERS, TRIOPHENES AND AROMATICS
Javier Pérez Pellitero
ISBN: 978-84-691-0377-7/DL: T.2195-2007

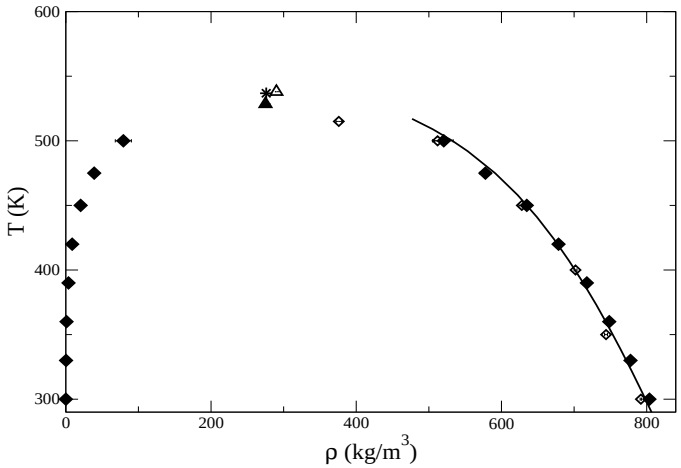

Figure 4.5: Coexistence curve of propanol. Solid line represents experimental data[88] for propanol. Up triangles denote critical point predictions. The star depicts the experimental critical point. Open symbols denote UA model results from ref. [39] with GEMC while filled symbols are AUA4 model results using GEMC

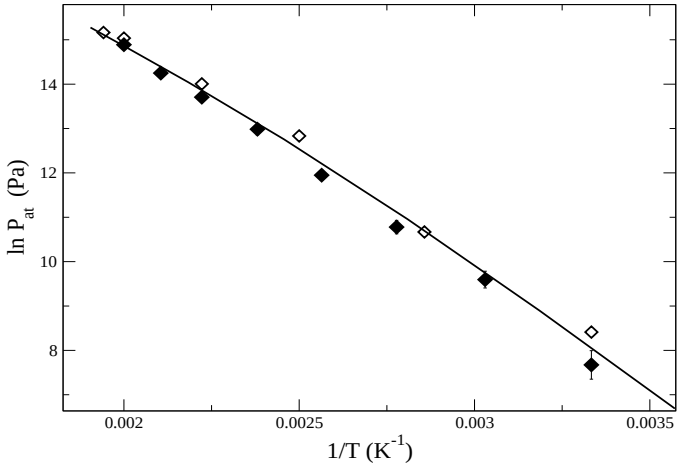

Figure 4.6: Saturated vapour pressures of propanol. Linestyles for experimental data and symbols as in figure 4.5

UNIVERSITAT ROVIRA I VIRGILI
IMPROVEMENT OF MONTE CARLO ALGORITHMS AND INTERMOLECULAR POTENCIALS FOR THE MODELLING OF ALKANOLS, ESTHERS, TRIOPHENES AND AROMATICS
Javier Pérez Pellitero
ISBN: 978-84-691-0377-7/DL: T.2195-2007

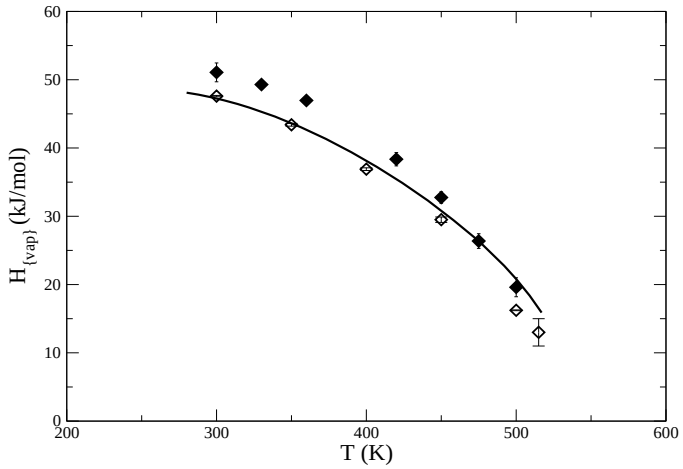

Figure 4.7: Heats of vaporization of propanol. Linestyles for experimental data and symbols as in figure 4.2

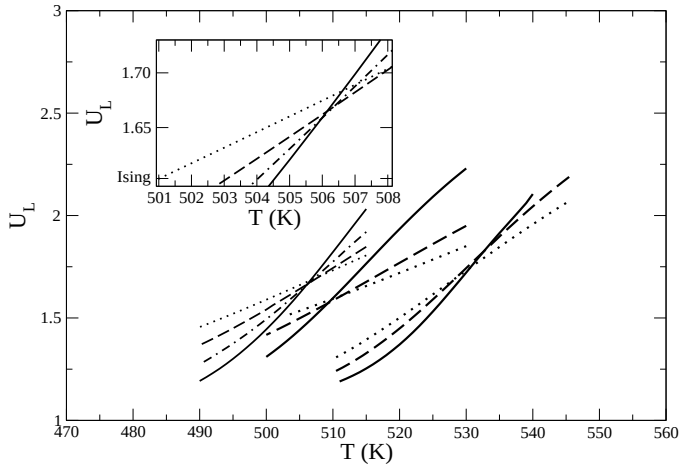

Figure 4.8: Binder parameter intersections for different system sizes for , ethanol, methanol and propanol.

UNIVERSITAT ROVIRA I VIRGILI
IMPROVEMENT OF MONTE CARLO ALGORITHMS AND INTERMOLECULAR POTENCIALS FOR THE MODELLING OF ALKANOLS, ESTHERS, TRIOPHENES AND AROMATICS
Javier Pérez Pellitero
ISBN: 978-84-691-0377-7/DL: T.2195-2007

T (K)	$\rho_{vap}(kg/m^3)$	$\rho_{liq}(kg/m^3)$	$\Delta H_{vap}(kJ/mol)$	ln $P_{sat}(kPa)$
		Methanol		
480	76.55±9	528.4±13	16.79±0.7	15.17±0.05
450	37.3±3	599.5±5.2	22.76±0.6	14.55±0.07
390	4.81±0.9	692.9±4.3	33.53±0.7	12.51±0.06
360	1.97±0.3	733.0±4.1	35.67±0.6	11.90±0.07
330	0.49±0.02	761.0±4.6	39.21±0.5	10.57±0.07
300	0.112±0.012	794.7±4.1	41.81±0.6	8.98±0.06
280	0.041±0.0098	817.8±3.9	43.70±0.2	7.98±0.03
		Ethanol		
480	70.3±7	556.0±10	19.86±0.8	14.90±0.06
450	26.7±1.3	613.2±8	25.39±0.7	14.12±0.07
420	11.3±0.8	660.5±5.6	33.23±0.7	13.34±0.06
390	4.91±0.53	706.1±4.5	35.70±0.6	12.51±0.07
360	1.44±0.14	738.6±6.6	41.92±0.6	11.28±0.05
330	0.344±0.05	767.0±5.5	44.08±0.7	9.89±0.05
300	0.058±0.008	791.9±2.1	46.57±0.4	8.03±0.06
280	0.0136±0.003	808.6±4.2	48.15±0.3	6.54±0.05
		Propanol		
500	79.3±7	520.6±8	19.60±0.8	14.89±0.09
475	39.1±3.8	578.0±7.3	26.37±0.7	14.25±0.09
450	20.5±1.4	634.9±5.7	32.75±0.8	13.71±0.09
420	8.79±0.9	678.6±6.4	38.36±0.8	12.98±0.08
390	3.69±0.9	717.6±4.5	40.32±0.8	11.95±0.09
360	0.99±0.2	748.4±4.5	46.96±0.3	10.78±0.08
330	0.33±0.07	777.7±3.1	49.29±0.4	9.59±0.08
300	0.048±0.01	803.8±2.8	51.08±0.6	7.67±0.07
		Octanol		
600	97.0±11	461.3±12	19.53±1.0	14.50±0.08
550	34.9±2	573.8±3	33.63±0.5	13.74±0.07
500	10.2±1.3	642.0±5.2	44.79±0.5	12.58±0.09
450	2.85±0.2	707.6±3.2	55.30±0.9	11.28±0.08
400	0.469±0.01	754.0±6.4	59.02±0.8	9.38±0.07
350	0.03130.001±	800.7±3.2	65.98±0.9	6.55±0.08
325	0.003±0.0004	816.1±5.3	67.81±0.9	4.20±0.07
		Phenol		
650	142.2±10	575.4±10	17.44±0.7	15.21±0.06
600	78.6±7	683.9±8	26.5±0.7	14.74±0.05
550	27.2±1.0	776.3±5.9	36.98±0.5	13.91±0.08
500	10.3±0.5	866.0±6.0	45.43±0.6	12.94±0.08
450	2.89±0.2	933.1±4.9	53.24±0.6	11.63±0.07
400	0.396±0.01	976.3±7	57.37±0.8	9.54±0.06
350	0.154±0.02	1022±3.0	61.0±0.3	8.46±0.06

Table 4.7: **Equilibrium properties of alcohols**

UNIVERSITAT ROVIRA I VIRGILI
IMPROVEMENT OF MONTE CARLO ALGORITHMS AND INTERMOLECULAR POTENCIALS FOR THE MODELLING OF ALKANOLS, ESTHERS, TRIOPHENES AND AROMATICS
Javier Pérez Pellitero
ISBN: 978-84-691-0377-7/DL: T.2195-2007

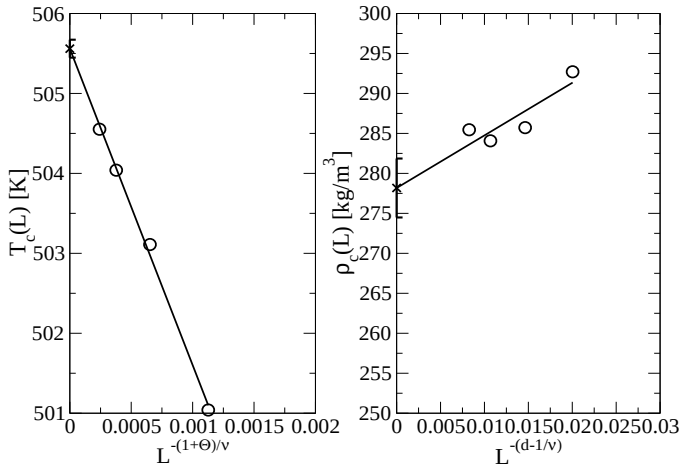

Figure 4.9: Finite Size scaling of the intersections with the universal Ising value of the Binder parameter for methanol.

attributed to the fact that the alcohols involved in the fitting process are the shortest ones: methanol and ethanol. The saturated vapour pressures shown in figure 4.11 are in very good agreement for both compounds presenting a slight overestimation in the case of phenol. Finally, in figure 4.12 are shown the predictions obtained for the heats of vaporization. In the case of octanol we have obtained an excellent agreement while in the case of phenol the AUA4 model fails to reproduce the experimental trend, overestimating the vaporization enthalpy at low temperatures. This fact could be attributed to the fact that the hydroxyl group has been fitted for short alkanols. In this case, probably an additional hydroxyl group for aromatic cycles should be optimised.

4.7

Calculation of Henry Constants of gases in alcohols

One of the advantages of the use of molecular simulation lies in the possibility to estimate Henry constants. The use of the particle insertion method, also referred to as the Widom method [104], associated with the statistical bias techniques previously described in section 1.10.1, allows for the simple and "smart" calculation of the chemical potential μ_i of a species i either in a pure fluid or a mixture. Consequently, the Henry constants of such a mixture can then be calculated. In this section, we show the application of this

UNIVERSITAT ROVIRA I VIRGILI
IMPROVEMENT OF MONTE CARLO ALGORITHMS AND INTERMOLECULAR POTENCIALS FOR THE MODELLING OF ALKANOLS, ESTHERS, TRIOPHENES AND AROMATICS
Javier Pérez Pellitero
ISBN: 978-84-691-0377-7/DL: T.2195-2007

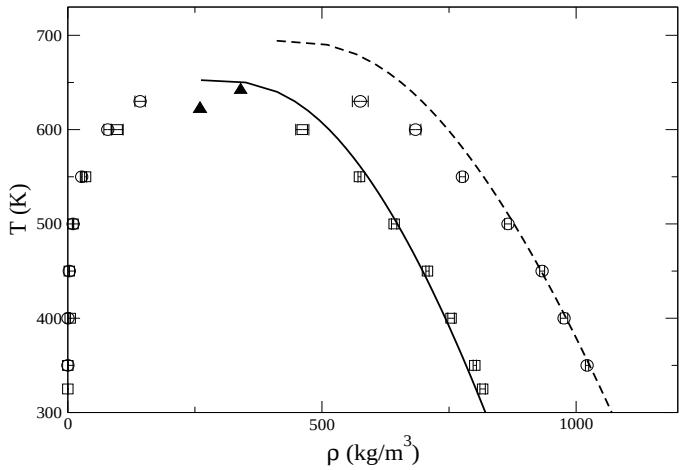

Figure 4.10: Coexistence curves of octanol and phenol. Solid and dashed lines represent experimental data[88] for octanol and phenol respectively. Square and circle symbols represent the simulation results for octanol and phenol respectively. Up triangles denote critical point predictions.

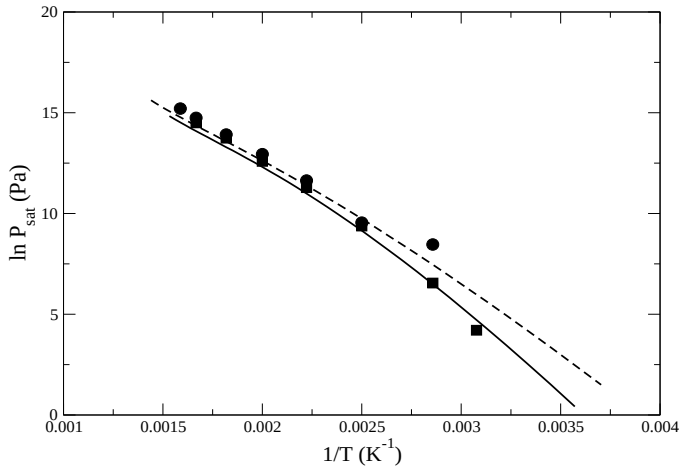

Figure 4.11: Saturated vapour pressures of octanol and phenol. Linestyles for experimental data and symbols as in figure 4.10

UNIVERSITAT ROVIRA I VIRGILI
IMPROVEMENT OF MONTE CARLO ALGORITHMS AND INTERMOLECULAR POTENCIALS FOR THE MODELLING OF ALKANOLS, ESTHERS, TRIOPHENES AND AROMATICS
Javier Pérez Pellitero
ISBN: 978-84-691-0377-7/DL: T.2195-2007

Molecule	Type	$T_c(K)$	$\rho_c(kg/m^3)$	$T_b(K)$
Methanol	This model	505.6(1)	278(3)	355
	TraPPE-UA	502(2)	285(4)	340(1)
	Experiment	512.5	273	338
Ethanol	This model	514.2(7)	271.5(3)	367
	TraPPE-UA	514(2)	281(3)	353(1)
	Experiment	514	274	351
Propan-1-ol	This model	528.5(9)	275(6)	377
	TraPPE-UA	538(2)	290(4)	368(2)
	Experiment	536.8	276	370.4
Octanol	This model	624.2(5)	252(4)	468
	TraPPE-UA	629(2)	270(2)	460(3)
	Experiment	652.5	262	468.4
Phenol	This model	642.8(5)	342(8)	590.9
	Experiment	694.2	411	455

Table 4.8: **Critical properties of the different alcohols**

methodology to the calculation of Henry constants of different gases in alcohols. The Henry constant of five different gases (methane, oxygen, nitrogen, carbon dioxide, hydrogen sulphide) have been determined for four different alcohols (methanol, ethanol, propanol, octanol) as a function of temperature.

The Henry constant K_H, which has the dimension of a pressure, is related in the limit of low concentration to the fugacity according to:

$$K_H x_i = f_i \tag{4.17}$$

where x_i is the concentration of the solute in the liquid phase and f_i is its fugacity in the quilibrium.

The use of the Widom method allows us to calculate the chemical potential μ_i of the species i, which is related to the fugacity. In particular, the chemical potential can be calculated by means of the next expression:

$$\mu_i = -kTln\left\langle \frac{V}{N_i+1} exp(-\beta\Delta U^+) \right\rangle \tag{4.18}$$

where ΔU^+ is the potential energy difference caused by the insertion of the test molecule, V is the volume of the system and N_i is the number of

UNIVERSITAT ROVIRA I VIRGILI
IMPROVEMENT OF MONTE CARLO ALGORITHMS AND INTERMOLECULAR POTENCIALS FOR THE MODELLING OF ALKANOLS, ESTHERS, TRIOPHENES AND AROMATICS
Javier Pérez Pellitero
ISBN: 978-84-691-0377-7/DL: T.2195-2007

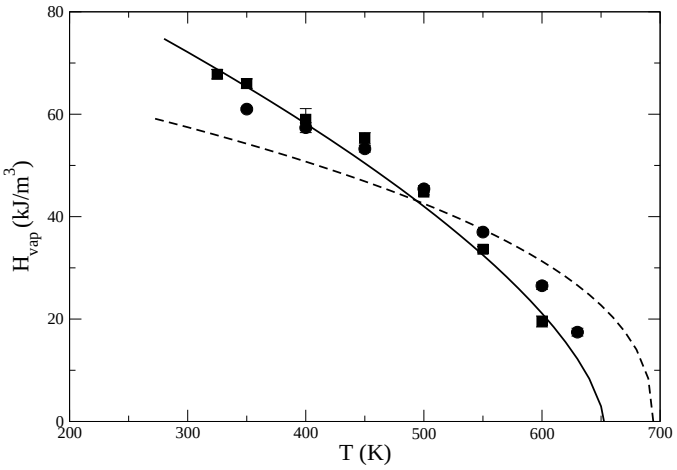

Figure 4.12: Vaporization enthalpies of octanol and phenol. Linestyles for experimental data and symbols as in figure 4.10

gas molecules in the solvent. As discussed by Frenkel and Smit [104], the de Broglie wavelength does not appear in the last expression due to the fact that it cancels out when the ideal gas at the same temperature is taken as the reference state, that is, when $\mu_i = 0$. According to Eqn. 4.18, these conditions are satisfied for a fluid of unit density $(V/(N_i + 1 = 1)$ and zero interaction energy $(\Delta U^+ = 0)$, which means an ideal gas of unit density. Although this reference state has no physical meaning, it makes the relationship with gas fugacity explicit through the equation of state of a system of $(N+1)$ molecules of an ideal gas:

$$P_0 = \frac{(N+1)kT}{V} = kT \tag{4.19}$$

Then the chemical potential defined by Eqn. 4.17 can be written as:

$$\mu_i = kTln\left(\frac{f_i}{P_0}\right) \tag{4.20}$$

Since the implicit reference pressure P_0 is not constant, it is more convenient to use a reference state with fixed pressure $P_{ref} = 1Pa$, i.e. the unit of the international system. Once we have defined this new reference state, we

UNIVERSITAT ROVIRA I VIRGILI
IMPROVEMENT OF MONTE CARLO ALGORITHMS AND INTERMOLECULAR POTENCIALS FOR THE MODELLING OF ALKANOLS, ESTHERS, TRIOPHENES AND AROMATICS
Javier Pérez Pellitero
ISBN: 978-84-691-0377-7/DL: T.2195-2007

can also define a chemical potential $\overline{\mu_i}$ wich is related to μ_i according to:

$$\overline{\mu_i} = kTln\left(\frac{P_0}{P_{ref}}\right) + \mu_i = kTln\left(\frac{f_i}{P_{ref}}\right) \tag{4.21}$$

Now making use of Eqns. 4.18 and 4.19 we can write:

$$\overline{\mu_i} = kTln\left(\frac{P_0}{P_{ref}}\right) - kTln\left\langle\frac{V}{N_i+1}exp(-\beta\Delta U^+)\right\rangle \tag{4.22}$$

The Henry constant in international system units can be determined by applying Eqns. 4.17 and 4.21 and by considering that $x_i = (N_i+1)/(N+1)$ where N is the total number of molecules in the solvent:

$$\frac{K_H}{P_{ref}} = \frac{f_i}{P_{ref}x_i} = \frac{(N+1)exp(\overline{\mu_i}/kT)}{N_i+1} \tag{4.23}$$

The Henry constant can then be determined in the limit of infinite dilution by making test insertions of the different gas molecules in the solvent. It is important to remark that the big advantage of this methodology is that different Henry constants can be determined from the same single simulation. This expression works correctly for methane, since it can be considered as a single center Lennard-Jones fluid. In the case of the other gases, which involve several force centers and electrostatic charges, as was previously mentioned, we need to use the statistical bias methods described in section 1.10.1

Finally, the variation of the Henry constant with the temperature is related to the infinite dilution hydration Gibbs energy $\Delta_{hyd}G^\infty$[105] according to:

$$\Delta_{hyd}G^\infty = RT\left(\frac{lnK_H}{p^0}\right) \tag{4.24}$$

and through its temperature derivatives to infinite dilution hydration enthalpy $\Delta_{hyd}H^\infty$:

$$\Delta_{hyd}H^\infty = -RT^2\left(\frac{dlnK_H}{dT}\right) \tag{4.25}$$

UNIVERSITAT ROVIRA I VIRGILI
IMPROVEMENT OF MONTE CARLO ALGORITHMS AND INTERMOLECULAR POTENCIALS FOR THE MODELLING OF ALKANOLS, ESTHERS, TRIOPHENES AND AROMATICS
Javier Pérez Pellitero
ISBN: 978-84-691-0377-7/DL: T.2195-2007

The infinite dilution solvation quantity corresponds to a transfer of one mol of the solute from the pure ideal gas state at standard pressure $P^0 = 100kPa$ to a hypothetical infinitely dilute solution. This quantity can also be determined from molecular simulation [106] by estimating the free energy with HR+GCMC simulations along a thermodynamic path.

4.7.1 Intermolecular potentials for gases

In table 4.9 are given the potential parameters of the different models for the five different gases considered.

To reproduce the methane molecule, the model proposed by Möller *et al* has been selected [107]. It involves a single LJ force center with the absence of electrostatic charges.

In the case of nitrogen, the model proposed by Delhomelle [85] has been chosen. It involves two LJ force centers separated by a fixed distance of 1.098 $\AA$ as well as two negative electrostatic charges located on the atomic centers and one positive charge on the center of mass. These charges were fitted respecting the experimental quadripolar moment of the molecule. The LJ parameters were fitted to reproduce the coexistence curve of the nitrogen molecule thus providing an excellent account of the liquid-vapor coexistence densities of pure nitrogen.

The model selected for oxygen has been proposed by Vrabec *et al*[109] who determined the parameters of several fluids with a two LJ centers plus point quadripole moment on the basis of the liquid-vapor coexistence properties. As our software does not at present allow for point quadripoles, three electrostatic charges have been introduced as in the case of nitrogen or carbon dioxide, but with a very close spacing of 0.2 $\AA$ The values of these charges were determined in such a way that the quadripolar moment indicated by Vrabec *et al*, i.e. 0.8081 D $\AA$, was exactly respected.

For carbon dioxide, the selected model is the EPM2 potential of Harris and Yung [110] wich involves three LJ force centers and three electrostatic charges on the atomic centers.

Finally, the model selected for the hydrogen sulfide is that proposed by Kristof and Liszi [78] involving one single LJ center of force and four electrostatic charges, three of them at the atomic centers of the different atoms of the molecule and the fourth one on the bisector of the angle formed by the hydrogens and the sulphur.

UNIVERSITAT ROVIRA I VIRGILI
IMPROVEMENT OF MONTE CARLO ALGORITHMS AND INTERMOLECULAR POTENCIALS FOR THE MODELLING OF ALKANOLS, ESTHERS, TRIOPHENES AND AROMATICS
Javier Pérez Pellitero
ISBN: 978-84-691-0377-7/DL: T.2195-2007

Although Lorentz-Berthelot combining rules were used in the development of the AUA potential, we have used Kong [111] [112] [113] combining rules to evaluate the cross-interactions between unlike groups. These rules are:

$$\epsilon ij\sigma_{ij}^6 = \sqrt{\epsilon_i\sigma_i^6\epsilon j\sigma_j^6} \tag{4.26}$$

$$\epsilon_{ij}\sigma_{ij}^{12} = \frac{\epsilon_i\sigma_i^{12}}{2^{13}}\left[1+\left(\frac{\epsilon_j\sigma_j^{12}}{\epsilon_j\sigma_j^{12}}\right)^{1/13}\right]^{13} \tag{4.27}$$

The use of Kong combining rules instead of Lorentz-Berthelot rules has been previously well justified for mixtures of carbon dioxide with alkanes[11]. Also, the these rules have been found to perform better for binary mixtures of noble gases[114] and carbon dioxide with hydrogen sulfide[115].

4.7.2 Results

The results obtained for the different gases in the different solvents are shown in figures 4.13-4.16. The Henry constant are ranked in the same order for a given temperature and solvent for all the figures. The Henry constant decreases as the critical temperature of the different solutes increases. In particular, nitrogen exhibits the highest critical temperature followed by oxygen, methane, carbon dioxide and hydrogen sulfide. The explanation for this phenomena is that the higher the critical temperature of the solute is, the larger the attraction energy in the liquid phase is and the higher the solubility in the solvent is. This behavior is also in good agreement with the available reference data for ethanol [116]

In the case of the temperature dependence, it differs from one component to the next. Except for octanol where all the solutes increase their solubilities as temperature is increased, in the other cases the Henry constant decreases with increasing temperatures for nitrogen, oxygen and methane, while it increases with increasing temperatures for carbon dioxide and hydrogen sulfide. Further investigation of the liquid structure would be required to understand the origin of the specific temperature dependence shown by these compounds. In the case of ethanol, where experimental data are available, the

UNIVERSITAT ROVIRA I VIRGILI
IMPROVEMENT OF MONTE CARLO ALGORITHMS AND INTERMOLECULAR POTENCIALS FOR THE MODELLING OF ALKANOLS, ESTHERS, TRIOPHENES AND AROMATICS
Javier Pérez Pellitero
ISBN: 978-84-691-0377-7/DL: T.2195-2007

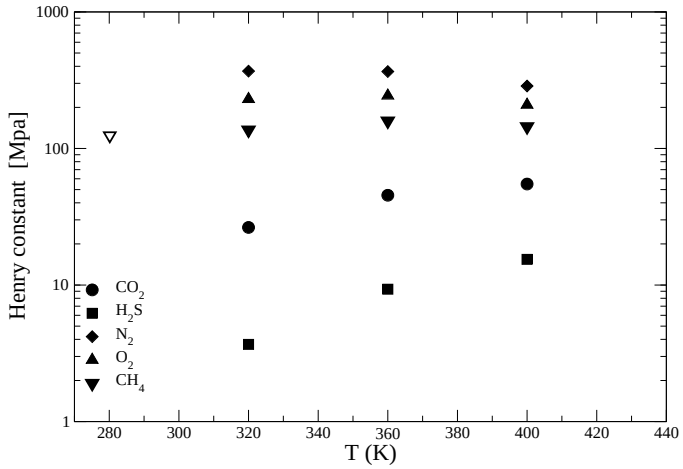

Figure 4.13: Henry constants for different gases in methanol as a function of the temperature. Filled symbols represent result from the simulations while open symbols represent experimental results [120]

obtained results are in good quantitative agreement for the different solutes and the predicted variations with temperature is reproduced satisfactorily. In the case of methane and oxygen, the effect of temperature on the Henry constant is found to be insignificant if statistical uncertainties are accounted for, in agreement with experiment.

Although it is generally recommended to use staged insertions for evaluating chemical potentials [117] in our case we have obtained reasonable estimations of the Henry constants for the different solvents. This can be explained because the temperatures are not too low, except in the case of octanol, where the lowest temperature considered is 130 K below its normal boiling point. This means that, in general, at these conditions, the liquid structure still presents sufficient ”holes” to accommodate the small solutes we have considered and a reasonable sampling can be obtained. The second explanation is the amount of computational time dedicated to the sampling of the solvent: at least 100 million MC moves in all cases and up to 400 million MC steps for octanol at the lower temperatures. This fact can be illustrated by the average statistical deviations obtained, whose values are around 5%. Staged insertion would probably have been required when considering significantly larger solutes or significantly lower temperatures, where the computational time necessary required to apply the Widom test at the same conditions obtained using the staged deletion method is significantly higher.[118][119]

UNIVERSITAT ROVIRA I VIRGILI
IMPROVEMENT OF MONTE CARLO ALGORITHMS AND INTERMOLECULAR POTENCIALS FOR THE MODELLING OF ALKANOLS, ESTHERS, TRIOPHENES AND AROMATICS
Javier Pérez Pellitero
ISBN: 978-84-691-0377-7/DL: T.2195-2007

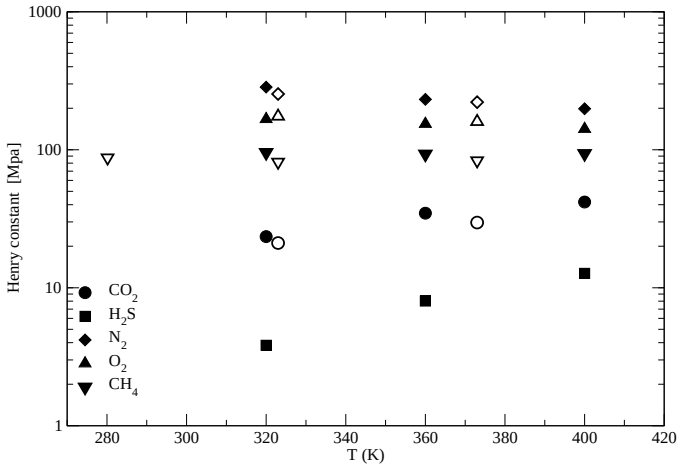

Figure 4.14: Henry constants for different gases in ethanol as a function of the temperature. Filled symbols represent result from the simulations while open symbols represent experimental results[116] [120]

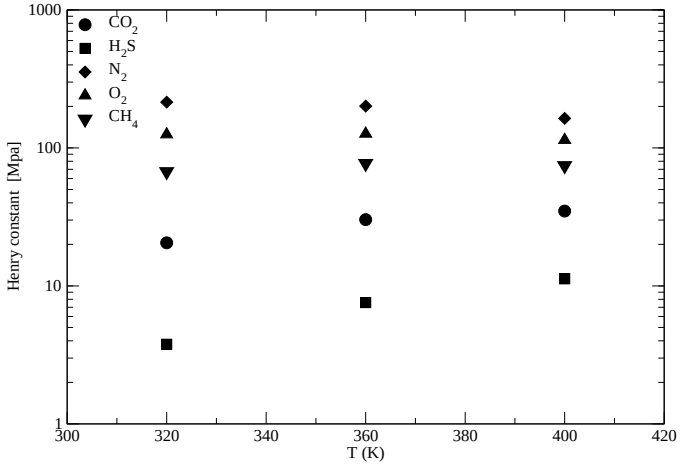

Figure 4.15: Henry constants for different gases in propanol as a function of the temperature.

UNIVERSITAT ROVIRA I VIRGILI
IMPROVEMENT OF MONTE CARLO ALGORITHMS AND INTERMOLECULAR POTENCIALS FOR THE MODELLING OF ALKANOLS, ESTHERS, TRIOPHENES AND AROMATICS
Javier Pérez Pellitero
ISBN: 978-84-691-0377-7/DL: T.2195-2007

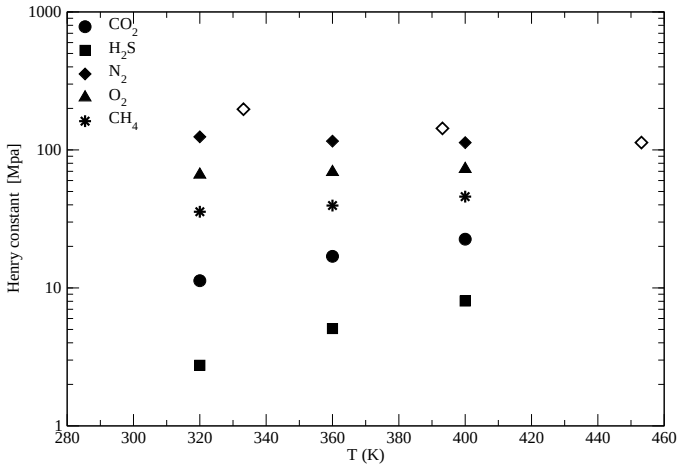

Figure 4.16: Henry constants for different gases in octanol as a function of the temperature. Filled symbols represent result from the simulations while open symbols represent experimental results [121]

4.8 Conclusions

The AUA4 potential has been extended to alcohols by adjusting the LJ parameters of the hydroxyl group and optimizing a set of charges so that they reproduce the electrostatic distributions of methanol and ethanol. Although the behavior of the model could be improved individually by optimizing different sets of LJ parameters for the carbon groups next to the hydroxyl, our goal is to produce parameters that are transferable to other molecules. In this way, we have kept the LJ parameters of the groups adjacent to the hydroxyl in order to maintain as far as possible the transferability of the AUA4 model, while still reproducing the equilibrium properties with an accuracy similar to previously proposed models. While the predictions for the saturated liquid densities and the vapor pressures agree well with the experimental data, the model has more difficulties to reproduce the heats of vaporization. Contrary to the TraPPE model, our model compares better near to the critical region while presenting higher deviations at low temperatures. From the finite size scaling study, we have shown that the presence of the electrostatic charges in this model does not change the universality class, belonging still to the Ising class.

UNIVERSITAT ROVIRA I VIRGILI
IMPROVEMENT OF MONTE CARLO ALGORITHMS AND INTERMOLECULAR POTENCIALS FOR THE MODELLING OF ALKANOLS, ESTHERS, TRIOPHENES AND AROMATICS
Javier Pérez Pellitero
ISBN: 978-84-691-0377-7/DL: T.2195-2007

We have also calculated the Henry law constants of different gases in different alcohols by applying the Widom particle insertion method and have obtained very good agreement with the available experimental data. In particular, the temperature dependence of the constants is well reproduced.

UNIVERSITAT ROVIRA I VIRGILI
IMPROVEMENT OF MONTE CARLO ALGORITHMS AND INTERMOLECULAR POTENCIALS FOR THE MODELLING OF ALKANOLS, ESTHERS, TRIOPHENES AND AROMATICS
Javier Pérez Pellitero
ISBN: 978-84-691-0377-7/DL: T.2195-2007

Force center / charge	Position			LJ parameters		Charge
	X	Y	Z	$\epsilon/k(K)$	$\sigma(\AA)$	
CH_4[107]						
C	0	0	0	149.92	3.7327	0
N_2[108]						
N	0.549	0	0	36.0	3.30	-0.5075
N	-0.549	0	0	36.0	3.30	-0.5075
q_1	0	0	0	-	-	1.015
O_2[109]						
O1	-0.485	0	0	43.183	3.1062	0
O2	0.485	0	0	43.183	3.1062	0
q_1	0	0	0	-	-	4.2
q_2	0.2	0	0	-	-	-2.1
q_3	-0.2	0	0	-	-	-2.1
CO_2[110]						
C	0	0	0	28.129	2.757	0.6512
O1	1.149	0	0	80.507	3.033	-0.3256
O2	-1.149	0	0	80.507	3.033	-0.3256
H_2S[78]						
H_2S	0	0	0	250	3.73	0
q_1	0	0	0	-	-	0.4
H1	1.149	0.9639	0.9308	-	-	0.25
H2	-1.149	-0.9639	0.9308	-	-	0.25
S	-1.149	0	0	-	-	-0.9

Table 4.9: **Intermolecular potential parameters of the five different gases considered**

UNIVERSITAT ROVIRA I VIRGILI
IMPROVEMENT OF MONTE CARLO ALGORITHMS AND INTERMOLECULAR POTENCIALS FOR THE MODELLING OF ALKANOLS, ESTHERS, TRIOPHENES AND AROMATICS
Javier Pérez Pellitero
ISBN: 978-84-691-0377-7/DL: T.2195-2007

Chapter 5

An Anisotropic United Atoms (AUA) potential for ethers

UNIVERSITAT ROVIRA I VIRGILI
IMPROVEMENT OF MONTE CARLO ALGORITHMS AND INTERMOLECULAR POTENCIALS FOR THE MODELLING OF ALKANOLS, ESTHERS, TRIOPHENES AND AROMATICS
Javier Pérez Pellitero
ISBN: 978-84-691-0377-7/DL: T.2195-2007

5.1 Introduction

The important role played by solvents in organic chemistry as well as in biochemistry is responsible for the need to model a variety of liquid compounds. Ether compounds are slightly polar, but not as much as the compounds of other families with similar structures like alcohols, esters or amides. The fact that ether compounds are not able to form hydrogen bonds between the molecules, results in lower boiling points compared to the analogous alcohols. Nonetheless, the lone pair of electrons on the oxygen atom allow for hydrogen bonding with water molecules. In particular, cyclic ethers such as tetrahydrofuran and 1,4-dioxane are totally miscible in water due to the fact that the oxygen atom is more exposed for hydrogen bonding as compared to aliphatic ethers. Due to their application as solvents, there is a considerable interest in the thermophysical properties of ethers. In particular, aliphatic ethers and polyethers are used in gasolines as additives, appear in chromatographic stationary phases and are also employed as cosolvents in supercritical fluids.

As has been shown in previous chapters of this thesis, molecular simulation is an alternative way to predict equilibrium thermodynamic properties of pure fluids and mixtures. Hence the need for accurate force fields able to describe the microscopic interactions of different compounds. In the case of ethers, the united-atom OPLS force field developed by Jorgensen *et al* for dimethyl, ethyl methyl and diethylether [122] was proposed to reproduce thermodynamic quantities at or near standard temperature and pressure. Far away from these conditions, such a model becomes less accurate. To account for a better and more general description, Siepmann and coworkers [123] have proposed the extension of the TraPPE [25] (transferable potentials for phase equilibria) force field by developing paramethers for the ether oxygen sites taking the rest of the groups from earlier works.

As in the case of alcohols in chapter 4, we have optimised an intermolecular potential for the oxygen atom of the ether molecules, based on an extension of the AUA 4 intermolecular potential already developed in previous works [32, 28]. A simple model of three different electrostatic charges placed on the oxygen and the adjacent carbons is proposed to reproduce the electronic structure of dimethylether before fitting the LJ parameters of the oxygen to reproduce selected equilibrium properties of ethers. As in the case of alcohols, we avoid the definition of new ”pseudo-atoms” for those carbons next to the oxygen group.

UNIVERSITAT ROVIRA I VIRGILI
IMPROVEMENT OF MONTE CARLO ALGORITHMS AND INTERMOLECULAR POTENCIALS FOR THE MODELLING OF ALKANOLS, ESTHERS, TRIOPHENES AND AROMATICS
Javier Pérez Pellitero
ISBN: 978-84-691-0377-7/DL: T.2195-2007

5.2 Model

5.2.1 Intermolecular Interactions

As in the case of alcohols in the previous chapter, to describe the dispersion interactions, the different molecules are represented by a set of interacting Lennard-Jones sites for each CH_3, CH_2, C or O group. The interaction between two different united atoms, i and j, from different molecules is calculated according to equation 4.1

To calculate the parameters between unlike united atoms, we use the Lorentz-Berthelot combining rules of equations 4.2 and 4.3.

As for the force field developed for alcohols, the different ethers considered have been modelled by using the AUA 4 model parameters for the CH_3 and CH_2 groups from Ungerer *et al.*[28] in order to mantain the transferability of the model and to keep to a maximum its simplicity. The oxygen group has then been fitted to reproduce experimental properties of ethylmethylether which has the advantage of incorporating both the effect of the adjacents CH_2 and CH_3 groups for the optimization of the LJ parameters. The parameters for the different potentials are shown in table 5.1. The length of the bond $C-O$ has been determined from *ab initio* calculations.

The bending angle is controlled by means of the following expression:

$$U_{bend}/k = \frac{1}{2}k_\theta \left(\theta - \theta_0\right)^2 \tag{5.1}$$

where k_θ is the bending constant and θ, θ_0 the bending and equlibrium angles respectively. The values for the bending angles have been taken as from the AMBER94 force field[100]. The different values of the bending parameters are listed in table 5.3. The torsional potentials are taken from the OPLS-UA force field [122]:

$$U_{tors}(\phi) = c_0 + \frac{1}{2}c_1(1 + cos\phi) + \frac{1}{2}c_2(1 - cos2\phi) + \frac{1}{2}c_3(1 + cos3\phi) \tag{5.2}$$

UNIVERSITAT ROVIRA I VIRGILI
IMPROVEMENT OF MONTE CARLO ALGORITHMS AND INTERMOLECULAR POTENCIALS FOR THE MODELLING OF ALKANOLS, ESTHERS, TRIOPHENES AND AROMATICS
Javier Pérez Pellitero
ISBN: 978-84-691-0377-7/DL: T.2195-2007

where ϕ is the dihedral angle and the Fourier coefficients are listed in table 5.4.

Group	$\sigma(\AA)$	$\epsilon/k(K)$	$\delta(\AA)$
CH_3[28]	3.607	120.15	0.216
CH_2[28]	3.461	86.29	0.384
O	2.991	59.69	—

Table 5.1: **Lennard-Jones parameters and distances of anisotropy**

bond	length $(\AA)$	angle	$\Sigma(deg)$
$C-C$	1.53	$C-O-C$	112
$C-O$	1.425		

Table 5.2: **Bond lengths and angles**

Angle	$\theta_0[deg]$	$k_\theta/k[K]$
CH_x-CH_y-O	112	50300
CH_x-O-CH_y	112	60400
$CH_x-CH_2-CH_y$	114	62500

Table 5.3: **Bending parameters**

5.2.2 Charges Optimization

By adjusting the values of the electrostatic charges in the oxygen group of the different compounds as well as of the neighbouring carbons, we have tried to reproduce the electrostatic potential of an isolated molecule of dimethylether determined from *ab initio* calculations. The charges have been optimized to reproduce the potential calculated in a grid placed over the envelope created by the spheres centered on the different atoms of the molecule. These spheres have been selected to have twice the *van der Waals* radius, and they have been constructed according to the methodology proposed by Singh *et al* [102]. We have then used the methodology previously described in section 4.2.2. The distribution proposed in this case is much simpler than the one used in the case of alcohols due to the moderate dipole moments of the ether molecules. In this case we have set a negative charge over the oxygen atom plus two positive and equal charges over the adjacent carbons with independence of the pseudoatom type.

UNIVERSITAT ROVIRA I VIRGILI
IMPROVEMENT OF MONTE CARLO ALGORITHMS AND INTERMOLECULAR POTENCIALS FOR THE MODELLING OF ALKANOLS, ESTHERS, TRIOPHENES AND AROMATICS
Javier Pérez Pellitero
ISBN: 978-84-691-0377-7/DL: T.2195-2007

Torsion	$c_0/k[K]$	$c_1/k[K]$	$c_2/k[K]$	$c_3/k[K]$
$CH_x - CH_2 - CH_2 - CH_y$	0	670.06	-136.38	1582.64
$CH_x - CH_y - O - CH_z$	0	1450.7	-327.5	1116.4
$O - CH_2 - CH_2 - O$	503.24	0	-503.24	2012.94
$CH_x - CH_2 - CH_2 - O$	0	353.24	-106.68	1539.86

Table 5.4: **Torsion potential constants**

5.3 Determination of the Lennard-Jones parameters

The oxygen group of the ether molecules has been fitted to the experimental properties of ethylmethylether. To optimize the Lennard-Jones parameters, two GEMC simulation were carried out. The first one at a reduced temperature of 0.95, concretely 420 K, while the second one was performed at 280 K. Once the simulations were done, the optimization methodology described in section 3.5 was applied. These two simulations optimizes the behavior of the oxygen LJ parameters over a total of 6 different properties of ethylmethylether including saturated liquid densities, saturation pressures and heats of vaporization. After applying the aforementioned methodology the LJ parameters shown in table 5.1 were obtained.

5.4 Performance of the parameters

Once the distribution of charges and the LJ parameters of the oxygen group were determined, the model has been tested with different compounds of the family: dimethylether, diethylether, 1,2-dimethoxyethane and tetrahydrofuran (THF). The results for dimethyl, ethylmethyl and diethylether are shown in figures 5.1-5.3 as well as in table 5.6. The saturated liquid densities compare well with the experimental results, 4% being the highest deviation obtained in the case of diethylether. In table 5.5 are shown the predictions for the critical point as well as for the normal boiling points of the AUA 4 model. The results are also in good agreement with the experimental data, particularly in the cases of dimethyl and ethylmethylether, where the obtained deviations are lower than 2%. As explained in previous chapters, the critical properties have

UNIVERSITAT ROVIRA I VIRGILI
IMPROVEMENT OF MONTE CARLO ALGORITHMS AND INTERMOLECULAR POTENCIALS FOR THE MODELLING OF ALKANOLS, ESTHERS, TRIOPHENES AND AROMATICS
Javier Pérez Pellitero
ISBN: 978-84-691-0377-7/DL: T.2195-2007

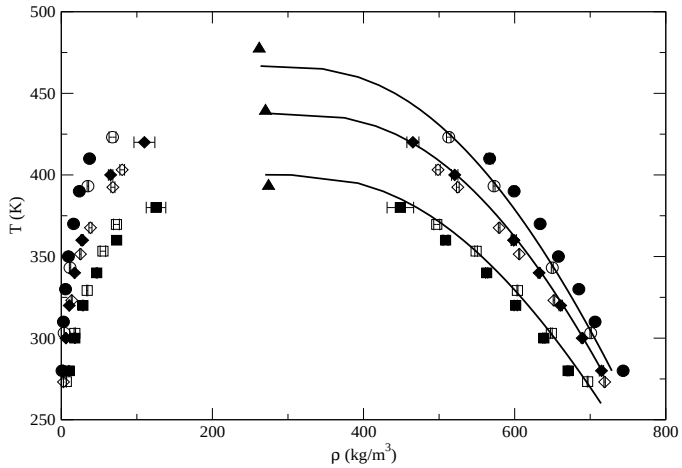

Figure 5.1: Coexistence curves of ethers. Solid lines represent experimental data[88] for dimethyl, ethylmethyl and diethylether. Square, diamond, and circle symbols represent the simulation results for dimethyl, ethylmethyl and diethylether respectively. Open symbols denote UA model results from ref. [123] with GEMC while filled symbols are GEMC results of this model. Up triangles denote the calculated critical points.

been determined by applying Finite Size Scaling techniques to the intersections with the universal value of the Binder parameter. The results obtained for the three shorter ethers are shown in figures 5.8- 5.10. The saturation pressures are in very good agreement with the experimental results in particular for ethylmethylether, where the normal boiling point is reproduced within 2%. Finally, the heats of vaporization compare well with the experimental results in particular for ethylmethylether. In the case of dimethylether this property is slightly underestimated as is expected from the fact that the saturated liquid densities are also.

Tetrahydrofuran and 1,2-dimethoxyethane have been selected to test the behavior of the parameters in the case of a cyclic molecule in the former and in the presence of a double ether functionality in the latter one. The results obtained for both molecules are shown in figures 5.4-5.6. The densities are very well reproduced for both compounds, and in particular in the case of 1,2-dimethoxyethane. The estimations of the critical temperatures are within 1 % for the two compounds. The saturation pressures are slightly overestimated in the case of THF, leading to higher deviations in the normal boiling point while in the case of 1,2-dimethoxyethane this property is reproduced within 1 %. Finally, in the case of the heats of vaporization, the predictions are this time better for THF than for 1,2-dimethoxyethane where this property is slightly

UNIVERSITAT ROVIRA I VIRGILI
IMPROVEMENT OF MONTE CARLO ALGORITHMS AND INTERMOLECULAR POTENCIALS FOR THE MODELLING OF ALKANOLS, ESTHERS, TRIOPHENES AND AROMATICS
Javier Pérez Pellitero
ISBN: 978-84-691-0377-7/DL: T.2195-2007

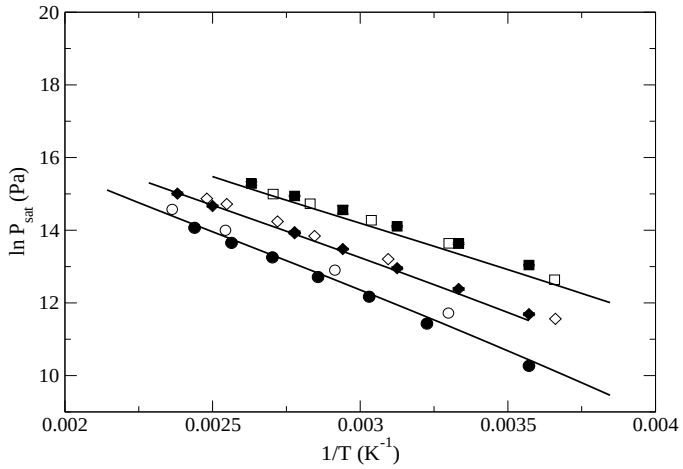

Figure 5.2: Saturated vapour pressures of ethers. Linestyles for experimental data and symbols as in figure 5.1

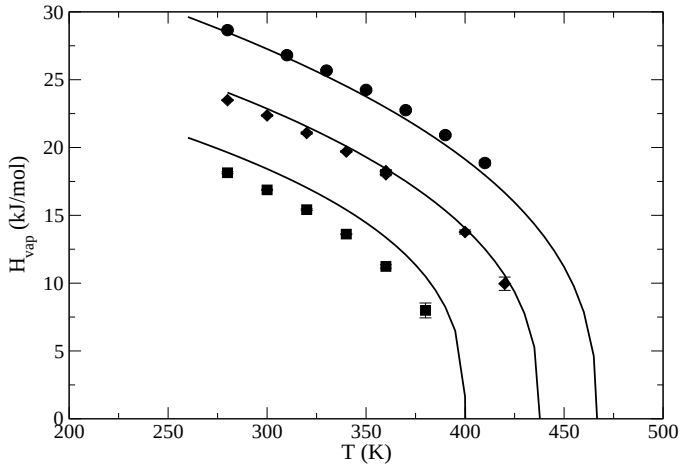

Figure 5.3: Heats of vaporization of ethers. Linestyles for experimental data and symbols as in figure 5.1

UNIVERSITAT ROVIRA I VIRGILI
IMPROVEMENT OF MONTE CARLO ALGORITHMS AND INTERMOLECULAR POTENCIALS FOR THE MODELLING OF ALKANOLS, ESTHERS, TRIOPHENES AND AROMATICS
Javier Pérez Pellitero
ISBN: 978-84-691-0377-7/DL: T.2195-2007

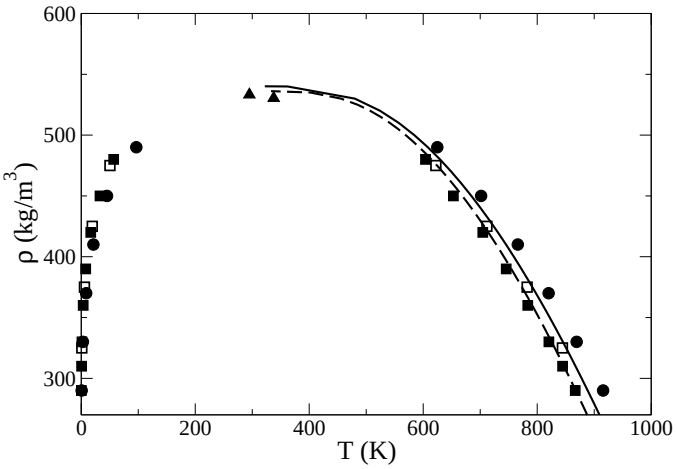

Figure 5.4: Coexistence curves of THF and 1,2-dimethoxyethane. Solid and dashed lines represent experimental data[88] for THF and 1,2-dimethoxyethane respectively. Circle and square symbols represent the simulation results for THF and 1,2-dimethoxyethane respectively. Open symbols denote UA model results from ref. [123] with GEMC while filled symbols are GEMC results of this model. Up triangles denote the calculated critical points.

underestimated.

5.5 Conclusions

The AUA-4 model has been extended to ethers by optimizing the LJ parameters of the oxygen and fitting a set of electrostatic charges to the electrostatic potential of an isolated molecule of dimethylether. The optimiztion of the LJ parameters has been done based on target properties of ethylmethyleter. It should be noted that the LJ parameters of the carbons adjacent to the oxygen group have not been reoptimized in order to keep to a maximum the simplicity and transferability of the model. Nevertheless, satisfactory results have been obtained for the different compounds considered. Saturated liquid densities have been calculated with mean errors of 2% while vaporization enthalpies and saturation pressures have also been reproduced with a good level of agreement. By considering THF we have shown that the transferability of the group to non linear ethers is also satisfactory. In the case of 1,2 dimethoxyethane the presence of a second ether functionality does not affect

UNIVERSITAT ROVIRA I VIRGILI
IMPROVEMENT OF MONTE CARLO ALGORITHMS AND INTERMOLECULAR POTENCIALS FOR THE MODELLING OF ALKANOLS, ESTHERS, TRIOPHENES AND AROMATICS
Javier Pérez Pellitero
ISBN: 978-84-691-0377-7/DL: T.2195-2007

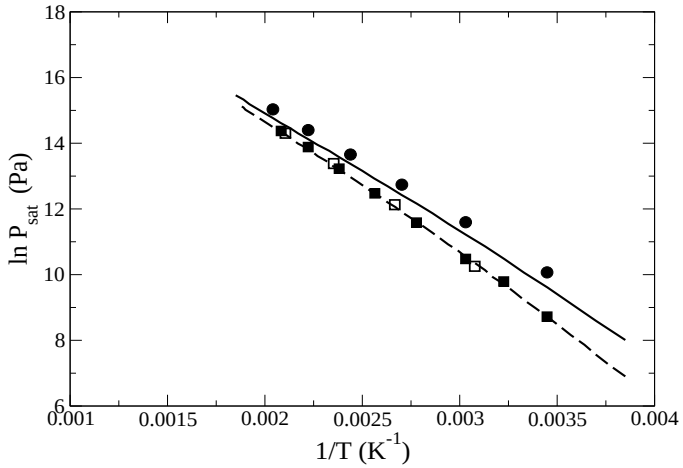

Figure 5.5: Saturated vapour pressures of THF and 1,2-dimethoxyethane. Linestyles for experimental data and symbols as in figure 5.4

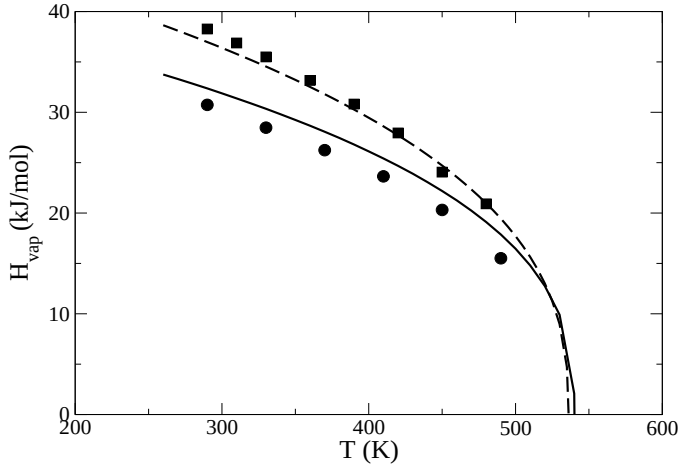

Figure 5.6: Heats of vaporization of THF and 1,2-dimethoxyethane. Linestyles for experimental data and symbols as in figure 5.4

UNIVERSITAT ROVIRA I VIRGILI
IMPROVEMENT OF MONTE CARLO ALGORITHMS AND INTERMOLECULAR POTENCIALS FOR THE MODELLING OF ALKANOLS, ESTHERS, TRIOPHENES AND AROMATICS
Javier Pérez Pellitero
ISBN: 978-84-691-0377-7/DL: T.2195-2007

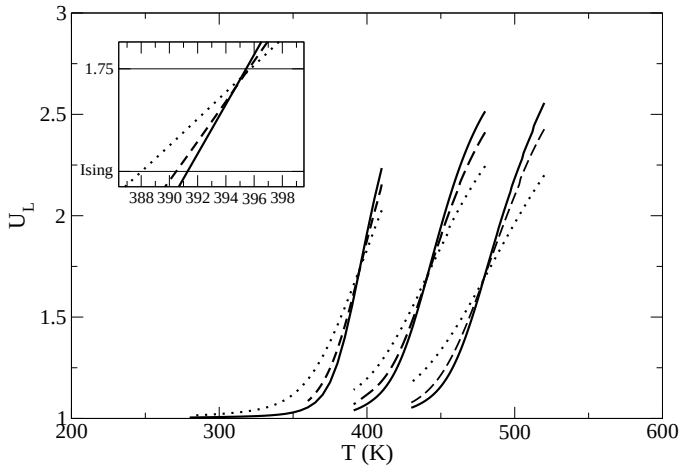

Figure 5.7: Binder parameter intersections for different system sizes for dimethyl, ethylmethyl and diethylether

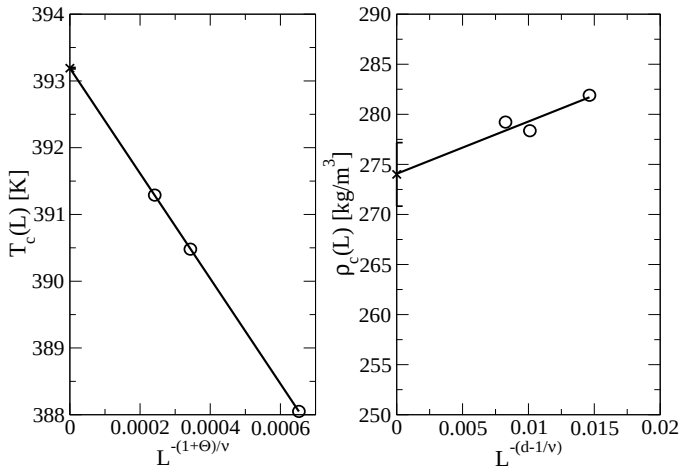

Figure 5.8: Finite Size Scaling for the critical temperature and density of dimethylether

UNIVERSITAT ROVIRA I VIRGILI
IMPROVEMENT OF MONTE CARLO ALGORITHMS AND INTERMOLECULAR POTENCIALS FOR THE MODELLING OF ALKANOLS, ESTHERS, TRIOPHENES AND AROMATICS
Javier Pérez Pellitero
ISBN: 978-84-691-0377-7/DL: T.2195-2007

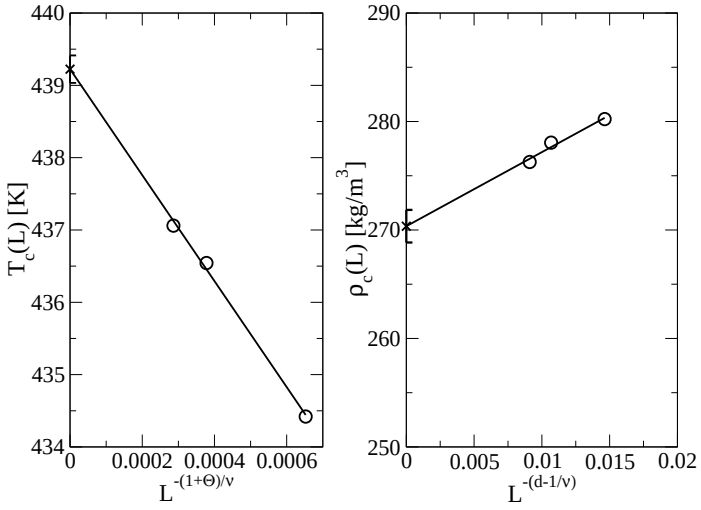

Figure 5.9: Finite Size Scaling for the critical temperature and density of ethylmethylether

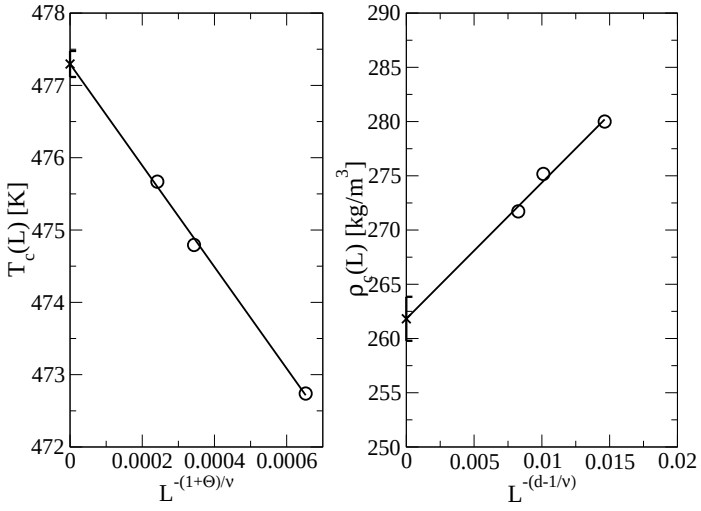

Figure 5.10: Finite Size Scaling for the critical temperature and density of diethylether

UNIVERSITAT ROVIRA I VIRGILI
IMPROVEMENT OF MONTE CARLO ALGORITHMS AND INTERMOLECULAR POTENCIALS FOR THE MODELLING OF ALKANOLS, ESTHERS, TRIOPHENES AND AROMATICS
Javier Pérez Pellitero
ISBN: 978-84-691-0377-7/DL: T.2195-2007

Molecule	Type	$T_c(K)$	$\rho_c(kg/m^3)$	$T_b(K)$
Dimethylether	This model	393.2(1)	274(3)	237.5
	TraPPE-UA	398(1)	277(2)	242(2)
	Experiment	402.1	271	248.3
Ethylmethylether	This model	439.2(2)	270.3(15)	274.8
	TraPPE-UA	435(1)	270(2)	272(1)
	Experiment	437.8	272	280.5
Diethylether	This model	477.3(2)	262(2)	312.1
	TraPPE-UA	466(2)	265(3)	297(1)
	Experiment	466.7	265	307.6
1,2-dimethoxyethane	This model	533.2(2)	295(3)	358.8
	TraPPE-UA	542(2)	291(2)	359(2)
	Experiment	539.2	333	357.8
THF	This model	530.4(5)	337(3)	328.7
	Experiment	540.2	322	339.1

Table 5.5: **Critical properties of the different ethers**

the quality of the predictions. In all cases, the calculation of the critical points has also been made through the methodology based on the calculation of a fourth order cumulant (Binder parameter) combined with the use of finite size scaling techniques. The predictions for the critical point compare well with the experimental data. In particular, the critical point of ethylmethylether has been located within 1% of its experimental value. As in the case of alkanols in chapter 4, we have not observed any evidence of a difference in the universality class due to the presence of the electrostatic charges in the model. The intersections takes place close to the universal Ising value indicating that this is the universality class to which the systems belong .

UNIVERSITAT ROVIRA I VIRGILI
IMPROVEMENT OF MONTE CARLO ALGORITHMS AND INTERMOLECULAR POTENCIALS FOR THE MODELLING OF ALKANOLS, ESTHERS, TRIOPHENES AND AROMATICS
Javier Pérez Pellitero
ISBN: 978-84-691-0377-7/DL: T.2195-2007

T (K)	$\rho_{vap}(kg/m^3)$	$\rho_{liq}(kg/m^3)$	$\Delta H_{vap}(kJ/mol)$	ln $P_{sat}(kPa)$
		Dimethylether		
380	125.4±12	448.7±13	7.99±0.55	15.28±0.05
360	73.2±2.7	508.6±3.4	11.23±0.12	14.94±0.02
340	46.9±0.7	563.0±1.4	13.61±0.04	14.56±0.01
320	28.6±0.8	601.4±2.2	15.42±0.06	14.10±0.02
300	17.9±0.5	638.7±1.4	16.88±0.04	13.63±0.02
280	10.2±0.3	670.7±1.4	18.14±0.07	13.04±0.02
		Ethylmethylether		
420	110±12	465.3±8	9.95±0.49	15.01±0.04
400	65.3±2.9	520.7±4.2	13.77±0.15	14.66±0.03
360	28.1±1.3	599.0±3.1	18.26±0.11	13.92±0.03
340	17.6±0.4	632.4±1.6	19.70±0.07	13.48±0.02
320	10.5±0.4	661.0±2.2	21.07±0.09	12.95±0.04
300	6.15±0.25	689.4±1.4	22.36±0.05	12.38±0.04
280	2.47±0.27	715.0±2.8	23.49±0.04	11.69±0.04
		Diethylether		
410	37.4±2.2	566.9±4.6	18.86±0.19	14.01±0.03
390	23.87±1.2	599.3±3.1	20.92±0.13	13.65±0.04
370	16.21±0.6	633.8±2.5	22.75±0.11	13.25±0.03
350	9.44±0.5	658.0±2.2	24.25±0.10	12.71±0.05
330	5.61±0.2	684.9±1.5	25.67±0.10	12.17±0.03
310	2.80±0.17	706.4±1.9	26.80±0.10	11.43±0.05
280	0.96±0.09	743.6±1.5	28.65±0.06	10.27±0.04
		1,2 dimethoxyethane		
480	56.9±1.7	604.0±5.9	20.92±0.3	14.37±0.07
450	32.8±1.1	653.0±2.2	24.06±0.11	13.88±0.03
420	16.65±0.6	704.5±2.1	27.95±0.13	13.22±0.03
390	7.89±0.3	745.7±1.7	30.82±0.11	12.47±0.03
360	3.40±0.21	783.5±1.3	33.16±0.13	11.58±0.06
330	1.20±0.11	820.5±2.1	35.50±0.40	10.48±0.08
310	0.63±0.05	844.6±1.0	36.88±0.52	9.79±0.09
290	0.23±0.04	866.7±2.2	38.27±0.45	8.72±0.08
		THF		
490	96.6±7.1	624.7±8.0	15.51±0.37	15.03±0.03
450	45.3±2.0	701.6±4.1	20.31±0.17	14.40±0.03
410	21.3±0.8	765.9±2.0	23.64±0.09	13.66±0.03
370	8.61±0.7	820.0±2.0	26.24±0.13	12.74±0.07
330	2.96±0.32	869.2±1.5	28.48±0.11	11.56±0.08
290	0.71±0.10	915.6±2.6	30.73±0.20	10.07±0.08

Table 5.6: **Equilibrium properties of ethers**

UNIVERSITAT ROVIRA I VIRGILI
IMPROVEMENT OF MONTE CARLO ALGORITHMS AND INTERMOLECULAR POTENCIALS FOR THE MODELLING OF ALKANOLS, ESTHERS, TRIOPHENES AND AROMATICS
Javier Pérez Pellitero
ISBN: 978-84-691-0377-7/DL: T.2195-2007

Appendix-1

UNIVERSITAT ROVIRA I VIRGILI
IMPROVEMENT OF MONTE CARLO ALGORITHMS AND INTERMOLECULAR POTENCIALS FOR THE MODELLING OF ALKANOLS, ESTHERS, TRIOPHENES AND AROMATICS
Javier Pérez Pellitero
ISBN: 978-84-691-0377-7/DL: T.2195-2007

A1-1
Probability distribution and partition function

The grand canonical partition function Ξ is given by:

$$\Xi(\mu, V, T) = \sum_N \frac{1}{N!\Lambda^{3N}} \exp(\beta\mu N) \int dr^N \exp(-\beta E) \tag{A-1}$$

where $\Lambda = \sqrt{\frac{h^2}{2\pi m k_b T}}$ is the de Broglie wavelength, $\beta = 1/k_b T$ and E is the configurational (potential) energy of the system with coordinates r^N

We introduce the density of states $\rho(N, V, E)$ through:

$$\Xi(\mu, V, T) = \sum_N \frac{1}{N!\Lambda^{3N}} \exp(\beta\mu N) \int dE \delta(E - E(r^n)) \exp(-\beta E) \tag{A-2}$$

$$\Xi(\mu, V, T) = \sum_N \frac{1}{N!\Lambda^{3N}} \exp(\beta\mu N) \int_{E_0}^{\infty} \rho(N, V, E) \exp(-\beta E) dE \tag{A-3}$$

Finally, we can write the histogram-reweighting inspired equation for both the partition function and the probability:

$$\Xi(\mu, V, T) = \sum_N \frac{1}{N!\Lambda^{3N}} \sum_E \rho(N, V, E) \exp(\beta\mu N - \beta E) \tag{A-4}$$

Following these definitions the probability of observing a configuration with a given number of particles N and a configurational energy E is:

$$P(N, E) = \frac{\frac{1}{N!\Lambda^{3N}} \exp(\beta\mu N - \beta E \rho(N, V, E)}{\Xi(\mu, V, T)} \tag{A-5}$$

UNIVERSITAT ROVIRA I VIRGILI
IMPROVEMENT OF MONTE CARLO ALGORITHMS AND INTERMOLECULAR POTENCIALS FOR THE MODELLING OF ALKANOLS, ESTHERS, TRIOPHENES AND AROMATICS
Javier Pérez Pellitero
ISBN: 978-84-691-0377-7/DL: T.2195-2007

Note that in this case the prefactor $\frac{1}{N!\Lambda^{3N}}$ is not cancelled out, due to the sumation over the number of particles present in the grand partition function.

A1-2

Histogram reweighting

If we perform a Monte Carlo simulation at inverse temperature β, chemical potential μ and volume V and make n measurements of the energy E of the system and the number of particles N, then we can make an estimate of the probability of a given energy and number of particles $P(N, E)$:

$$P(N, E) = \frac{H(N, E)}{n} \tag{A-6}$$

where the histogram $H(N, E)$ is the number of times that the system was measured to have energy E and number of particles N. From equation A-5 we can write the density of states as follows:

$$\rho(N, V, E) = \frac{H(N, E)}{n} \frac{\Xi}{exp(\beta\mu N - \beta E)} N!\Lambda^{3N} \tag{A-7}$$

Supposing that we perform severa simulations at a different number of inverse temperatures β_i and chemical potential μ_i we obtain a number of different estimations of the density of states:

$$\rho_i(N, V, E) = \frac{H_i(N, E)}{n_i} \frac{\Xi_i}{exp(\beta_i\mu N - \beta_i E)} N!\Lambda_i^{3N} \tag{A-8}$$

What we want to do is form a weighted average over the estimates $\rho_i(N, V, E)$ to get the best estimate of the whole range of energies covered by the different histograms. The standard way of performing such a weighted average is as follows. If we have a number of measurements x_i of a quantity x, each of which has an associated standard error σ_i, then the best estimate x_{avg} of x is:

UNIVERSITAT ROVIRA I VIRGILI
IMPROVEMENT OF MONTE CARLO ALGORITHMS AND INTERMOLECULAR POTENCIALS FOR THE MODELLING OF ALKANOLS, ESTHERS, TRIOPHENES AND AROMATICS
Javier Pérez Pellitero
ISBN: 978-84-691-0377-7/DL: T.2195-2007

$$x_{avg} = \frac{\sum_i x_i/\sigma_i^2}{\sum_j 1/\sigma_j^2} \tag{A-9}$$

Assuming as in [44] that the true error on the number of samples in each bin of our histograms should be Poissonian and a function of the average histogram $\overline{H_i(N,E)}$ (which is the real value of the histogram obtained with perfect sampling, the exact density of states is:

$$\rho_i(N,V,E) = \frac{\overline{H(N,E)}}{n_i}\frac{\Xi_i}{exp(\beta_i\mu N - \beta_i E)}N!\Lambda_i^{3N} \tag{A-10}$$

Note, that the value of $\overline{H_i(N,E)}$ is not known.

Making the previous assumptions, the error σ_i for $\rho_i(N,V,E)$ is:

$$\sigma_i = \frac{\sqrt{\overline{H_i(N,E)}}}{n_i}\frac{\Xi_i}{exp(\beta_i\mu N - \beta_i E)}N!\Lambda_i^{3N} \tag{A-11}$$

and the variance is:

$$\sigma_i^2 = \frac{\overline{H_i(N,E)}}{n_i^2}[\frac{\Xi_i}{exp(\beta_i\mu N - \beta_i E)}]^2[N!\Lambda_i^{3N}]^2 = \frac{\rho^2(N,V,E)}{\overline{H_i(N,E)}} \tag{A-12}$$

Performing the weighted average of equation A-9 our best estimate of $\rho(N,V,E)$ is:

$$\rho(N,V,E) = \frac{\sum_i \overline{H_i(N,E)}H_i(N,E)/n_i[\Xi_i/\exp(\beta_i\mu_i N - \beta_i E)]N!\Lambda_i^{3N}}{\sum_j \overline{H_j(N,E)}} \tag{A-13}$$

Making use of equation A-10 to cancel out the quantities $\overline{H_i(N,E)}$ whose values we do not know, we obtain:

UNIVERSITAT ROVIRA I VIRGILI
IMPROVEMENT OF MONTE CARLO ALGORITHMS AND INTERMOLECULAR POTENCIALS FOR THE MODELLING OF ALKANOLS, ESTHERS, TRIOPHENES AND AROMATICS
Javier Pérez Pellitero
ISBN: 978-84-691-0377-7/DL: T.2195-2007

$$\rho(N,V,E) = \frac{\sum_i H_i(N,E)}{\sum_j n_j \Xi_j^{-1} \exp(\beta_j \mu N - \beta_j E) \frac{1}{N! \Lambda_j^{3N}}} \tag{A-14}$$

where the well known factor $\frac{1}{N!\Lambda^{3N}}$ now appears. (note that the value of Λ depends also on the temperature of each simulation). This factor is not given in the normal formulation of the histogram reweighting.

In order to determine the partition function we have still to find the values of Ξ_i, whose values we do not know.

To do that we apply the definition of the partition function in equation A-4:

$$\Xi_k = \sum_N \frac{1}{N! \Lambda_k^{3N}} \sum_E \rho(N,V,E) \exp(\beta_k \mu_k N - \beta_k E) \tag{A-15}$$

Substituting the value of the density of states by our best estimate we obtain:

$$\Xi_k = \sum_N \sum_E \frac{\frac{1}{\Lambda_k^{3N}} \exp(\beta_k \mu_k N - \beta_k E) \sum_i H_i(E,N)}{\sum_j n_j \Xi_j^{-1} \exp(\beta_j \mu_j N - \beta_j E) \frac{1}{\Lambda_j^{3N}}} \tag{A-16}$$

where now a factor $\frac{1}{\Lambda^{3N}}$ appears at different temperatures (it does not cancel out) both in the numerator and the denominator. As in [19] [18] we can define a virtual chemical potential shifted by the temperature-dependence of the DeBroglie wavelength, according to:

$$\frac{\exp(\mu \beta N)}{\Lambda^{3N}} = \exp(\mu \beta N - 3N \ln \Lambda) = \exp(\overline{\mu} \beta N) \tag{A-17}$$

with

$$\overline{\mu} = \mu - \frac{3}{\beta} \ln \Lambda \tag{A-18}$$

to obtain finally:

UNIVERSITAT ROVIRA I VIRGILI
IMPROVEMENT OF MONTE CARLO ALGORITHMS AND INTERMOLECULAR POTENCIALS FOR THE MODELLING OF ALKANOLS, ESTHERS, TRIOPHENES AND AROMATICS
Javier Pérez Pellitero
ISBN: 978-84-691-0377-7/DL: T.2195-2007

$$\Xi_k(\mu,V,T) = \sum_{N,E} \frac{\sum_i H_i(E,N)}{\sum_j n_j \Xi_j^{-1} \exp(\beta_j \overline{\mu_j} N - \beta_k \overline{\mu_k} N - (\beta_j - \beta_k)E)} \tag{A-19}$$

Also we could consider using the activity instead of chemical potential where the activity a can be defined as follows:

$$a = \frac{exp^{\beta\mu}}{\Lambda^3} \tag{A-20}$$

Each of the values of Ξ_k corresponding to the different simulations must be found by solving the previous set of equations iteratively.

Once we have calculated these values, we can calculate the partition function at any other temperature or chemical potential generalizing the previous equation:

$$\Xi(\mu,V,T) = \sum_{N,E} \frac{\sum_i H_i(E,N)}{\sum_j n_j \Xi_j^{-1} \exp(\beta_j \overline{\mu_j} N - \beta \overline{\mu} N - (\beta_j - \beta)E)} \tag{A-21}$$

A1-3
Relation with the computational code

In the grand canonical algorithm of the Gibbs code we are sampling the phase space with a probability:

$$P(N \to N+1) = min\left(1, \frac{V}{N+1} \exp(\beta\mu - \beta E\right) \tag{A-22}$$

Hence, we are ignoring the DeBroglie wavelength in the acceptance probability. As a consequence, we are shifting the value of the chemical potential by an ammount $-3 \ln \Lambda$. This is equivalent to the use of the modified chemical potential defined in equation A-18 or to use activity in the acceptance probability. In this way we can use directly equation A-21 to reweight our data.

UNIVERSITAT ROVIRA I VIRGILI
IMPROVEMENT OF MONTE CARLO ALGORITHMS AND INTERMOLECULAR POTENCIALS FOR THE MODELLING OF ALKANOLS, ESTHERS, TRIOPHENES AND AROMATICS
Javier Pérez Pellitero
ISBN: 978-84-691-0377-7/DL: T.2195-2007

Bibliography

[1] Redlich O. Kwong J.N.S.
Chemical Reviews, 44:233, 1949.

[2] Soave G.
Chemical Engineering Science, 27:1197, 1972.

[3] Peng D. Robinson D.B.
Industrial and Engineering Chemical Fundamentals, 15:59, 1976.

[4] Renon H. Prausnit J.M.
Chemical Engineering Science, 22:299, 1967.

[5] Lee B.I. Kesler M.G.
AICHE Journal, 21:510, 1975.

[6] Hansen J.P. McDonald I.R.
Theory of Simple Liquids.
Academic Press, London 1990.

[7] A.Z. Panagiotopoulos.
Molecular Physics, 61:813–826, 1987.

[8] K.K Mon and K. Binder.
Journal of Chemical Physics, 96:6989, 1992.

[9] J.R. Recht and A.Z Panagiotopoulos.
Molecular Physics, 80:843, 1992.

[10] B. Smit S Karaborni J.I. Siepmann.
Journal of Chemical Physics, 102:2126, 1995.

[11] J.J. Potoff J.R.Errington A.Z. Panagiotopoulos.
Molecular Physics, 97(10):1073–1083, 1999.

[12] A.Z. Panagiotopoulos.
Molecular Physics, 63(4):527–545, 1988.

[13] B. Smit.
J. Chem. Phys., 96:8639–8640, 1992.

UNIVERSITAT ROVIRA I VIRGILI
IMPROVEMENT OF MONTE CARLO ALGORITHMS AND INTERMOLECULAR POTENCIALS FOR THE MODELLING OF ALKANOLS, ESTHERS, TRIOPHENES AND AROMATICS
Javier Pérez Pellitero
ISBN: 978-84-691-0377-7/DL: T.2195-2007

[14] N.B. Wilding.
Physical Review E, 52(1), 1995.

[15] A.M. Ferrenberg R.H. Swendsen.
Phys. Rev. Lett., 61:2635–2638, 1988.

[16] A.M. Ferrenberg R.H. Swendsen.
Phys. Rev. Lett., 63:1195–1198, 1989.

[17] N.B. Wilding and A.D. Bruce.
Journal of Physics-Condensed Matter, 4:3087–3108, 1992.

[18] J.M. Caillol.
Journal of Chem. Phys., 109(12), 1998.

[19] W. Shi J.K. Johnson.
Fluid Phase Equilibria, 187-188:171–191, 2001.

[20] J.J. Potoff and A.Z. Panagiotopoulos.
J. Chem. Phys., 109(24), 1998.

[21] R.O. Contreras-Camacho P. Ungerer M.G. Ahunbay V Lachet J. Perez-Pellitero A.D. Mackie.
J.Phys. Chem. B, 108:14115–14123, 2004.

[22] GIBBS code supplied by the Institut Français du Pétrole.

[23] K. Binder.
Phys B: Condens. Matter, 43(119), 1981.

[24] W.L. Jorgensen J.D. Madura C.J. Swenson.
Journal of the American Chemical Society, 106:6638, 1984.

[25] M.G. Martin J.I. Siepmann.
Journal of Physical Chemistry B, 102:2569, 1998.

[26] J.R. Errington A.Z. Panagiotopoulos.
Journal of Physical Chemistry B, 103:6314, 1999.

[27] B. Chen J.I. Siepmann.
Journal of Physical Chemistry B, 103:5370, 1999.

[28] P. Ungerer C. Beauvais J. Delhommelle A. Boutin B. Rousseau A.H. Fuchs.
J.Phys. Chem., 112(12):5499–5510, 2000.

[29] S. Toxvaerd.
Journal of Chemical Physics, 107:5197, 1997.

[30] S. Toxvaerd.
Journal of Chemical Physics, 107:4290, 1990.

[31] T. J. Bandosz C. O. Ania.
Energy & Fuels, 20:1076, 2006.

UNIVERSITAT ROVIRA I VIRGILI
IMPROVEMENT OF MONTE CARLO ALGORITHMS AND INTERMOLECULAR POTENCIALS FOR THE MODELLING OF ALKANOLS, ESTHERS, TRIOPHENES AND AROMATICS
Javier Pérez Pellitero
ISBN: 978-84-691-0377-7/DL: T.2195-2007

[32] M.G. Ahunbay J. Perez-Pellitero R.O. Contreras-Camacho J.M. Teuler P. Ungerer A.D. Mackie and V. Lachet.
J. Chem. Phys., 109:2970, 2005.

[33] W.L. Jorgensen.
Journal of the American Chemical Society, 102:543, 1980.

[34] W.L. Jorgensen.
Journal of the American Chemical Society, 103:335, 1981.

[35] M Haughney.
Journal of Physical Chemistry, 91:4934, 1987.

[36] M.E. Van Leeuwen.
Molecular Physics, 87:87, 1996.

[37] M.E. Van Leeuwen B. Smit.
Journal of Physical Chemistry, 99:1831, 1995.

[38] J.I. Siepmann S. Karaborni B. Smit.
Nature, 365:330, 1993.

[39] B. Chen J.J. Potoff J.I Siepmann.
Journal of Physical Chemistry B, 105(3093), 2001.

[40] B. Widom.
Statistical Mechanics: A concise introduction for chemists.
Cambridge University Press, United Kingdom 2002.

[41] A.Z. Panagiotopoulos N. Quirke M. Stapleton D. J. Tildesley.
Molecular Physics, 63:527, 1988.

[42] A.Z. Panagiotopoulos.
Molecular Simulation, 9:1, 1992.

[43] A.Z. Panagiotopoulos.
Molecular Physics, 68:951, 1989.

[44] M.E.J. Newman G.T. Barkema.
Monte Carlo Methods in Statistical Physics.
Oxford University Press, Oxford 1999.

[45] G. Jen.
Ind. Eng. Chem., 38:803, 1946.

[46] U. Wolff.
Computational Methods in Field Theory.
1992.

[47] Data for the ”universal operator distribution” Private communication N.B. Wilding.

[48] IMSL Math and Stat Libraries.

UNIVERSITAT ROVIRA I VIRGILI
IMPROVEMENT OF MONTE CARLO ALGORITHMS AND INTERMOLECULAR POTENCIALS FOR THE MODELLING OF ALKANOLS, ESTHERS, TRIOPHENES AND AROMATICS
Javier Pérez Pellitero
ISBN: 978-84-691-0377-7/DL: T.2195-2007

[49] E. Luijten M.E. Fisher A.Z. Panagiotopoulos.
Physical Review Letters, 88:185701, 2002.

[50] R.A. Aziz.
J. Chem. Phys, 99:4518, 1993.

[51] Laso M de Pablo J. J. Suter U. W.
Journal of Chemical Physics, 97:2817, 1992.

[52] Siepmann J.I Frenkel D.
Molecular Physics, 75:59, 1992.

[53] P. Ungerer B. Tavitian A. Boutin.
Applications of molecular simulation in the oil and gas industry. Monte Carlo methods.
Paris 2005.

[54] Neubauer B. Boutin A. Tavitian B. Fuchs A. H.
Molecular Physics, 97:769, 1999.

[55] Macedonia M. D. Maginn E. J.
Molecular Physics, 96:1375, 1999.

[56] E. Bourasseau P. Ungerer A. Boutin.
J. Phys. Chem B, 106:5483, 2002.

[57] M.P. Allen and D.J. Tildesley.
Computer Simulation of Liquids.
Oxford University Press, Oxford 1989.

[58] Nymand T. M. Linse P.
J. Chem. Phys, 112:6386, 2000.

[59] J.J. Rehr and N.D. Mermin.
Phys. Rev. A, 8:472, 1973.

[60] M.E Fisher and G. Orkoulas.
Physical Review Letters, 85:696, 2000.

[61] G. Orkoulas M.E Fisher and A.Z. Panagiotopoulos.
Physical Review E, 5(63):051507, 2001.

[62] A.Z. Panagiotopoulos.
International Journal of ThermoPhysics, 15:1057–1072, 1994.

[63] B. Smit.
Simulations of phase coexistence: from atoms to surfactants.
PhD thesis, Universiteit Utrecht, The Netherlands, 1990.

[64] Y.C. Kim M.E Fisher.
Computer Physics Communications, (169):295–300, 2005.

[65] Y.C. Kim.
Physical Review E, (71):051501, 2005.

UNIVERSITAT ROVIRA I VIRGILI
IMPROVEMENT OF MONTE CARLO ALGORITHMS AND INTERMOLECULAR POTENCIALS FOR THE MODELLING OF ALKANOLS, ESTHERS, TRIOPHENES AND AROMATICS
Javier Pérez Pellitero
ISBN: 978-84-691-0377-7/DL: T.2195-2007

[66] S. Moghaddam A.Z Panagiotopoulos.
Fluid Phase Equilibria, 222:221, 2004.

[67] A.M. Ferrenberg and D.P. Landau.
Phys. Rev. B, 44:5081, 1991.

[68] J.H. Chen M.E. Fisher and B.G. Nickel.
Phys. Rev. Lett, 48:630, 1982.

[69] A. Lotfi J. Vrabec J.Fischer.
Mol. Phys., 76:1319–1333, 1992.

[70] J.J Potoff and A.Z.Panagiotopoulos.
J. Chem. Phys., 112:6411, 2000.

[71] Y.C. Kim M.E. Fisher G. Orkoulas.
Physical Review E, 67(6):061506, 2003.

[72] D.P. Landau and K. Binder.
Monte Carlo Simulations in Statistical Physics.
Cambridge University Press, Cambridge 2000.

[73] H.W.J. Blöte M.E. Luijten and J.R. Heringa.
J. Phys. A, 28:6289, 1995.

[74] E. de Miguel.
Physical Review E, 55:1347–1355, 1997.

[75] V.I. Harismiadis N.K. Koutras D.P. Tassios A.Z. Panagiotopoulos.
Fluid Phase Equilibria, 65:1–18, 1991.

[76] R. Goodwin.
National Bureau of Standards Report, (No NBSIR 83-1964), 1983.

[77] S. Stamataki and K. Magoulas.
Oil Gas Sci. Technol., (55):511, 2000.

[78] T. Kristof J. Liszi.
J.Phys. Chem. B, 101:5480–5483, 1997.

[79] C. Nieto-Draghi A.D. Mackie and J. Bonet Avalos.
J. Chem Phys, (123):014505, 2005.

[80] O. Elizalde-Solis L.A. Galicia-Luna.
Fluid Phase Equilibria, 236:178, 2005.

[81] H Toghiani R.K Toghinai D.S Viswanath.
Journal of Chemical and Engineering Data, 39:63, 1994.

[82] M.I. Zaretskii V.B Kogan N.F Kononov.
Journal of Applied Chemistry o the USSR, 47:2327, 1974.

[83] M.I. Zaretskii V.B. Kogan N.F. Kononov A.A. MiroshniChenko I.V. Usyushkina V.G. Podolyak.
Journal of Applied Chemistry o the USSR, 47:2142, 1974.

UNIVERSITAT ROVIRA I VIRGILI
IMPROVEMENT OF MONTE CARLO ALGORITHMS AND INTERMOLECULAR POTENCIALS FOR THE MODELLING OF ALKANOLS, ESTHERS, TRIOPHENES AND AROMATICS
Javier Pérez Pellitero
ISBN: 978-84-691-0377-7/DL: T.2195-2007

[84] C. Tsonopoulos D. Ambrose.
Journal of Chemical and Engineering Data, 46:480, 2001.

[85] J. Delhommelle C Tschirwitz P. Ungerer G. Granucci P. Millié D. Pattou and A.H. Fuchs.
J. Phys. Chem. B, 104:4745, 2000.

[86] E. Bourasseau M. Haboudou A. Boutin A.H. Fuchs P. Ungerer.
New optimization method for intermolecular potentials: Optimization for a new anisotropic united atoms potential for olefins: Prediction of equilibrium properties.
J. Chem. Phys., 118:3020, 2003.

[87] *Handbook of Chemistry and Physics*.
CRC Press, 1993.

[88] BYU DIPPR 801.
Thermophysical properties database public release january 2005.

[89] The positions of the functional groups can be calculated from the condition of having them placed on the external bisector of the angle formed by the carbon where the functional group is attached to.

[90] R.O. Contreras-Camacho P. Boutin A. A.D. Mackie.
J.Phys. Chem. B, 108:14109, 2004.

[91] A.D. Mackie B. Tavitian A. Boutin A.H. Fuchs.
Mol. Sim., 19, 1997.

[92] M. Lagache P. Ungerer A. Boutin A.H. Fuchs.
Phys. Chem. Chem. Phys., 3:4333, 2001.

[93] E. Bourasseau P. Ungerer A. Boutin A.H. Fuchs.
Molecular Simulation, 28:317–336, 2002.

[94] J. Pérez-Pellitero P. Ungerer G. Orkoulas A.D. Mackie.
J. Chem Phys, 125(054515), 2006.

[95] N. Lubna G. Kamath J.J. Potoff N. Rai J.I Siepmann.
J. Phys. Chem. B, 109:24100–24107, 2005.

[96] A. Boutin A.D Mackie R.O. Contreras-Camacho, P. Ungerer.
J. Phys. Chem. B, 108:14109, 2004.

[97] P. Ungerer C. Nieto-Draghi P. Bonnaud.
J. Phys. Chem. B, 111:3730, 2007.

[98] O.K. Bates G. Hazzard.
Industrial and Engineering Chemistry, 37:193–195, 1945.

[99] E. Bourasseau.
Prédiction des propriétés d'équilibre de phases par simulation moléculaire. Développement d'algorithmes et optimisation de potentiels.
PhD thesis, Université de Paris-Sud, 2003.

UNIVERSITAT ROVIRA I VIRGILI
IMPROVEMENT OF MONTE CARLO ALGORITHMS AND INTERMOLECULAR POTENCIALS FOR THE MODELLING OF ALKANOLS, ESTHERS, TRIOPHENES AND AROMATICS
Javier Pérez Pellitero
ISBN: 978-84-691-0377-7/DL: T.2195-2007

[100] W.D. Cornell P. Cieplak C.I. Baily I.R. Gould K.M. Merz D.M. Ferguson D.C. Spellmeyer T. Fox J.W. Caldwell P.A. Kollman.
Journal of the American Chemical Society, 117:5179, 1995.

[101] W.L. Jorgensen.
J. Phys. Chem., 90:1276, 1986.

[102] Singh U. C. Kollman P. A.
Journal of Computational Chemistry, 5:129, 1984.

[103] W.L. Jorgensen J.Chandrasekhar J.D. Madura R.W. Impey M.L. Klein.
Journal of Physical Chemics, 79:926, 1983.

[104] D. Frenkel and B. Smit.
Understanding Molecular Simulation: From Algorithms to Applications.
Academic Press, San Francisco 2001.

[105] Dohnal V. Fenclová D. Vrbka Pavel.
J. Phys. Chem. Ref. data, 35:1621, 2006.

[106] Hernández-Cobos J. Mackie A. D. Vega L. F.
Journal of Chemical Physics, 114:7527, 2001.

[107] Moller D. Oprzynski J. Muller A. Fischer J.
Molecular Physics, 75:363, 1992.

[108] J. Delhommelle.
Etablissement de potentiels d'interaction pour la simulation moléculaire-application à la prédiction des équilibres liquide-vapeur de mélanges binaires alcane-molécule multiolaire.
PhD thesis, Université de Paris XI Orsay France, 2000.

[109] Vrabec J. Stoll J. Hasse H.
Journal of Physical Chemistry B, 105:12126, 2001.

[110] Harris J. G. Yung K.H.
Journal of Physical Chemistry, 99:12021, 1995.

[111] Kong C. L.
J. Chem. Phys., 59:1953, 1973.

[112] Kong C. L.
J. Chem. Phys., 59:2464, 1973.

[113] Kong C. L.
J. Phys. Chem., 77:2668, 1973.

[114] Delhommelle J. Millie P.
Molecular Physics, 99:619, 2001.

[115] Ungerer P. Wender A. Demoulin G. Bourasseau E. Mougin P.
Molecular Simulation, 30:631, 2004.

UNIVERSITAT ROVIRA I VIRGILI
IMPROVEMENT OF MONTE CARLO ALGORITHMS AND INTERMOLECULAR POTENCIALS FOR THE MODELLING OF ALKANOLS, ESTHERS, TRIOPHENES AND AROMATICS
Javier Pérez Pellitero
ISBN: 978-84-691-0377-7/DL: T.2195-2007

[116] Boutard Y. Ungerer Ph. Teuler J. M. Ahunbay M. G. Sabater S. F. Pérez-Pellitero J. Mackie A. D. Bourasseau E.
Fluid Phase Equilibria, 236:25, 2005.

[117] Kofke D. A.
Molecular Physics, 102:405, 2004.

[118] Boulougouris G. C. Economou I. G. Theodorou D. N.
Journal of Chemical Physics, 115:8231, 2001.

[119] Boulougouris G. C. Economou I. G. Theodorou D. N.
Molecular Physics, 96:905, 1999.

[120] Ukai T. Kodama D. Miyazaki J. Kato M.
J. Chem. Eng. Data, 47:1320, 2002.

[121] Weng W. L. Lee J. M.
Fluid Phase Equilibria, 122:243, 1996.

[122] Briggs J. M. Matsui T. Jorgensen W. L.
Journal of Computational, 96:905, 1990.

[123] Stubbs J. M. Potoff J. J. Siepmann J. I.
J. Phys. Chem. B, 108:17596, 2004.